Development of Biomechanical Models that Represent Members of the South African National Defence Force

Karen Bredenkamp
B. Ing (Mechanical)

Dissertation for M.Sc. (Med) in Biomedical Engineering
University of Cape Town

Supervisor : Prof. C.L. Vaughan

December 2010

DECLARATION

I, Karen Bredenkamp, hereby declare that the work on which this dissertation/thesis is based is my original work (except where acknowledgements indicate otherwise) and that neither the whole work nor any part of it has been, is being, or is to be submitted for another degree in this or any other university. I empower the university to reproduce for the purpose of research either the whole or any portion of the contents in any manner whatsoever.

SIGNATURE : signature removed

Date : 28/01/2011

ACKNOWLEDGEMENTS

First and foremost, thank you to our Creator for the gift of health, vitality, time and intellect to conduct this thesis to the best of my ability.

In addition, this work was made possible with the help and support of a series of people and organisations. I would therefore like to acknowledge the following persons/organisations for their contribution which allowed completion of this master's thesis.

I would like to acknowledge the support of the South African National Defence Force as well as ERGOnomics TECHnologies. Without the financial and organisational backing provided by these organisations, this work would not have been possible. I would also like to acknowledge the University of Cape Town, and specifically the administrative staff at the postgraduate office for their assistance. Thank you for the help of my colleagues, especially Petrie Marais and Heinrich Nolte, in setting up equipment, solving software problems and helping me understand Biomechanics. A special thanks to all persons who participated in the data collection. Their time and the enthusiasm with which they diligently completed (and repeated) the tasks as instructed is invaluable.

To my supervisor, Prof Vaughan, thank you for your patience with my busy work and family schedule, for always being available and willing to provide inputs (even over Christmas and New Year!) and for keeping me motivated to finish this thesis.

And lastly but most importantly, for my family and friends: to my husband, Riaan, for not always agreeing with what I set out to do, but being an amazing support throughout none the less. To my sister, Jeanne, for believing in me and being the driving force behind me "finishing what I've started". And to my friend and ex-colleague, Lorraine Mac Duff, for being an exceptional friend and inspiration, and for leading by example.

My sincerest thank you,

The author
January 2011

ABSTRACT

Biomechanical analysis plays a key role in task and job analysis to reduce musculoskeletal risk to the worker. In a military environment, manual material handling tasks that place military personnel under extreme biomechanical strain are almost certainly encountered. The aim of this study was to build a range of biomechanical models that represent members of the South African National Defence Force (SANDF) in terms of anthropometry and functional body strength. These models would have the potential to serve as biomechanical risk analysis tools, and would indicate specific military tasks, identified during job analysis, that would put SANDF personnel members at risk. This biomechanical analysis tool would provide the crucial step in the process to ensure that SANDF personnel members are not placed in jobs or posts that might expose them to biomechanical risks.

A combination of analysis techniques was used to attain the most complete understanding of the body form variation for the males and females in the SANDF. These included investigation of BMI distribution, correlations between anthropometric variables and principle component analysis. This analysis approach was successful in highlighting variation in body forms of males and females in the SANDF. Eight biomechanical models, four male and four female, were created in the dynamics biomechanical software package LifeMod^{TM}. The modelling process required multiple iterations to identify optimal model characteristics such as joint stiffness and damping, foot-floor contact characteristics, motion tracking settings and muscle properties. In spite of the efforts made to ensure that all aspects of the models were optimised, modelling errors occurred which resulted in no data being obtained for two of the eight biomechanical models. In addition, validation of the functional body strength capabilities of the models indicated a maximum of 34 % estimation error when compared to the actual functional body strength data. Errors in functional strength values predicted by the model could be attributed to a range of modelling anomalies, such as inconsistencies between motion data and the model, poor muscle representation in specific areas such as the abdomen and shoulders, as well as joint instability and poor force exertion at large (> 90 degrees) joint angles.

Taking all the results and conclusions into consideration, it was finally concluded that the LifeMod™ software does not lend itself to the current approach of using a range of models to investigate biomechanical risks by representing functional body strength of a population. It is recommended that the current approach used for investigating biomechanical risk for the SANDF population by representing functional body strength in biomechanical models created in the LifeMod™ software, be re-assessed and that joint loads and joint angles be investigated further to predict muscular skeletal risk during task and job analysis.

CONTENTS

CHAPTER 1 : INTRODUCTION

Occupational biomechanics is the discipline concerned with the mismatch of human physical capacities and human manual performance requirements in industry; and so involves the physical interaction of the worker with his/her tools, machines and materials. This mismatch of human physical capabilities and manual performance requirements leads to injury, such as impact or overexertion trauma (Chaffin *et al.,* 1999). The costs incurred by occupational injury would include the medical expenses, sick leave, replacement staff and training, and perhaps of greatest concern is the loss of productivity, temporary or otherwise, of a fully trained employee. Biomechanical analysis plays a key role in task and job analysis as well as in equipment design and development to reduce musculoskeletal risk to the worker (Lavender *et al.,* 2000; Ren *et al.,* 2005; Chaffin *et al.,* 2004 and Cooper and Ghassemieh, 2007).

In a military environment, manual material handling tasks that put military personnel under extreme biomechanical strain are almost certainly encountered (Mac Duff and Slabbert, 2003). Following the end of the Apartheid era in South Africa, the South African National Defence Force (SANDF) has seen a huge change in the human resource profile as a result of the transformation process and the implementation of the Employment Equity Act No. 55 of 1998. Women were introduced into jobs which incorporated material handing tasks such as ammunition handlers. Unfortunately this was done without taking into consideration the inherent physical demands and requirements of the tasks associated with these jobs. These changes in the SANDF population resulted in obvious mismatches between the physical capability of the employee and the expected task requirements. As a result, biomechanical risk analysis has become a crucial step in task analysis during the description of job profiles.

Biomechanical risk analysis has to date been conducted for SANDF task analysis by means of generalised, ergonomics risk analysis tools such as the American National Institute of Occupational Safety and Health (NIOSH) (Waters *et al.,* 1996), Rapid Upper Limb Assessment (RULA) (McAtamney and Corlett, 1993) and the Ovaco Working Posture Analysis System (OWAS™) (Louhevaara and Suurnakki, 1992). At a later stage, analytical postural analysis in combination with ground force

reaction data were utilised to evaluate and predict biomechanical risk to the soldier (Load carriage programme (Mac Duff and Smit, 2002; Mac Duff and Smit, 2004[1]) and lower extremity programme (Mac Duff and Smit, 2004[2])). Finally, a database was compiled on the functional body strength of SANDF members for specific functions (such as pushing and pulling forces), by which capabilities and limitations for the SANDF population could be specified and used as reference for analysis of job demands (RSA-MIL-STD-127 Vol. 5, 2001; Mac Duff *et al.,* 2003; Mac Duff, 2004[2]). However, none of these techniques fulfilled the requirements for biomechanical risk prediction for the SANDF. In several instances it was found that the abovementioned international biomechanical risk analysis tools are overly conservative, provided impractical job limits and did not accurately predict biomechanical risk for the South African military population (Shaba and Slabbert, 2002). Other tools such as direct camera postural analysis is time intensive, costly and obtaining test subjects with whom to conduct the analysis became increasingly difficult. In addition, the functional body strength data, although providing actual guidelines for the SANDF population, does not contain data for all tasks and postures and can therefore not be used for all biomechanical analysis scenarios used in military task analysis.

Digital Human Modelling (DHM) has become increasingly popular as a biomechanics risk assessment tool (Wagner *et al.,* 2007; Cholewicki *et al.,* 1995; Marras *et al.,* 2003; Lavender *et al.,* 2000; Korkmaz *et al.,* 2006; Cooper and Ghassemieh, 2006; Daynard *et al.,* 2001). DHM provides the freedom to assess biomechanics risks of a range of postures/tasks for a range of male and female users. Of the first DHM biomechanics risk assessment tools include the University of Michigan 3D static strength prediction program (3DSSPP) and in-house developed software models that conducts lumbar spine compressive load assessments (Wagner *et al.,* 2007). One major drawback of the 3DSSPP is that it can only solve static biomechanical problems. For sagittal plane lifting, Dysart and Woldstad (1996) and McGill and Norman (1985) reported that dynamic analysis were significantly more accurate than the static or quasi-static equivalent in the prediction of external joint torques. The dynamic mode of analysis includes all the aspects of motion in the calculation of joint forces and internal stresses, including the effects introduced by changing velocity and acceleration components. The largest drawback of software models that relies on the assessment of lumbar spine

compressive loads, are that they rely on "universal" risk criteria. Factors such as physical conditioning (which plays an important role in a military population) are not taken into consideration.

The advancement in computer technology and data processing capability has allowed the improvement of modelling software packages to a point where dynamic problems can now be simulated and analysed in a digital environment (Zenk *et al.*, 2007; Kim and Martin, 2007; Wagner *et al.*, 2007). LifeMod™ (Biomechanics Research Group, 2005) is a plug-in developed in the dynamics analysis Computer Aided Design (CAD) software package, ADAMS (MSC.Software Corporation, 2005), and enables the modelling of a human body with biomechanical properties including bone segments, joints and muscles.

The aim of this study is to build a range of biomechanical models that are based on South African National Defence Force (SANDF) anthropometry and functional body strength data. These models are to be representative of 90 present of the male and female SANDF population in terms of anthropometry and functional body strength (ranging from small to large and from weak to strong). The modelling was executed using the dynamics biomechanical software package LifeMod™. The aim of these models is to be used in the assessment of specific military tasks, identified during job analysis as potential biomechanical risks to SANDF personnel members. The range of models enables the assessment of a range of tasks with varying biomechanical risk. Biomechanical risks could include from manual material handling or arm/leg force exertions in potentially awkward postures for large persons or in potentially out of reach areas for small persons. The biomechanical risk could also include manual material handling or arm/leg force exertion task requirements that fall outside the physical capability of the weaker SANDF personnel members. The biomechanical risk analysis that this range of biomechanical models would enable, provides the crucial step in the process to ensure that SANDF personnel members are not placed in jobs/posts which will expose them to biomechanical risk.

CHAPTER 2 : LITERATURE REVIEW

2.1 ANTHROPOMETRY ANALYSIS

The characterisation of body forms is of interest to a variety of disciplines, including: sport and health sciences, apparel design, and engineering and ergonomics. The approach in defining and evaluating body form differs within these disciplines, which is primarily due to the purpose of the application. The approaches of these disciplines used to characterise body form are discussed below.

2.1.1 Sport and health science body typing

Somatotyping and body mass index (BMI) are techniques widely used for characterising body types in sport science and health.

Somatotyping characterises any person into three physical classifications of the human body: endomorph, mesomorph and ectomorph. According to the Sheldon Somatotype (Fox *et al.,* 1993) the first component, endomorphy, is characterised by roundness and softness, or rather "fatness", of the body. Typical features of this component are predominance of the abdomen over the thorax, high square shoulders and a short neck. The second component, mesomorphy, is characterised by a square body with hard, rugged and prominent musculature. Outstanding characteristics of this type are forearm thickness and heavy wrists, hands and fingers. The thorax is large and the waist is relatively slender, shoulders are broad, the trunk is usually upright, and the trapezius and deltoid muscles are well developed. The third component, ectomorphy, includes as predominant characteristics linearity, fragility, and delicacy of body. This is the leanness component; the bones are small and the muscles thin. The shoulders are mostly narrow, lacking muscle relief and regularly drooping. There is no bulging of muscle at any point on the physique and the scapulae tend to wing out posteriorly.

Sheldon's method of somatotyping requires a photograph of the individual in three planes. From these pictures, a number of measurements are taken and, with the aid of tables developed by Sheldon, the somatotype is determined. The tables numbered 1 to 7 indicate the degree of each of the three components, with number

1 representing the least amount of the component and 7 the maximum amount. Therefore, a somatotype of 7-1-1 would indicate extreme endomorphy (fatness), 1-7-1 extreme mesomorphy (muscularity) and 1-1-7, extreme ectomorphy (thinness). The somatotyping of an individual would typically involve a combination of these three components. The typing is determined from visually inspecting the photographs of subjects, and also the Sheldon method represents a subjective method for evaluating body form. A more objective method than the Sheldon method is the Heath-Carter Anthropometric method. With the Heath-Carter method, ten anthropometric variables are measured and used to calculate the anthropometric somatotype: stature, body mass, four skinfolds (triceps, subscapular, supraspinale, and medial mid-calf), two bone widths (bi-epicondylar width for both the humerus and femur), and two limb girths (flexed upper arm girth and calf girth) (Carter, 2002; Fox *et al.*, 1993). Figure 1 illustrates the front and side views of the three body types.

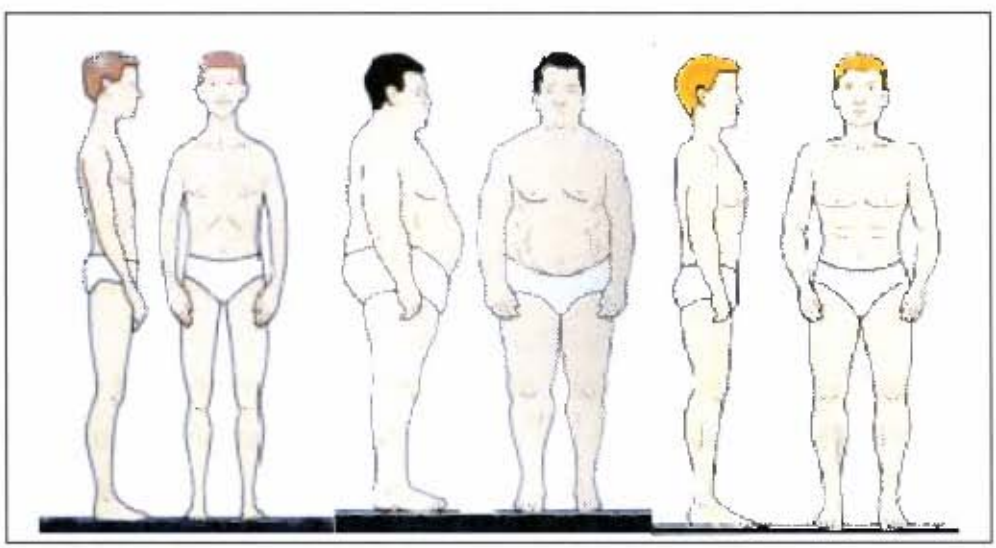

Figure 1 : Ectomorph, endomorph and mesomorph body types (in the tests Heath-Carter body types (2008))

The BMI is an easy and practical technique for estimating body composition (body fat) that is regularly used in sport science and health surveys (Fox *et al.,* 1993). BMI uses stature and body mass to classify body composition by means of the following equation :

$$BMI = \frac{stature^2}{mass}$$

Where : $stature$ = height of person (m)
$mass$ = mass of person (kg)

Typical classifications include:

- Underweight (BMI < 18.5)
- Normal (BMI : 18.5 – 24.9)
- Overweight (BMI > 24.9)

- Pre-obese (BMI : 25 – 29.9)
- Obese class I (BMI : 30 – 34.9)
- Obese class II (BMI : 35 – 39.9)
- Obese class III (BMI > 39.9)

When investigating body form, body composition might be one component, but is not successful in describing aspects such as how upper and lower body dimensions (circumferences) relates, or how limb length relate to body (trunk) length. Limitations to BMI are possible "overestimations" in body composition classifications due to high mesomorph components and/or differences in skeletal mass (typically in sporting population groups).

2.1.2 Apparel industry body typing

Although linear grading techniques which assume that humans have mathematically proportional bodies are still being used in the apparel industry (Simmons *et al.*, 2004), studies have indicated that population variation cannot be accommodated by linear grading rules for the size range (Gupta *et al.*, 2006, Simmons *et al.*, 2004). As

a result, some national sizing systems (such as the United Kingdom, Germany, Netherlands, Canada and America) do attempt to incorporate body form variation by including variables such as height, ratio value (difference between hip and bust circumference) and hip type (hip circumference) for females, and body length and ratio values (chest to waist circumference) for males (Fan *et al.*, 2004). The American sizing systems commonly use the figure types called junior petite, junior, miss petite, miss, half-size, and woman. These figure types vary from each other with regard to body length (back length for upper body garments and inside leg length for lower body garments) and body circumference (bust, waist and hip for upper body garments, and waist and hip for lower body garments). Gaetan (1989) identified body shapes for the Italian population that incorporated the relationship between stature and chest circumference for men, and stature and hip circumference for females. He called the different body shapes slim, athletic, regular, robust, corpulent and extra corpulent for males, and slim, harmonious, regular, robust, and corpulent for females.

Several different body shapes have furthermore traditionally been identified in the apparel industry, especially for females. Examples of these are the pear, barrel and box shapes for plus sizes (Zangrillo, 1990); inverted triangle, diamond, rectangle, oval, triangle and hourglass (Rasband, 1994) as illustrated in Figure 2, or hourglass, bottom hourglass, top hourglass, spoon, rectangle, diamond, oval, triangle and inverted triangle (Simmons *et al.*, 2004). The identification of these body forms are however not customarily done in an objective, or rather mathematical manner and requires a large amount of experience or a "seeing eye", as referred to by Douty (1954), to do correctly.

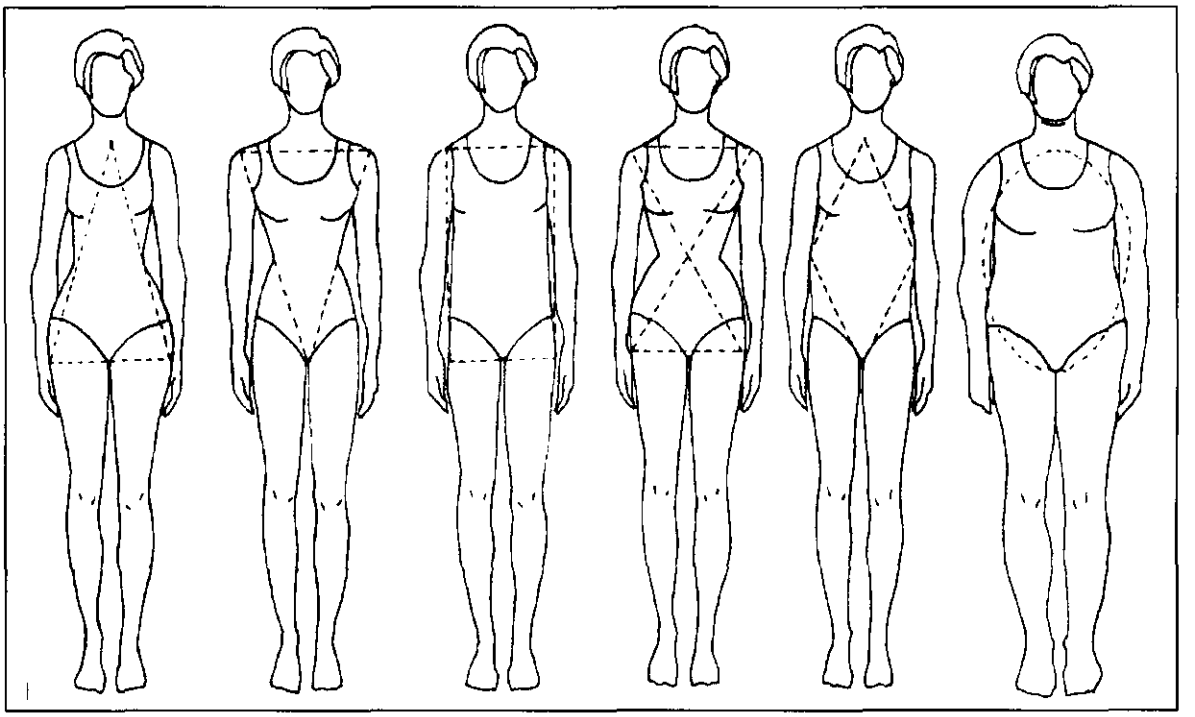

Figure 2 : Body types: Triangle, Inverted triangle, Square, Hourglass, Diamond and Oval (Rasband, 1994)

Techniques typically used in the apparel industry to identify these body forms include subjective visualization by clothing fit experts, self-analysis/identification, outlining a figure on a grid paper or, probably the most "objective", analysing a photo (taken against a grid background) (Douty, 1954). An exception to this subjective form of identification is a software program, called FFIT© (Female Figure Identification Technique) for Apparel, that was developed by Karla Simmons (2004). The software program compares body measurements of a person to a mathematical model of the body forms and so determines a person's body form.

Ms Daisy Veitch of Australia is one of few in the apparel industry who has applied a multivariate statistical analysis technique, principal component analysis (PCA). Veitch *et al.* (2007) reported using hip circumference, waist circumference, bust circumference, C7-waist length (posterior and anterior), C7-nipple length, bust width, back width, waist tilt, sleeve length, C7-wrist length and waist height to identify body forms characteristic for a specific demographic of the Australian

population for the apparel industry. These results have been applied in the production of realistic clothing fit manikins.

2.1.3 Engineering and ergonomics body form analyses

The techniques most commonly used to characterise body form in engineering and ergonomics design, are multivariate statistical analysis techniques. Of the multivariable statistical analysis techniques available, PCA and cluster analysis are the two most widely used (Ben Azous *et al.,* 2005; Paquet, 2004; Whitestone and Robinette, 1994; Hudson *et al.,* 1998; Smit, 2003; Kim and Whang, 1997; Mochimaru and Kouchi, 2007; Bataller *et al.,* 2001; Gordon and Brantley, 1997; Godil, 2007; Alemany *et al.,* 2006; Robinette and Whitestone, 1992; Bredenkamp and Skelton, 2009).

The majority of these studies mentioned above made use of linear measurement data collected by means of traditional anthropometric measurement techniques or extracted from landmarks identified on three dimensional (3D) point cloud data as input to the multivariate analysis techniques. However, some of the later studies made use of two or three dimensional (2D or 3D) form data as input to the multivariate analysis techniques (Mochimaru and Kouchi, 2007; Alemany *et al.,* 2006; Hennessy *et al.,* 2005; Ben Azouz *et al.,* 2005; Godil, 2007; Bredenkamp and Skelton, 2009).

In order to facilitate the multivariate statistical analysis such as PCA on 2D or 3D form data, some organisations have been developing software packages in-house. This software firstly enables complex calculations, such as is required when analysing 2D and 3D form data. Secondly, the software makes it possible for the user to view the dimensional association of each principal component (PC) which in turn assists in a better understanding of the form characteristics represented by each PC. Examples of such software package includes Cleopatra, developed by the National Research Council of Canada (from the text 3D Imaging, modelling and visualisation (2007)), MAM, developed by the Air Force Research Laboratory in USA (G.F. Zehner and J. Hudson, personal communication, June 14, 2007), and Body Shape Browser, developed by Ergovision in Japan (Mochimaru and Kouchi, 2007).

Coblentz *et al.* (1991) also utilised multiple anthropometric variables. However, instead of relying on PCA to identify PCs that indicate the largest variance, or clustering techniques to identify groups (clusters) of people with similar relationships between anthropometric variables (body form), they selected fewer variables and identified variances in form as different combinations of these variables and variable ranges. Smit (2001; 2003) used a similar approach in characterising facial and head form variations for the SANDF population.

The variables that are used during the multivariate statistical analysis should be selected according to the application of the anthropometric data (Hudson *et al.*, 1998). Hudson *et al.* (1998) used sitting height, sitting eye height, thumb tip reach, sitting acromion height, buttock to knee length and sitting knee height in order to identify body shapes and sizes representative of the air force population for cockpit design. Godil (2007) used upper leg length, lower leg length, foot length, hip width, upper arm length, lower arm length, shoulder width, head width and head length in an attempt to describe body shape variation. Mollard (2007) and Bataller *et al.* (2001) used all the variables that they had (38 and 23 respectively) during the multivariate statistical analysis to identify body and foot form. The inference of the different approaches is that expertise is still inherent in the decision regarding which of the variables to include in the analysis and that it should be in accordance with the intended application.

2.2 INVESTIGATING CORRELATION BETWEEN ANTHROPOMETRY AND FUNCTIONAL BODY STRENGTH VARIABLES

In a study conducted by Pompeu *et al.* (2004), a reasonably strong correlation (R^2=0.66) was found between arm transverse muscle area and a maximal load lifted once. A much weaker correlation (R^2=0.36) was observed between the arm total cross-section and maximal load lifted. The arm transverse muscle area was calculated by subtracting a triceps skinfold factor from the measured arm circumference before calculating the area. The arm total cross-section was calculated from only the arm circumference. These calculations are demonstrated in the equations below.

$$A_{TB} = C^2 \div (4 \times \pi)$$

Where : A_{TB} = arm total cross-section (cm^2)
C = arm circumference (cm)

$$A_{MB} = \left[C - (T \times \pi)\right]^2 \div (4 \times \pi)$$

Where : A_{MB} = arm transversal muscular area (cm^2)
C = arm circumference (cm)
T = triceps skinfold (cm)

Hornby *et al.* (2005) on the other hand found a medium correlation between left and right hand grip strength and mid-arm muscle circumference as well as mid-arm circumference for males. They found no medium or higher correlation between grip strength and mass, height, mid-arm muscle or mid-arm circumference for females.

Xiao *et al.* (2005) investigated the correlation between isometric strength measurements and anthropometry variables. The anthropometry variables included mostly length components (stature, acromial height, iliac height, knuckle height, knee height) and some mass and depth components (mass, BMI, chest depth and abdominal depth). The isometric strength measurements included right and left hand grip, arm and shoulder lift, and torso pull. Medium correlations were observed for females between mass, BMI and abdominal depth and arm lift and shoulder lift, as well as chest depth and arm lift (r^2 ranging between 0.31 and 0.53). No medium or higher correlations were observed for males between anthropometry and strength variables.

Meyer *et al.* (1996) investigated the correlation between isokinetic strength measurements and anthropometric variables. The anthropometric variables included mostly length components (stature, thumb-tip reach, sitting height, sitting eye height, sitting acromial height, buttock-knee length, sitting knee height and functional leg length) and a few depth, width and circumference measurements (mass, bi-deltoid breadth, abdominal extension depth, sitting hip breadth, thigh clearance and thigh circumference). Strength measures included peak torque, torque acceleration energy, total work and average power at knee, shoulder and

elbow for males and knee and shoulder for females. Medium positive correlations were observed for males between mass and peak torque for knee and elbow flexion (r^2=0.3 for each). For females, several medium positive correlations were observed. Positive correlations were observed between peak torque knee extension and mass, stature, buttock-knee length, knee height and leg length (r^2 ranging between 0.3 and 0.48); for peak torque knee flexion and mass (r^2=0.31); total work for knee extension and mass, height, buttock-knee length and leg length (r^2 ranging 0.3 and 0.37); as well as average power for knee extension and mass (r^2=0.38).

Maeda *et al.* (2001) investigated the relationship between muscle strength and length and width of the head of the long bones for females. The anthropometry (bone length and width) parameters included distance between styloid process of ulna and radius (DUR), distance between medial and lateral humeral epicondyles (DMLH), distance between medial and lateral femoral epicondyles (DMLF), width of patella (WP), distance between medial and lateral maleoli (DTF), radius length, spina malleolar distance and stature. The muscle strength variables included left hand grip strength and isometric left knee extension muscle strength (force and torque). The study indicated a medium correlation between grip strength and DUR, DMLH, spinal malleolar distance and stature (r^2 ranging from 0.36 to 0.55). A strong correlation was found between grip strength and DTF (r^2=0.6). A medium correlation was found between knee joint extension force and DMLF (r^2=0.5), and between knee joint extension torque and DMLF, WP, DTF and spina malleolar distance (r^2 between 0.3 and 0.4).

In a study conducted by Sinaki *et al.* (2001), anthropometric variables (stature and mass) were compared to body strength variables (right and left hand grip, left and right knee extensor strength and back extensor strength) for males and females. A medium correlation was observed between stature and left and right hand grip and back extensor strength for males, and stature and left and right grip strength for females.

Several researchers investigated the relationship between anthropometry and functional (often sport specific) performance (Sekulic *et al.*, 2005; Geladas *et al.*, 2005; and Van den Tillaar and Ettema, 2004). Sekulic *et al.* (2005) found no medium or high correlation between stature, mass or BMI and push-ups, sit-ups,

high jumps, 1500m run or 50m freestyle swimming for males. Geladas *et al.* (2005) found a medium correlation between 100m freestyle swimming and stature, mass, upper extremity length, hand length, chest circumference, biacromial breadth and horizontal jump for boys aged 12 to 14 years. No medium or higher correlation was found between 100m freestyle swimming and any of the anthropometric variables for girls aged 12 to 14 years. Van den Tillaar and Ettema (2004) observed a medium to strong correlation between over arm throwing velocity and fat-free mass, mass and stature for males and females. They also observed a medium correlation between horizontal maximal isometric arm strength at shoulder height and fat-free mass as well as mass for males and females.

The topic of correlation between anthropometric and functional strength variables remains a controversial one. Several studies have published contradictory results. Although correlations between anthropometric and functional strength variables are regularly found, no such correlations are consistently found between studies. Transversal muscular area (calculated either from circumference measures or circumference – skinfold measures), stature and mass are among the anthropometric variables most widely found to be correlated with functional strength variables (Xiao et al, 2005; Meyer et al, 1996; Geladas et al, 2005; Van den Tillaar and Ettema, 2004).

2.3 BIOMECHANICS RISK ANALYSIS

One of the primary application areas of biomechanics analysis is injury prevention (Knudson, 2007). When looking at injury prevention, several approaches are used in quantitative and qualitative analyses. Three of these approaches include :

- Assessment of joint loads
- Assessment of muscle forces
- Assessment of functional strength limits.

2.3.1 Assessment of joint loads

In order to assess the risk of injury due to specific tasks, the assessment of joint loads is often used as risk criteria. This risk analysis could include assessment of risks of joints related to specific isolated movements (such as the knee joint during a leg push function) or for whole body tasks. During the assessment of whole body tasks, the spinal joint loads are most commonly assessed. During the assessment

of spinal loads, two aspects are evaluated: 1) Spinal compression and 2) lateral as well as anterior/posterior sheer loading. The most widely used limits for spinal compression are those published by NIOSH (American National Institute of Occupational Safety and Health) (Waters *et al.,* 1994) specifically for the lumbosacral disc compression, which includes an action limit (AL) of 3433N and maximum permissible limit (MPL) of 6376N (Cooper and Ghassemieh, 2007). The most widely used limits for anterior/posterior shear are values published during studies conducted by McGill and colleagues and are between 500 – 1000 N (McGill *et al.*, 1998; McGill, 1996) (Korkmaz *et al.*, 2006; Daynard *et al.*, 2001; Marras *et al.*, 2009).

One of the most frequently used generalized lifting limits has been compiled by NIOSH and is based on the spinal loading limits (Waters *et al.,* 1994).

2.3.2 Assessment of muscle forces

The assessment of muscle forces is most often used during the comparison of postures or tasks to identify postures causing the least amount of muscle strain (Cholewicki *et al.*, 1995; Laursen *et al.*, 1998; Pel *et al.*, 2008; Amarantini *et al.*, 2010; Rohlmann *et al.*, 2006).

2.3.3 Assessment of functional strength limits

Functional body strength limits that are unique to specific populations are commonly measured and used during biomechanical risk assessment of specific tasks. The functional body strength limits are either used directly in manual materials handling tables (Snook, 1978; Snook and Ciriello, 1991; RSA-MIL-STD-127 (Vol. 5), 2001), incorporated in a set of mathematical models (Shoaf *et al.,* 1997) or in strength based generalized lifting limits (Louhevaara and Suurnakki, 1992; McAtamney and Corlett, 1993; Chaffin, 1997). Examples of such generalized mass lifting limits include OWAS™ (Ovaco Working Posture Analysis System) (Louhevaara and Suurnakki, 1992), RULA (McAtamney and Corlett, 1993), and 3DSSPP (3D Static Strength Prediction Program) developed by the University of Michigan (Chaffin, 1997).

One of the techniques used to determine the maximum acceptable mass of lift (MAWL) is by means of operator perceived exertions. Although this technique provides magnitudes of loads that are unique to the population under investigation, some researchers do not agree that this technique truly represent the biomechanical limit of the human lifting ability. Thompson and Chaffin (1993) reported that there was no correlation between perceived exertion and compressive force on the lumbosacral joint. Jorgensen *et al.* (1999) and Davis *et al.* (2000) found that spinal loads (i.e. compression and shear forces) were not associated with changing the mass toward the MAWL during the psychophysical decision process. Individuals adjusted the mass based on cues other than loading on the spine and thus psychophysically determined limits may not be protective of discogenic injuries. Rather, perceived MAWLs may be an indication of muscle force sensation and fatigue and/or cardiovascular exertion (Davis *et al.*, 2000). Muscle force sensation and fatigue are typically measured with electromyography (EMG) and cardiovascular exertion by means of measuring heart rate (Davis *et al.*, 2000), oxygen consumption or metabolic rate (Robertson, 1982).

Another technique commonly used to measure maximum lifting limits or force exertions is to measure peak isometric and isokinetic exertions (Kumar, 1996; MacDuff, 2001).

2.3.4 Modelling in biomechanics risk analysis

The majority of modelling tools can be divided into three analysis modes: static, quasi-static and dynamic. The static analysis assesses a single posture assumed to be associated with the greatest injury risk of tissue stress during the task. The quasi-static analysis applies a static analysis at multiple time steps of a motion. Inertial effects are neglected, effectively setting the velocity and acceleration components of the body during each frame to zero. The dynamic mode of analysis includes all the aspects of motion in the calculation of joint forces and internal stresses, including the effects introduced by changing velocity and acceleration components.

An example of static modelling includes EMG-assisted biomechanical models used to predict muscle forces and spinal loading (Granata and Marras, 1993 and 1995; Marras and Granata 1995 used by Korkmaz *et al.*, 2006, Marras *et al.*, 2009; Davis

et al., 2000). 3DSSPP is another example of a static biomechanical model (Dolan and Adams, 1993; Hughes *et al.*, 1994). Several finite element models have also been used to solve biomechanical risk problems in a static environment (Dietrich *et al.*, 1991; Rohlmann *et al., 2006*). Wilke *et al.* (2003) and Calisse *et al.* (1999) utilized direct *in vivo* measurement of loads of internal fixators and of intradiscal pressure in experimental and finite element model studies. Arjamand and Shirazi-Adl (2006) developed a kinematics-based non-linear FEM of the spine to analyse static muscle and internal loads by means of optimization.

Examples of quasi-static biomechanical computer models are the lumbar spine biomechanical models developed by Norman *et al. (*1998) as well as by Gardner-*Morse et al.(*1995) (Gardner-Morse and Stokes, 1998; Stokes and Gardner-Morse, 1995, 2001).

With the advances of computer technology over the past couple of years, dynamics modelling has become much more prevalent. Two examples of commercially available dynamic biomechanical whole-body modelling software include the Anybody Modelling System (Anybody Technology A/S, 2008) and LifeMod™ (Biomechanics Research Group, 2005). Other examples of dynamic modelling are an EMG-driven Hill-type model developed in open-access version of SIMM, OpenSim (Delp *et al.*, 2007; de Oliveira and Menegaldo, 2010) and a Hill-type whole body model using motion and force plate data as input in SIMM (Delp *et al.*, 1990) referenced by Goldberg and Kepple (2009). Several researchers also utilized EMG-assisted and optimization models (Cholewicki and McGill, 1994; Gagnon *et al.*, 2001; Amarantini *et al.*, 2010). Lu *et al.* (2010) developed a visco-hyperelastic model for skeletal muscle tissue under high strain rates.

2.4 MECHANICAL PROPERTIES OF MUSCLES

Soft connective tissue in the human body such as muscles, tendons and ligaments are structurally complex with complex mechanical behaviour in response to loading. The mechanical behaviour of the muscle-tendon unit (MTU) under passive tension is discussed in brief below :

1. Biological tissues are *anisotropic*, which means that their strength properties are different for each major direction of loading,

2. When compared to a typical load-deformation graph of elastic material, most soft connective tissue has an additional region referred to as the *"toe region"*. The "toe region" is indicated in Figure 3 and corresponds to the straightening of the wavy collagen fibres (Carlsteds and Nordin, 1989),
3. Biological tissues are *viscoelastic*, which means that the stress and strain in the tissues are dependent on the rate of loading, so the timing of the force application affects the strain response of the material. The implications of this are :
    a. The slope of the elastic region will vary depending on the *rate of stretch*. This is illustrated in Figure 4 where a faster rate of stretch results in a higher stiffness and a slower rate of stretch results in a lower stiffness,
    b. *Creep*, thus the gradual elongation (increased strain) of a material over time under constant stress, occurs,
    c. *Stress relaxation*, where reduced stress over time when elongated to a set length, occurs,
    d. *Hysteresis*, where different response to loading and unloading and therefore energy is lost, occurs.
4. The nature of protein fibres as well as the amount of calcification determines the mechanical response to loading; thus the mechanical response will be *variable between individuals* and a universal mechanical response applicable to all individuals does not exist.

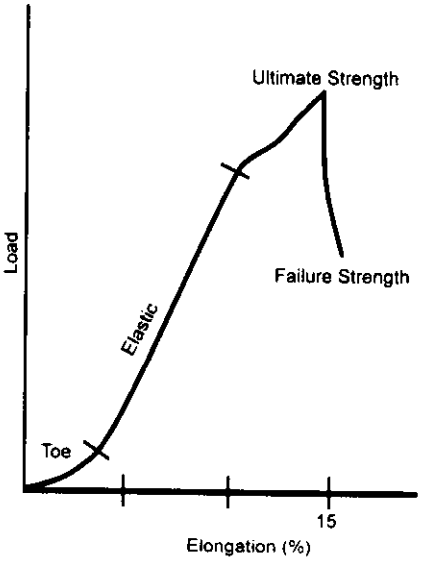

Figure 3 : The typical load-deformation (elongation) curve for the human tendon (Knudson, 2007)

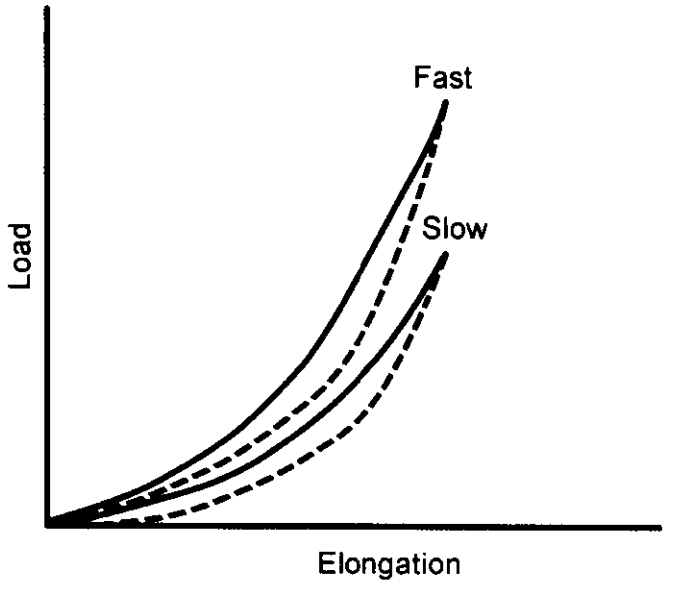

Figure 4 : Load-deformation curves for tendon stretched at a fast and a slow rate to the same length (Knudson, 2007)

In addition to the factors listed above, mechanical properties measured on muscle tissue are affected by factors such as training, age and disease of the individual. Methodological factors such as how the human tissue was stored, attached to the machine or preconditioned (warm-up before testing) also affect the measured mechanical properties. In light of these factors, the identification of a generalised maximum specific tension or ultimate strength (σ) for muscle tissue (see Figure 3) is not a trivial task and as a result, the values reported in the literature are very variable. Wickiewicz *et al.* (1983) reported σ to be 73 N/cm^2, Brand *et al.* (1986) and Friederich and Brand (1990) reported 30 N/cm^2, Bodine *et al.*, 1987 reported σ for muscle tissue to be between 17.2 and 23.5 N/cm^2 and Powel *et al.* (1984) 22.5 N/cm^2. Sverdlova and Witzel (2010) used an σ value of 50 N/cm^2, McGill and Norman (1986) 35 N/cm^2, and Amarantini *et al.* (2010) 40 N/cm^2 during their modelling of muscle forces. Tendons have parallel arrangement of collagen fibres and cross-links between fibres, and this makes tendons approximately 3 times stronger in tension than muscles. The ultimate strength of tendons is approximately 100 N/cm^2.

In addition to the mechanical properties discussed above for MTU under passive loading, the force potential of a MTU varies during active loading together with

passive muscle conditions and can be described by the following three mechanical characteristics:

1. Force-Velocity Relationship

The force generated by a fully activated muscle varies with velocity. This relationship is illustrated in Figure 5. During concentric muscle action (shortening) the force potential of a muscle decreases with the speed of movement. During eccentric muscle action (lengthening) the muscle force potential increases with the increase in speed of motion. Isometric muscle force, that is the maximum muscle force without motion, is also illustrated on this figure.

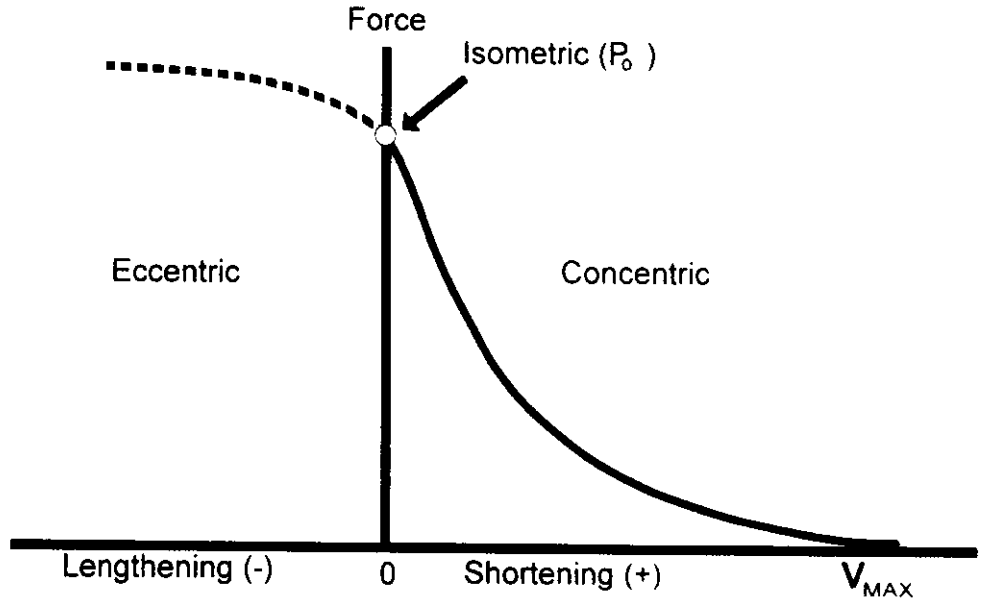

Figure 5 : The Force-Velocity Relationship of muscle (Knudson, 2007)

2. Force-Length Relationship

The Force-Length Relationship documents how muscle tension varies at different muscle lengths. This is illustrated in Figure 6. The active component of the Force-Length Relationship has a logical association with the potential numbers of the cross-bridges between the actin and myosin filaments in the sliding filament theory. The peak muscle force is generated when there are the most cross bridges, at the resting length (L_o in Figure 6). This is usually related to a point near the middle of the range of motion. The potential active muscle tension decreases for shorter or longer muscle lengths because fewer cross-bridges are available for binding.

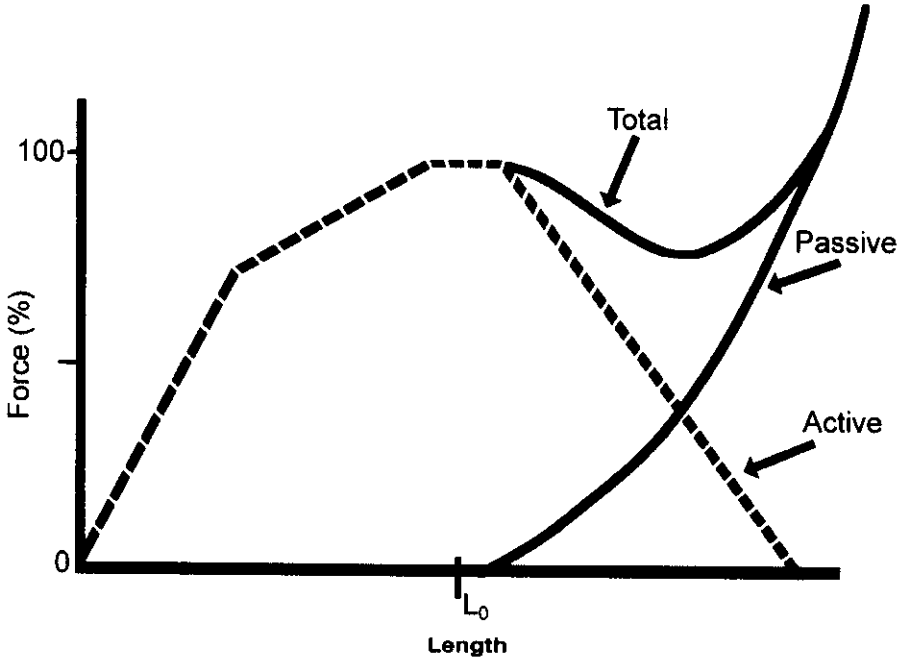

Figure 6 : The Force-Length Relationship of human skeletal muscle (Knudson, 2007)

3. Force-Time Relationship

The Force-Time Relationship refers to the delay in the development of muscle tension of the whole MTU and is equal to the time from motor action potential to the rise or peak in muscle tension.

In addition to this Force-Time Relationship, muscles are comprised out of two types of muscle fibres : Type I which is referred to as the slow twitch or Slow Oxidative (SO) and Type II which is referred to the fast twitch or Fast Glycolytic (FG) muscle fibres. These two types of muscle fibres have a varying response rate and reach the maximum muscle force over varying time rates. This is illustrated in Figure 7. The human muscles are a mix of fibres, where certain sets of muscles have higher percentages of certain fibres (i.e. the antigravity muscles (Soleus, Erector spinae and Abdominalis) have a higher percentage of SO), and the percentages of muscle fibres varies between individuals.

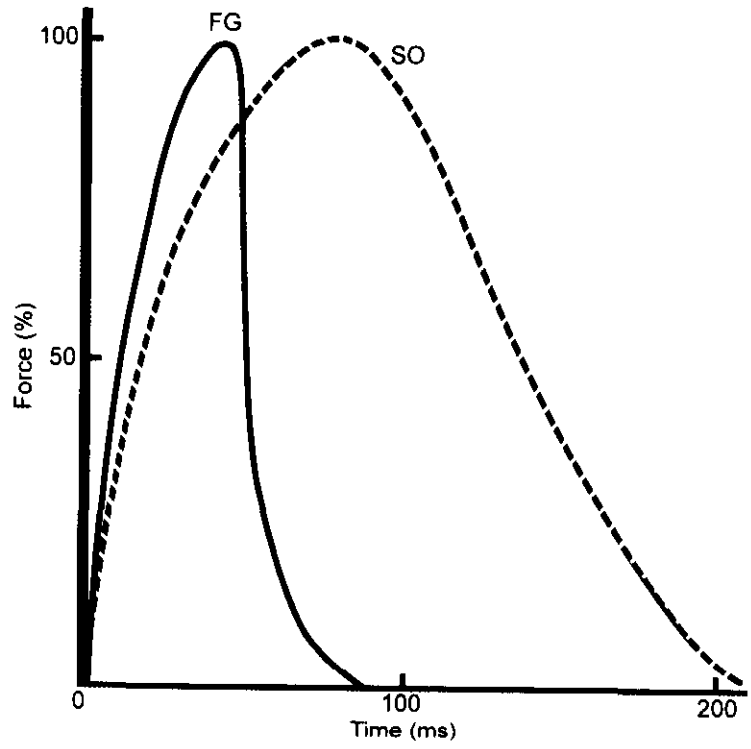

Figure 7 : The twitch response of fast-twitch (FG) and slow-twitch (SO) muscle fibres (Knudson, 2007)

CHAPTER 3 : METHODOLOGY

3.1 OVERVIEW OF PROJECT

An overview of the stages and integration of individual aspects used to develop the biomechanical models that represent members of the SANDF is illustrated in Figure 8. This overview will be followed by the detailed methodology of how the separate analyses were conducted. Section 3.2 describes the analysis method used for the identification of body forms that are characteristic to the SANDF males and females. Section 3.3 describes the method used to investigate the relationship between anthropometry and functional body strength in the attempt to combine these to represent the members of the SANDF. Finally Section 3.4 describes the method used in creating biomechanical models that will represent members of the SANDF.

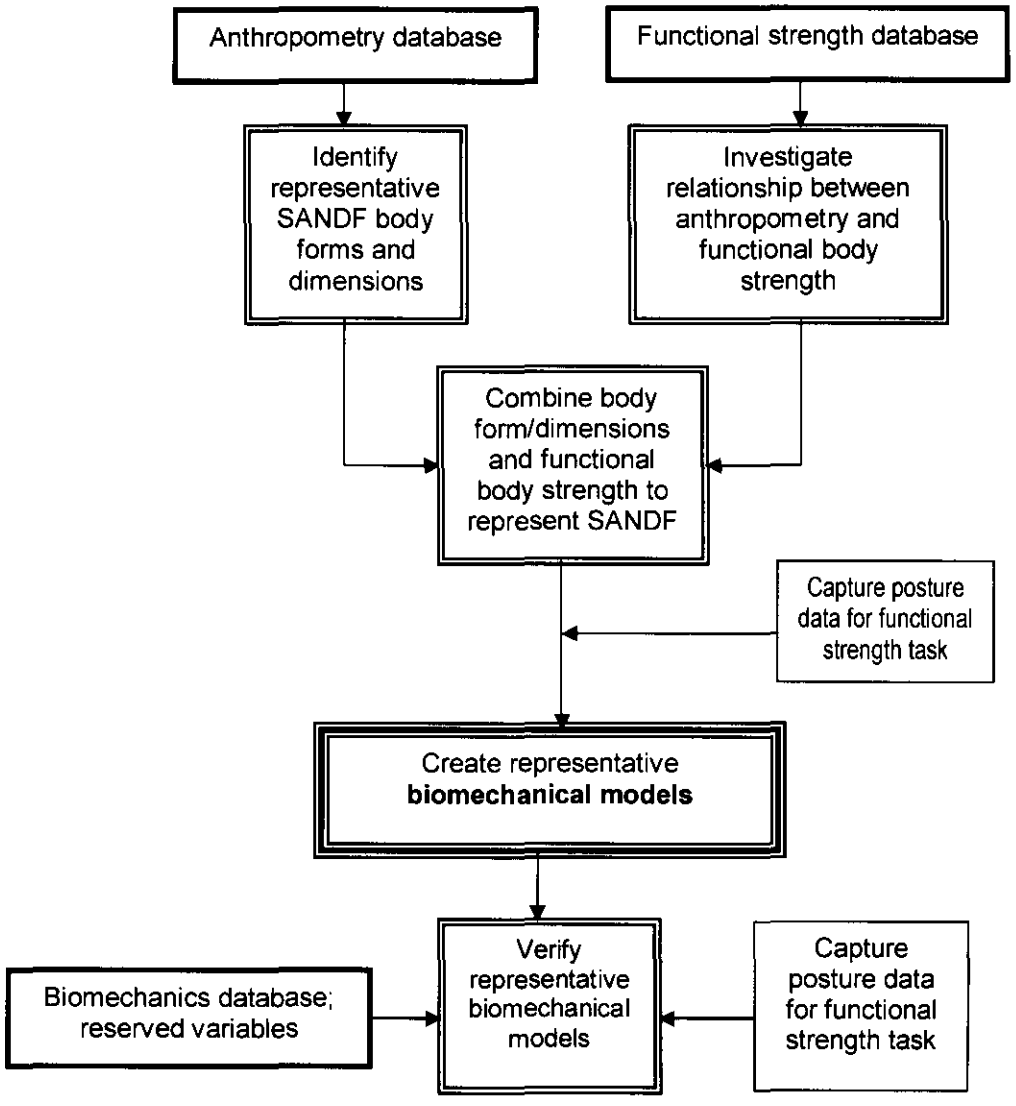

Figure 8 : Integration of individual aspects of modelling process

3.2 ANTHROPOMETRY ANALYSIS

The body form analysis for the South African National Defence Force (SANDF) males and females included in this study integrated investigation of Body Mass Index (BMI) distribution, correlations between anthropometric variables and Principal Component Analysis (PCA). The variables that were included in the analyses were selected for the application of creating whole body models in a predictive biomechanical modelling software package.

The anthropometric data used during this study was obtained from the SANDF anthropometric database which has been populated between 2000 and 2007 (Slabbert, 2001[1]; Slabbert, 2001[2]; Slabbert, 2002[1]; Slabbert, 2002[2]; Slabbert, 2003; Mac Duff, 2004[1]; Van Schalkwyk, 2004; Shaba, 2005[1]; Shaba, 2005[2]; Shaba, 2006[1]; Shaba, 2006[2]; Shaba, 2007). The data for males and females were analysed separately and for each gender was stratified according to current representation of ethnic groupings (African Black, White, Coloured and Asian) in the SANDF as presented in the Department of Defence Annual Report FY 2006-2007 (2007). The definitions of anthropometric variables are given in the RSA-MIL-STD -127 Volume 1 (2004).

The percentages of males and females that could be classified into typical body composition classifications (that are underweight, normal mass and different levels of obesity) based on BMIs were determined. This provided an understanding of the distribution of the SANDF population with regards to body composition.

Linear correlations between body variables were furthermore investigated by means of Pearson's correlation test. Strong correlations were marked for $r^2 \geq 0.6$ (thus $r > 0.77$).

In order to investigate body form as the relationship between multiple variables, PCA was used. The analysis was based on correlations and not covariances, thus standardizing data to ensure that the size of the variable did not influence the size of its contribution to the PC. The variances were computed with the formula $\frac{SS}{(N-1)}$ (where SS = sum of squares and N = valid number of cases) since variances are estimated for the population and not for the sample only. PCA identifies principal

components (PCs) characterized by a collection of body anthropometric variables which describes the largest variances in the sample data. A PC can therefore be described as a body form variable, such as segment length or circumference in relation to the overall body height variable. By identifying PCs, the form variances that are characteristic of the sample data can be identified. The number of PCs is determined by the percentage of variance in the sample data that it represents.

The following variables were included in the PCA to characterise body forms focusing mainly on trunk shape and length proportions (specifically between upper limb, lower limb, trunk and stature):

1. Stature
2. BMI
3. Cormic index (sitting height divided by stature)
4. Upper limb index (outside arm length divided by stature)
5. Lower limb index (trochanterion height divided by stature)
6. Chest to waist ratio
7. Waist to hip ratio
8. Waist circumference
9. Hip circumference
10. Chest circumference
11. Inside arm length
12. Inside leg length
13. Trunk length (7^{th} cervical height – inside leg length)

For males, abdominal and buttock depth were included in addition.

No consistent set of anthropometric variables have been identified in the literature for the identification of body form variances. The anthropometric variables selected in other research studies are based on the specific application and body variances that would be applicable to the research study in question (see Section 2.1). As a result, the anthropometric variables included in the PCA in this thesis were selected based on the body form variances that these variables would describe and how they would impact the application of the biomechanical models. Stature provided an indication of the overall height variances while inside arm length, inside leg length

and trunk length provided an indication of how the arm, leg and body lengths of individuals vary. In addition to these anthropometric variables, the cormic index, upper limb index and lower limb index provided additional body form variances with regards to how the segment lengths vary in relation to an individual's overall body height. The variances in overall height and segment lengths play an important role when assessing postures during task analysis. BMI, body circumferences (waist, hip and chest) and body depths (abdominal and buttock for men) provided an indication of mass and body size in relation to overall stature. In addition to body circumferences and depths, chest to waist as well as waist to hip ration's provided an indication of how the trunk shape varies. Body mass and trunk shape in combination with stature and segment lengths are related to functional strength and therefore variances in these anthropometric variables would be accommodated in variances in the functional strengths of SANDF personnel members (see Section 2.2).

In order to facilitate a better understanding of the variables included in the PCA, the definitions of these body measurements are presented in Table 1 below.

Table 1 : Anthropometric (body measurement) definitions for body measurements used in the principal component analysis

Anthropometric measurement name [unit]	Measurement definition
B1: Stature (erect) [mm]	The vertical distance from a standing surface to the top of the head. The subject stands erect with the head in the Frankfort plane. The heels are together with the mass distributed equally on both feet. The shoulders and upper extremities are relaxed.
B3 : Inside arm length [mm]	Distance between the mid axilla fold to the distal end of the stylion landmark at the wrist. Subject stands erect with the arms rested against the body. Can be calculated from: Axilla height – wrist height
B4 : Buttock depth [mm]	The distance between the anterior and posterior maximum buttock point. The subject stands erect and is measured from the side
B5 : Crotch height [mm]	The vertical distance between the standing surface and the crotch. The subject stands erect looking straight ahead. The heels are together and the mass is distributed equally on both feet
I1 : Body mass index [kg/m^2]	Body mass index represents the proportion between the mass (in kg) and the stature (in m), using the following formula: B.M.I = mass ÷ stature^2

Anthropometric measurement name [unit]	Measurement definition
I2 : Cormic Index [%] (relationship trunk/stature)	Proportion between the trunk and the stature, using the following formula: 100 x sitting height ÷ stature
I3 : Upper limb index [%] (relationship upper limb/stature)	Proportion between the arm length and the stature, using the following formula: 100 x arm length ÷ stature
I4 : Lower limb index [%] (relationship lower limb/stature)	The lower limb index represents the proportion between the lower limb and the stature, using the following formula: 100 x trochanterion height ÷ stature
I5 : Chest waist ratio index [none]	The ratio between the chest circumference and the waist circumference at the level of the natural indentation, can be calculated as follows: chest circumference ÷ waist circumference (natural indentation)
I6 : Waist hip ratio index [none]	The ratio between the waist circumference at the level of the natural indentation and the maximum hip circumference, can be calculated as follows: Waist circumference (natural indentation) ÷ maximum hip circumference
Bs18 : Abdominal depth [mm]	Horizontal distance between the anterior point of the abdomen and the back at the same level of the omphalion. The subject sits erect and symmetrically
C1 : Chest circumference [mm]	Maximum horizontal circumference at fullest part of breast measured at maximum quiet respiration. The subject stands erect, with the arms raised slightly out from the body
C2 : Waist circumference (natural indentation.) [mm]	The circumference of the waist at level of natural indentation
C3 : Hip circumference (maximum) [mm]	The circumference of the hip at the point where the hips are the widest
C4 : Trunk length [mm]	Linear distance calculated by subtracting B41 crotch height from B3 cervical height

The statistical analyses were completed using the STATISTICA© software package (Statsoft, 2008).

3.3 INVESTIGATING CORRELATION BETWEEN ANTHROPOMETRY AND FUNCTIONAL BODY STRENGTH VARIABLES

The linear correlations were investigated by means of the Pearson's correlation test between anthropometry and functional body strength data from the SANDF biomechanics database. Correlations were taken to be statistically significant with a p-value of less than 0.05. Medium correlations were marked at $r^2 \geq 0.3$ and $r^2 \leq 0.6$ (r value between 0.55-0.775) and strong correlations for $r^2 \geq 0.6$ (thus $r > 0.775$).

Functional body strength data were collected during the years 2001, 2002 and 2003 (Mac Duff, 2001; Mac Duff *et al.*, 2003; Mac Duff, 2004[2]). The datasets contained different anthropometry and functional body strength variables and therefore correlations between variations of combinations of variables could not be conducted. The variables for which correlations were investigated per dataset are indicated in Appendix B.

The statistical analyses were completed using the STATISTICA© software package (Statsoft, 2008).

3.4 REPRESENTATIVE FULL BODY BIOMECHANICAL MODELS

3.4.1 LifeMod™ model

The LifeMod™ biomechanics modelling software (Biomechanics Research group, 2008) was used to develop a full body human model. The model included standard LifeMod™ bone segments, joints and muscle elements. The full-body muscle set included 118 muscles (see Appendix C) which are created automatically and attached (origin and insertion points) to bone elements at pre-defined anatomical landmarks. Eight biomechanics full body models, four male and four female, were created. A summary of the eight models are indicated in Table 2. A human model was created by using the Gebod anthropometry database (default database used in the software) with the following settings: Full body, hands grip, units = mm, kg, N. The stature and body mass characteristics of each model were similar to the anthropometric cases identified and described in Section 3.2 as well as Section 3.4.2.1 that follows. The model was created to be symmetrical, with right and left anthropometric dimensions of equal value. The bone elements, muscle elements and muscle attachments were scaled automatically according to the skeletal geometry when the body segments were created.

Table 2 : Description of the eight biomechanical models

Model number	Gender	Anthropometric variance (see Sections 3.2 and 3.4.2.1)		Biomechanical model name
		Principal component	Boundary case	
1	Male	1	Small	MPC1-
2			Large	MPC1+
3		2	Small	MPC2-
4			Large	MPC2+
5	Female	1	Small	FPC1-
6			Large	FPC1+
7		2	Small	FPC2-
8			Large	FPC2+

3.4.2 Input data to model

3.4.2.1 Anthropometric data

The process to characterize the body forms of SANDF males and females described in Section 3.2 was applied. Body form variances described by two PCs for the SANDF males and two PCs for SANDF females were included in the modelling process. The number of PCs was selected based on the percentage form variance described by these PCs, impact of the form variances described by these PCs on functional strength variances, as well as the practicality of the number of biomechanical models. In order to derive anthropometric dimensions (design limits) from the body form variances (PCs) identified, a technique described by Gordon and Brantley (1997), regularly used in designing for anthropometric variances in a population (Kim and Whang, 1997; Veitch *et al.*, 2007; Wirsching and Premkumar, 2007; Mochimaru and Kouchi, 2007), was used. All the cases (SANDF persons included in the anthropometric database/sample population) were plotted on the PC space (see Figure 9). These plots indicated the relationship of the cases to each PC, and distribution of cases in the PC space. An equal probability ellipsoid was plotted for the sample population in the PC space. An ellipsoid that included 90

present of the sample population was used to identify the design boundaries/limits (illustrated as A, B, C and D in Figure 9) (data in Figure 9 not based on real data; only an illustration of the concept). At least three actual cases (subjects) that fell closest to these design limits, representing the smallest and largest extremes of the PCA, were selected to represent the boundary condition that that was modelled. The anthropometric body dimensions of these three cases were averaged to obtain the body dimensions that the respective biomechanical models should have.

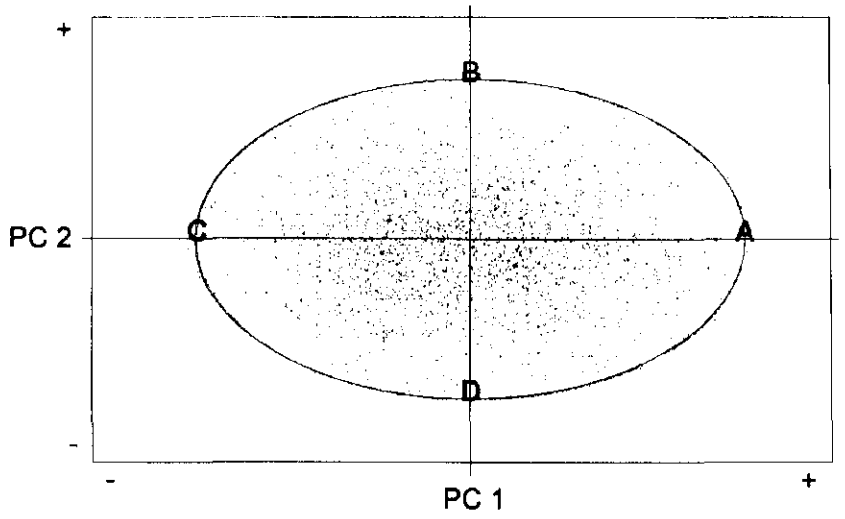

Figure 9 : Illustration of cases plotted on PC space with 90 percentile boundary ellipsoid indicating design limits A, B, C and D

3.4.2.2 Functional body strength data

In order to model biomechanical properties representative of the SANDF, functional body strength data were retrieved from the SANDF functional strength database. The SANDF functional strength database consists of a range of functional strength measurement variables for SANDF males and females collected between 2001 and 2003.

Functional body strength values were assigned to the eight biomechanical models based on body mass index (BMI) (see discussion in Section 4.2). For each biomechanical model, a range of BMI values was assigned based on the anthropometric variances of the three boundary cases/subjects (see Section 3.4.2.1). Functional body strength values were selected from the SANDF functional

strength database for males and females with BMI values that fell within these ranges. The functional body strength values selected for each biomechanical model were averaged to provide one functional strength value for each functional strength variable.

Three functional body strength variables were selected for incorporation into the biomechanical model. These included peak isokinetic pedal push leg strength (30 °/sec) (see Figure 10), peak isometric back strength at knee level (see Figure 11) and peak isokinetic overhead lift (30 °/sec) (see Figure 12). These three variables were selected to represent upper body, lower body and torso strengths.

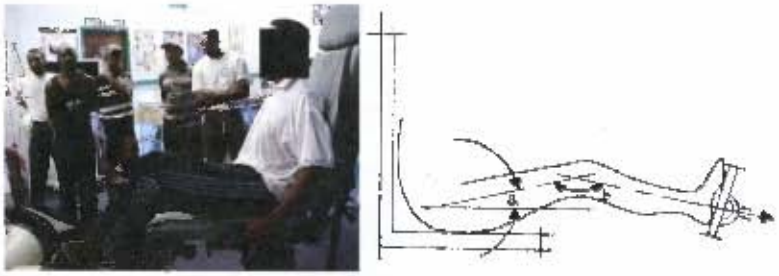

Figure 10 : Peak isokinetic pedal push leg strength

Figure 11 : Peak isometric back strength at knee level

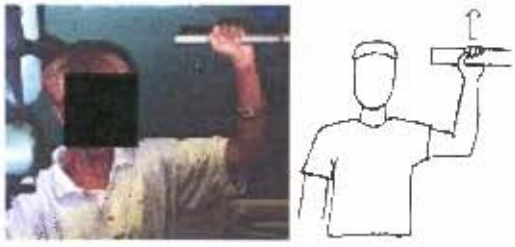

Figure 12 : Peak isokinetic overhead lift arm strength

3.4.2.3 Posture and motion data

A 6 camera Qualisys (Qualisys AB, 2006) postural analysis system (see equipment list in Appendix A) was used for the collection of kinematic data during this study (postural and motion data that are representative of postures adopted during the measurement of functional body strength data). Kinematic data were collected for a test participant with anthropometric dimensions similar to that described in Section 3.3.2.1. All segment lengths as defined in the LifeMod™ User Manual (Biomechanics Research Group, 2008) were measured and modelled for each participant. Reflective passive markers were placed on the participant in accordance with the golf marker placement as specified in the LifeMod™ User Manual (Biomechanics Research Group, 2008). The setups for the three functional body strength scenario's used to build the biomechanics model as well as scenario used for the verification of the model is demonstrated in Figures 13 to 16 below.

Figure 13 : Motion data capture for overhead push

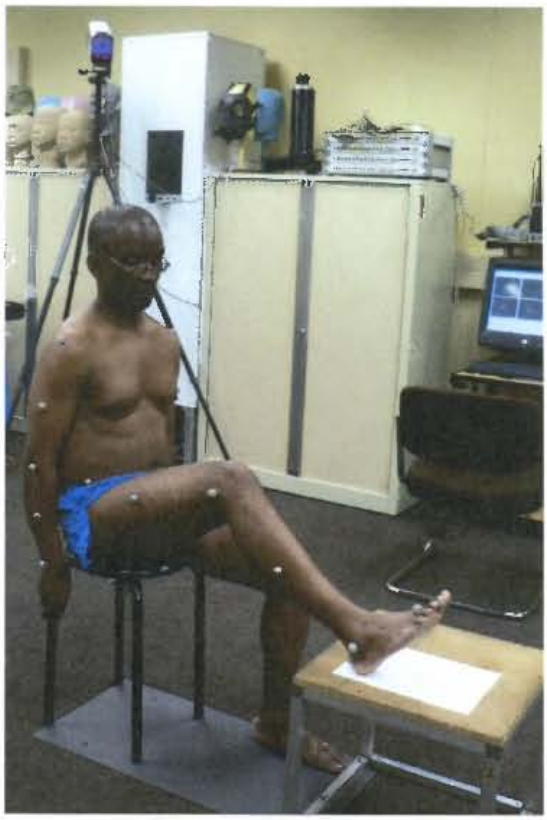

Figure 14 : Motion data capture for functional leg push

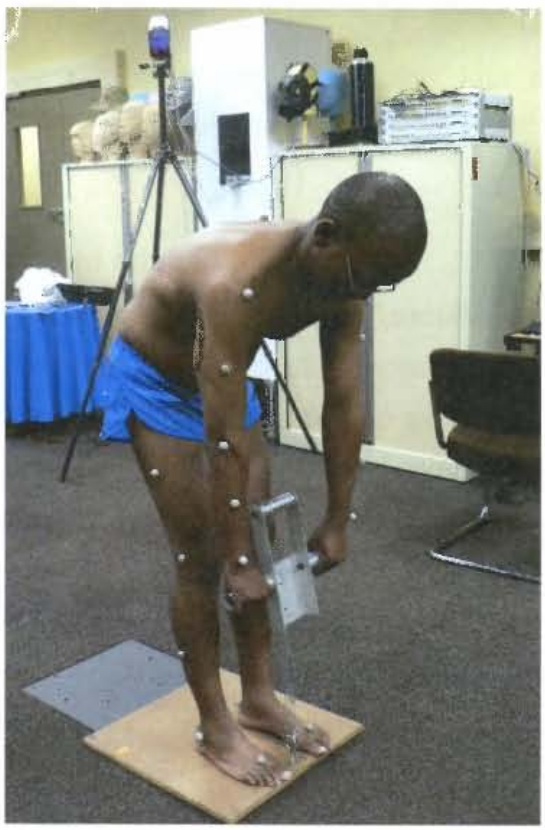

Figure 15 : Motion data for back strength

Figure 16 : Motion data for box lift

The Qualisys motion capture data were translated into a format that could be imported into LifeMod™ by a script written in active PERL.

3.4.3 Simulation and analysis

3.4.3.1 Muscle properties for maximum functional strength exertion

The muscles used during the modelling of Biomechanical Models that represent members of the SANDF are referred to in LifeMod as Closed Loop muscles. Closed loop muscles contain proportional-integral-differential (PID) controllers. The PID controller algorithm uses a target length-time curve to generate the muscle activation and the muscles follow this curve. Because of this approach, an inverse dynamics simulation using passive recording muscles is required prior to simulation with closed loop muscles. The closed loop algorithm is governed by the following formula :

$$F - P_{gain}(P_{error}) + I_{gain}(I_{error}) + d_{gain}(d_{error})$$

Where : P_{error} = (targetValue-currentValue)/rangeOfmotion
D_{error} = first derivative of P_{error}
I_{error} = time integral of P_{error}

The maximum force generated by a closed loop muscle is limited by the muscle strength conditioning formulas :

$$F = A(t) \times F_{\max} \times tone \times preload$$

Where : $A(t)$ = 1 for activation
F_{max} = maximum force that a muscle can exert
$tone$ = muscle force output filter value between 0 and 2
$preload$ = user-defined constant force value

If the PID calculations result in a larger value than this, the force is limited and the controller will not force the model to exceed this physiological limit.

Simple muscle elements were modelled. Simple muscles consist of active muscle elements only, and no passive muscle elements. These muscles fire with no constraints except for the physiological cross-sectional area (pCSA), which designates the maximum force a muscle can exert. The graphs of simple muscle activation curves will generally peak at a flat force ceiling value. The maximum force that can be exerted by each muscle is calculated as follows :

$$F_{\max} = \sigma_{\max} \times pCSA$$

Where : F_{max} = maximum force that a muscle can exert
$pCSA$ = physiological cross sectional area of muscle
σ_{max} = maximum isometric muscle stress

The muscle forces required to execute the maximum functional strengths as described by current SANDF functional body strength data were determined by running a first line analysis with very high cross sectional muscle areas or maximum tissue stress settings (pCSA and/or σ_{max}). The maximum tissue stress values were then reduced to 35 N/cm^2 and pCSA reduced to ensure that the maximum muscle forces that could be generated by each of the muscles were equal to the muscle forces that enabled the maximum functional strength exertions under investigation.

Since the muscles of the whole body contributed to the overall strength of the model, but only certain muscles were involved in the limited functional body strength tasks used to build the models, some form of scaling factor was needed with which all muscle pCSA's could be scaled to enable the overall functional strength of the model. One functional strength scaling factor was therefore used for each functional body strength task. This scaling factor was then applied to all the muscles of the portion of the body associated with the respective functional body strength tasks. Therefore, all the muscles in the leg were multiplied by the leg strength scaling factor calculated from the functional leg strength task, all the arm muscles with the arm strength scaling factor calculated for the overhead strength task, and all the trunk muscles with the back scaling factor calculated for the back strength task.

The functional strength scaling factors were determined as follows :

1. The primary muscles responsible for producing the specific functional body strength force and task were identified
2. A scaling factor for each of the primary muscles was calculated. This scaling factor was the number by which the default pCSA value for the muscle had to be multiplied to obtain the final model pCSA, which when multiplied by σ_{max} of 35 N/cm^2 would produce the maximum muscle force required to execute the functional body strength being modelled,
3. The functional strength scaling factor for the function body strength task = the mean of the scaling factors for each of the primary muscles for that task.

3.4.3.2 Joint parameters

The original joints created in the biomechanical model had default joint parameters (Stiffness (K) =1E4, Dampening (C) =1000). Joints with such high joint stiffness are created to ensure a relatively "rigid" model that provides a stable and smooth motion when manipulated by motion splines. This is especially important during the movement of the model into the initial posture as well as to ensure smooth model motion during inverse dynamics. Since no muscle force data were recorded during inverse dynamics, high joint stiffness did not have an effect on the final muscle forces.

After the muscle lengths had been recorded in the inverse dynamics, the joint stiffness was changed to near zero, to represent actual stiffness in human joints. Since the biomechanical model is being driven by the forces generated in the muscles, any joint stiffness values that are higher than that of the scenario being represented, will result in muscle forces that are higher than the actual circumstances being modelled (since additional muscle forces will have to be generated to overcome the artificial joint torques).

3.4.3.3 Floor contact settings

Contact between the model and the floor is required in the vertical direction to prohibit the model from "falling through the floor" when the gravitational forces are activated in the dynamic environment. Different contacts between the model and the floor were created according to the specific scenarios modelled. Where body parts were not required to move from a location for the entire duration of the analysis, these parts were fixed to the ground by means of bushing elements. Bushing elements are preferred to fixed joint elements because they allow for limited translational and rotational motion. Also, the amount of motion can be controlled by changing stiffness and damping characteristics in all three Cartesian coordinates. Objects such as chairs or box surfaces (representing raised surfaces) were fixed to the floor by means of fixed joints since no movement between the floor and object was required.

For the pedal push leg strength, the model's pelvis was fixed to a chair and the foot not exerting the force to the floor with a bushing element with the following settings :

- Translational stiffness : (1e6, 1e6, 1e6)
- Translational damping : (1e5, 1e5, 1e5)
- Rotational stiffness : (1e4, 1e4, 1e4)
- Rotational damping : (1e3, 1e3, 1e3)

The heel of the foot exerting the pushing force was fixed to a raised foot surface by means of a bushing element. The bushing properties were set as follows to prohibit translational moment in the vertical direction only :

- Translational stiffness : (0, 0, 1e6)
- Translational damping : (0, 0, 1e5)
- Rotational stiffness : (0, 0, 0)
- Rotational damping : (0, 0, 0)

The chair, the box surface (representing the raised foot surface) and the torso at the level of the fourth thoracic vertebra were fixed to ground with a fixed joint element, allowing no translation or rotation movement.

For the overhead lift arm strength, the model's feet were fixed to the ground and the pelvis to the chair with a bushing element. The bushing elements had similar settings to those used for the pelvis and feet during pedal push leg strength.

For the back strength, the feet were fixed to the floor with bushing elements with similar settings to those used in the overhead lift arm strength modelling scenario.

3.4.3.4 Body postures and inverse dynamics

LifeMod™ advises that the model should be moved from a normal standing posture to the posture in which the motion is started, by means of freezing the motion agents and conducting an inverse dynamics simulation run. During this run, spring elements between the marker locations on the model and the actual motion data, "pull" the model into the motion start position. Once the model has been moved to the start position, the marker locations on the model are synchronized with motion data marker locations (model markers moved to coincide with motion data marker locations) and the joint angles are changed to those of the start body posture. However, it was found that any inconsistencies in the location of markers as well as discrepancies in segment lengths between the test subject used during collection of

motion data and the model, resulted in awkward or incorrect joint angles and body postures. Incorrect body posture had severe effects on the muscle response and ability of the model to execute the intended task. As a result, the starting posture was obtained by means of importing the motion data and manually adjusting the joint angles to line marker locations on the model up with motion markers. Once the correct joint angles were obtained, marker locations were synchronized. By using this technique, more representative muscle responses were obtained when executing the recorded motion.

Movement (body motion) was modelled by means of Inverse dynamics simulations. Inverse dynamics simulations were performed on the model which was being manipulated, by the use of movement splines and external forces. Movement splines were generated from motion agents. The data used to drive the motion agents were recorded with the Qualisys posture analysis system (see Section 3.3.2.3) and was entered into the system by importing the marker trajectory set generated from the motion capture system. The mass of each motion agent (marker) was set according to the importance of the marker's contribution to the motion as well as to the stability of the model. The massing factors used were determined by means of running several modelling iterations to identify the best combination of massing factors per functional body strength modelling scenario. The massing factors used for each of the three functional body strength body scenarios (left and right side massing factors were set the same for all postures) were set as follows :

Pedal push:

Shoulder, epicondyle, wrist, ASIS and T4 = 5
Femoral condyles and heels = 10
Sacrum = 20
Rest of markers = 1

Back strength :

Shoulder, T4 and sacrum = 20
Wrist = 10
ASIS, femoral condyles and heels = 5
Rest of markers = 1

Overhead lifts :

Shoulders, epicondyles, wrists = 10

Femoral condyles, heels = 5

T4 = 30

Sacrum = 20

Rest of markers = 1

The translational stiffness and damping, as well as linear and angular conversions were set to default values. Markers with coordinate axes that coincided with those of the motion data were created to indicate the orientation according to which the motion data had to be imported.

The inverse dynamics simulation replicated kinematics only. During this simulation, the changes in lengths of the muscle elements and the angles of the joint elements were recorded for each muscle and joint element. This recorded kinematics information was then used during the forward dynamics simulation to generate the forces required in the muscle elements of the model to make the intended motion possible without the guidance of motion splines.

3.4.3.5 Simulation of functional body strength

In order to simulate the muscle output required to execute the functional strength task, a force (LifeMod™ SFORCE element) that moves with the respective body parts was placed on the heel (for pedal push leg strength) and to the model's hand (for overhead lift arm strength). The LifeMod™ force element had the same magnitude, but in an opposing direction, as the peak body strength being modelled. The LifeMod™ function builder was used to gradually increase the force over the first 0.5 seconds (from 0N to full magnitude) where after the force remained constant at full magnitude for the remaining duration of the simulation (STEP (0,0,0.5, force)). In the back strength simulation (isometric), the movement of the model was constrained by the motion data while a bar fixed to the model's hands had a mass similar to the functional back strength. The inverse dynamics simulations were performed for durations ranging from 2 to 3 seconds. The average functional body strength values, derived as described in Section 3.4.2.2, were used to provide force values required to simulate the respective peak muscles contractions.

3.4.3.6 Forward dynamics

After the inverse dynamics simulation was performed, the motion agents imported from the Qualisys system were deactivated for the forward dynamics simulation. Muscles generated contractile forces in order to simulate the muscle length history recorded during inverse dynamics. During the forward dynamics simulation the model was guided by the internal muscle forces and influenced by external forces (gravity, contact and pushing/pulling forces). A tracking agent was applied to ensure stability to the model. A tracking agent is a motion agent created at the centre of mass location of the model using the inverse dynamics simulation data and is used only during the forward dynamics simulation. It applies small spring forces via a connector bushing to account for various minor instabilities in the model. Instabilities could occur due to a mathematical round-off error or model imbalances.

3.4.4 Validation of model

Several iterations of simulation and analysis were completed for each to the three functional body strength scenarios, to obtain the optimum joint stiffness and damping settings as well as muscle characteristics to execute the respective body strengths. The joint stiffness and damping settings of the three scenarios were amalgamated into one biomechanical model.

The biomechanical strength of this model was validated against SANDF biomechanics data reserved for the validation process. This variable included a box lift from knee to waist height (see Figure 17).

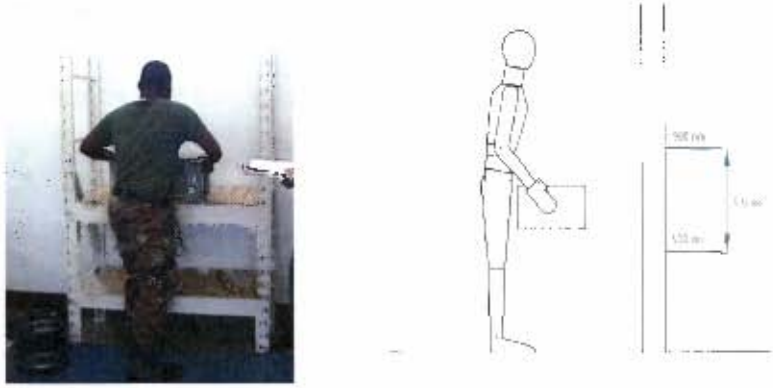

Figure 17 : Box lift functional strength, knee to hip

During the validation process, the biomechanical model with anthropometric dimensions, joint and muscle detail as described and determined in Section 3.3.3 of this report was utilised. Motion data were captured and imported into LifeMod™ as described in Section 3.3.2.3. The simulation and analysis were conducted according to Section 3.3.3, with the addition of the following characteristics :

- Contact forces were created between both feet and the floor by use of LifeMod™ bushing elements with the following settings :
    - Translational stiffness : (1e6, 1e6, 1e6)
    - Translational damping : (1e5, 1e5, 1e5)
    - Rotational stiffness : (1e4, 1e4, 1e4)
    - Rotational damping : (1e3, 1e3, 1e3)
- The motion agents were imported with the following massing factors :
    - Shoulders, epicondyles, wrists, femoral condyles, heels = 10
    - T4 and Sacrum = 20
    - Rest of markers = 1
- The maximum mass was modelled as a box with mechanical properties representing the maximum mass. The box was fixed to the model's hands by means of a LifeMod™ fixed joint element.

The maximum mass that the model could lift was determined by means of visual inspection of the model and observing whether the model could execute the expected task. The mass for which the model was not able to lift the box was determined to be above the maximum. This maximum mass was then compared to what SANDF males and females with similar anthropometric characteristics would be able to lift (as found in the SANDF biomechanics database) to determine the accuracy of the model to represent the modelled functional capability.

CHAPTER 4 : RESULTS

4.1 ANTHROPOMETRY ANALYSIS

The number of SANDF members included in the anthropometric data included in this evaluation is indicated in Table 3.

Table 3 : Sample description

Ethnic grouping	Number of people (included in stratified sample)	
	Males	**Females**
African Black	1501	1251
White	356	670
Coloured	278	278
Asian	25	28
Total	***2160***	***2227***

This analysis incorporates body lengths (leg, arm, trunk and stature) together with BMI and body circumferences to ensure representation of the varying relationship between these variables in males and females in the SANDF. There were certain aspects of body form that could not be described within the 1D data without shape information (such as obtained from 3D data) or at least visual tools (photo's or 3D scans).

4.1.1 Females

4.1.1.1 Body Mass Index

The distribution plots of BMIs (Figures 18 to 21) indicated that a small percentage of females (less than 4%) were underweight. A very large percentage of the female population, almost half, were classified as obese (ranging between 38% of Coloured females to 58% of African Black females). This body factor has a large impact on the investigation of correlation between BMI and functional body strength.

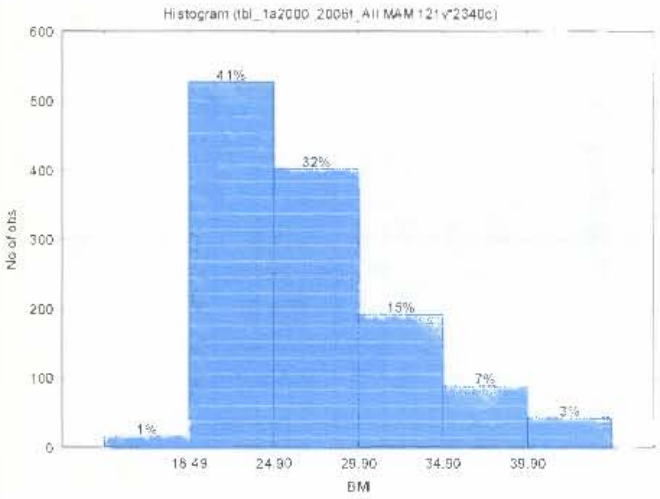

Figure 18 : BMI distribution for African Black females

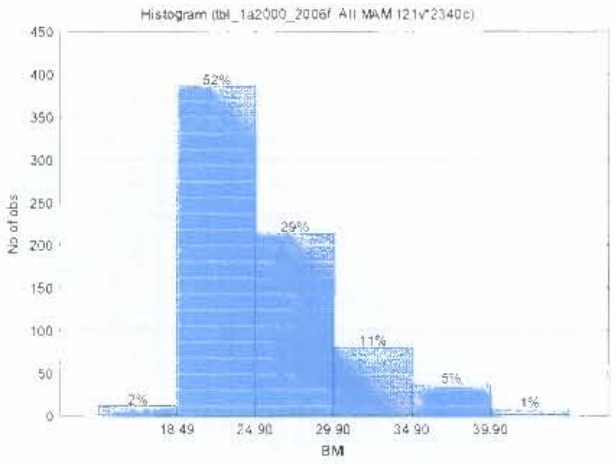

Figure 19 : BMI distribution for White females

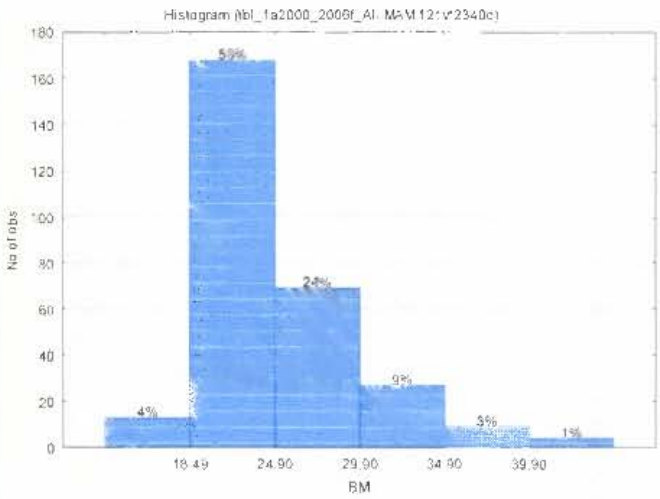

Figure 20 : BMI distribution for Coloured females

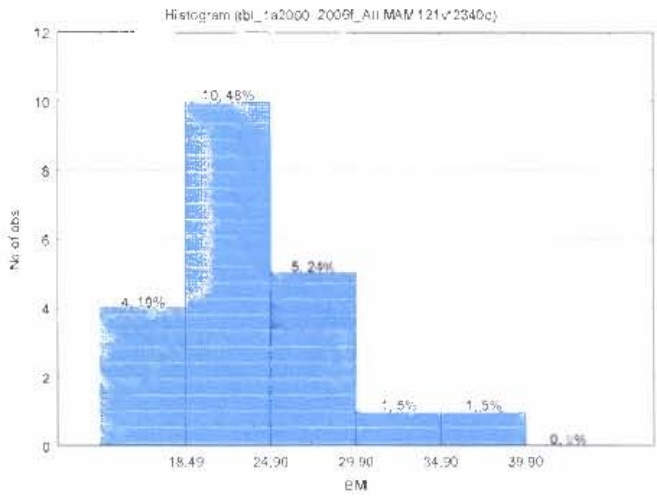

Figure 21 : BMI distribution for Asian females

4.1.1.2 Correlations

The Pearson's correlation coefficients are presented in Tables 4 to 6. Strong correlations were marked for $r^2 \geq 0.6$ (thus $r > 0.77$).

Table 4 : Correlation coefficients for females (stratified according to SANDF distribution of four ethnic groupings, as presented in the Department of Defence Annual Report FY 2006-2007 (2007)

	Mass	B1 Stature	B5 Acromial height	B6 Axilla height	B7 Chest height	B12 Elbow rest height	B13 Wrist height	B19 Armspan	B22 Inside arm length	B23 Outside arm length	B26 Cervical to waist back	B27 Cervical to waist front	B29 Under bust to waist	B30 Shoulder length	B35 Body rise	B40 Total crotch length	B41 Crotch height	B43 Thigh link	B44 Calf link	B48 Lateral malleolus height	Bs1 Sitting height	Trunk length
B1 Stature	0.32		0.90	0.89	0.84	0.88	0.77	0.78	0.50	0.55	0.38	0.33	0.09	0.25	0.24	0.12	0.65	0.29	0.37	0.21	0.70	0.59
B22 Inside arm length	-0.01	0.50	0.55	0.68	0.65	0.35	0.03	0.60		0.73	0.02	0.00	-0.10	-0.02	-0.07	-0.09	0.49	0.13	0.12	0.17	0.11	0.21
B41 Crotch height	0.08	0.65	0.67	0.63	0.64	0.59	0.42	0.63	0.49	0.56	0.14	0.09	-0.01	0.08	-0.08	-0.09		0.29	0.10	0.24	0.27	-0.07
Trunk length	0.40	0.59	0.58	0.53	0.46	0.56	0.53	0.38	0.21	0.33	0.34	0.36	0.06	0.18	0.34	0.31	-0.07	0.21	0.25	0.00	0.58	

Table 5: Correlation coefficients for females (representative of four ethnic groupings (continued...)

	Bs8 Horizontal wrist reach	Bs15 Bi-acromial width	Bs18 Abdominal depth	Bs20 Thigh clearance height	Bs21 Knee height	Bs22 Popliteal height	Bs23 Buttock to popliteal length	Bs24 Buttock to knee length	Bs25 Functional leg length	f1 Foot length	h1 Hand length	C1 Head circ	C2 Neck circ	C3 Shoulder circ	C4 Chest circ	C5 Standing vertical trunk circ	C6 Armscye circ	C9 Waist circ	C12 Wrist circ	C13 Hip circ	C14 Thigh circ	C18 Ankle circ
B1 Stature	0.36	0.39	0.02	0.28	0.73	0.66	0.33	0.44	0.61	0.61	0.54	0.04	0.25	0.23	0.19	0.44	0.25	0.15	0.30	0.10	0.07	0.29
B22 Inside arm length	0.29	0.06	-0.16	0.01	0.46	0.49	0.14	0.19	0.39	0.37	0.34	0.04	-0.04	-0.03	-0.11	0.01	-0.05	-0.10	0.05	-0.24	-0.08	0.01
B41 Crotch height	0.31	0.13	-0.11	0.19	0.59	0.56	0.27	0.34	0.54	0.49	0.41	0.01	-0.01	0.02	-0.04	0.10	0.06	-0.05	0.04	-0.13	-0.06	0.06
Trunk length	0.28	0.35	0.20	0.25	0.41	0.29	0.22	0.32	0.26	0.28	0.28	0.02	0.31	0.32	0.32	0.49	0.31	0.27	0.33	0.20	0.20	0.29

Table 6: Correlation coefficients for females (representative of four ethnic groupings (continued...)

	C2 Neck circ	C3 Shoulder circ	C4 Chest circ	C5 Standing vertical trunk circ	C6 Armscye circ	C7 Upper arm circ	C8 Forearm circ	C9 Waist circ natural ind	C11 Elbow circ	C12 Wrist circ	C13 Hip circ	C14 Thigh circ	C16 Knee circ	C17 Calf circ	C18 Ankle circ	C19 Over bust circ	C20 Under bust circ	C21 Hip circ - 10cm below waist	C22 Hip circ - 20cm below waist	C23 Hip circ - 25cm below waist
C1 Head circumference	0.21	0.24	0.18	0.15	0.16	0.18	0.27	0.20	0.21	0.22	0.21	0.25	0.29	0.24	0.24	0.15	0.16	0.12	0.24	0.22
C2 Neck circumference		0.73	0.73	0.61	0.61	0.52	0.65	0.73	0.64	0.63	0.54	0.52	0.51	0.54	0.46	0.67	0.69	0.58	0.57	0.44
C3 Shoulder circumference			0.85	0.70	0.71	0.71	0.72	0.84	0.68	0.61	0.61	0.69	0.59	0.61	0.49	0.82	0.79	0.72	0.74	0.58
C4 Chest circumference				0.70	0.72	0.64	0.68	0.89	0.64	0.61	0.70	0.69	0.58	0.59	0.48	0.81	0.85	0.72	0.74	0.58
C5 Standing vertical trunk circumference					0.62	0.58	0.59	0.70	0.59	0.58	0.61	0.62	0.59	0.60	0.52	0.70	0.68	0.67	0.69	0.59
C6 Armscye circumference						0.70	0.60	0.71	0.59	0.53	0.56	0.58	0.53	0.51	0.45	0.65	0.68	0.59	0.61	0.49
C7 Upper arm circumference biceps (max)							0.65	0.68	0.63	0.50	0.45	0.61	0.55	0.55	0.40	0.66	0.63	0.58	0.63	0.53
C8 Forearm circumference max								0.70	0.71	0.70	0.57	0.64	0.66	0.66	0.57	0.64	0.65	0.60	0.66	0.53
C9 Waist circumference natural ind									0.67	0.61	0.71	0.71	0.62	0.62	0.48	0.84	0.87	0.79	0.78	0.59
C11 Elbow circumference										0.66	0.50	0.58	0.59	0.59	0.53	0.63	0.63	0.56	0.60	0.51
C12 Wrist circumference											0.50	0.50	0.59	0.58	0.60	0.59	0.58	0.51	0.51	0.46
C13 Hip circumference												0.71	0.61	0.57	0.47	0.60	0.64	0.63	0.75	0.66
C14 Thigh circumference													0.73	0.71	0.52	0.65	0.64	0.71	0.87	0.79
C16 Knee circumference mid-patella														0.74	0.62	0.55	0.55	0.59	0.71	0.65
C17 Calf circumference max															0.68	0.59	0.57	0.61	0.69	0.62
C18 Ankle circumference																0.44	0.48	0.37	0.49	0.48
C19 Over bust circ																	0.88	0.75	0.71	0.54
C20 Under bust circ																		0.70	0.69	0.53
C21 Hip circ - 10cm below waist																			0.80	0.53
C22 Hip circ - 20cm below waist																				0.80

For the females, representative of the SANDF population with regard to percentages of African Black, White, Coloured and Asian females included in the sample population, strong correlations were observed between the following anthropometric variables:

- Stature and acromial, axilla, chest and elbow rest heights as well as armspan
- Shoulder circumference and bust, natural waist, over bust, under bust circumferences
- Bust circumference and waist, over bust, under bust circumferences
- Waist circumference and over bust, under bust, hip 10cm below waist, hip 20cm below waist circumferences
- Thigh circumference and hip 20cm below waist, hip 25cm below waist circumferences
- Over bust and under bust circumferences
- Hip 10cm below waist and 20cm below waist circumferences
- Hip 20cm below waist and 25cm below waist circumferences

The correlations listed above indicated that there are very few correlations between length variables such as arm, leg, hand and feet lengths and stature or between upper and lower arm and upper and lower leg lengths. The correlations furthermore indicated strong correlations between upper torso circumferences (shoulder, chest, over bust, under bust and waist) which would imply that very few females with a so-called "inverted triangle" body shape will be observed in this population. Finally, strong correlations were observed between waist circumference and higher hip circumference measurements (hip circumference measurements taken relatively close to the waist height) (hip 10cm and 20cm below waist circumference) as well as between thigh and hip circumferences, which implies that females with large hips will also have large thighs.

4.1.1.3 Principal Component Analysis

The results of the PCA for the different combination of body variables for females are presented in Figure 22 and Tables 7 and 8.

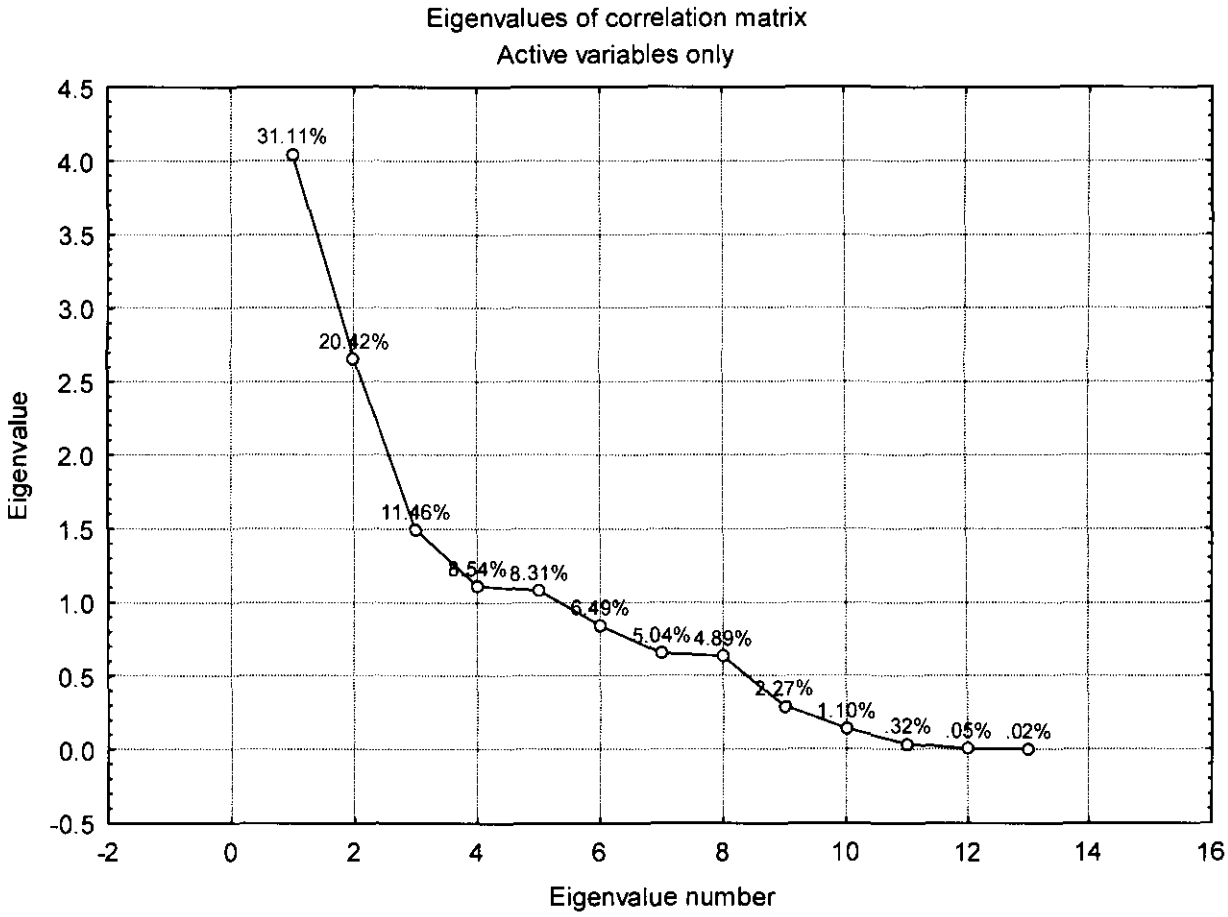

Figure 22 : Scree plot of eigenvalues of PCA (tabulated in Table 7)

Table 7 : Eigenvalues of PCA

	Eigenvalue	% Total	Cumulative Eigenvalue	Cumulative %
1	4.044	31.11	4.04	31.11
2	2.654	20.42	6.70	51.53
3	1.490	11.46	8.19	62.99
4	1.110	8.54	9.30	71.53
5	1.080	8.31	10.38	79.83
6	0.843	6.49	11.22	86.32
7	0.655	5.04	11.88	91.36
8	0.636	4.89	12.51	96.25
9	0.295	2.27	12.81	98.51
10	0.144	1.10	12.95	99.62
11	0.041	0.32	12.99	99.93
12	0.006	0.05	13.00	99.98
13	0.003	0.02	13.00	100.00

Visual inspection of the Scree plot (Figure 22) indicated that the majority of the variance of the data (and so the body shape of the SANDF female population) is described by the first four PCs. Due to the small amounts of variances described by each of the remaining components, it is impractical to consider, and design for, these variances. The first four PCs describe 72% of the variance in the data.

The anthropometric variances described by each PC are indicated in Table 8.

Table 8 : Contribution of variables to Principal Components

	Factor 1	Factor 2	Factor 3	Factor 4
B1 Stature	-0.04	**0.84**	-0.42	0.18
I1 BMI	**0.92**	-0.05	0.00	-0.10
I2 Cormic Index	0.20	**-0.55**	0.05	0.21
I3 Upper limb index	-0.09	0.40	**0.63**	-0.02
I4 Lower limb index	0.01	0.10	-0.21	**-0.76**
I5 Chest to Waist Drop	**-0.60**	-0.11	-0.38	0.09
I6 Waist to Hip Drop	0.40	0.28	**0.59**	0.18
B22 Inside arm	-0.22	**0.75**	0.27	-0.02
B41 Crotch height	-0.26	**0.74**	-0.08	-0.32
C4 Chest circumference	**0.90**	0.15	-0.11	0.00
C9 Waist circumference (natural indentation)	**0.97**	0.17	0.07	-0.03
C13 Hip circumference	**0.83**	0.00	-0.33	-0.16
B49 Trunk length	0.22	0.47	-0.42	**0.53**

The first PC describes the "fatness" variance in the population. Anthropometric variances included are bust, waist and hip circumferences together with BMI and bust to waist ratio. This PC describes people who range from thin (a small bust, waist and hip circumference coupled with a low BMI) and who naturally have a bigger bust, than waist (see Figure 23) (typically an hourglass body form), to those that are fatter (has large bust, waist and hip circumference coupled with a high BMI) and with bust and waist circumferences that are similar (see Figure 24) (typically square or oval body forms).

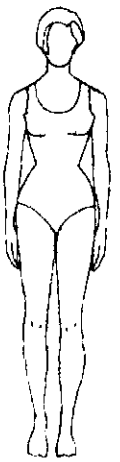

Figure 23 : Thinner females with low BMI and waist smaller than bust

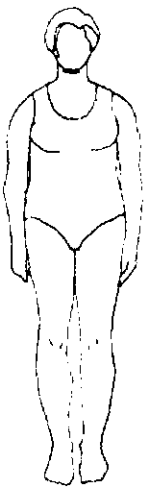

Figure 24 : Fatter females with high BMI and waist and bust similar circumferences

The second PC describes the "length" variance in the population. Anthropometric variables included are stature, inside arm length, crotch length and cormic index. The variances described ranges of females that are short (with arms, legs and upper body proportionally short) (see Figure 25) to females that are tall (with arms, legs and upper body proportionally long) (see Figure 26).

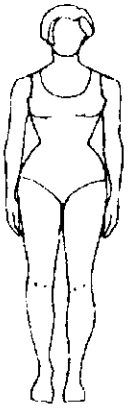

Figure 25 : Females that are shorter with shorter arms and legs

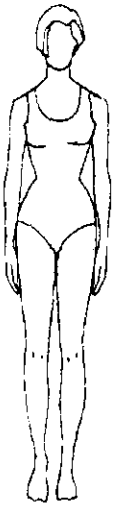

Figure 26 : Females that are taller with longer arms and legs

The third PC describes the lower trunk "curviness" and upper arm length variances. Included in this PC are waist to hip ratio and upper limb index. Therefore, this PC describes females who range from ones with waist and hip circumference that are

similar with longer arms in relation to stature (see Figure 27), to females with much larger hips than waist and shorter arms in relation to stature (see Figure 28).

Figure 27 : Females with similar waist and hip circumferences with longer arms

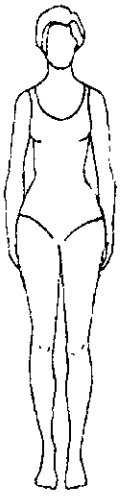

Figure 28 : Females with wider hips than waists with shorter arms

The final PC describes the relationship between trunk and legs in relation to stature. Anthropometric variables that are included are the lower limb index and trunk length. The variances described range from females with longer upper bodies and shorter legs to females with shorter upper bodies and longer legs.

4.1.2 Males

4.1.2.1 Body Mass Index

The distribution plots of BMIs (Figures 29 to 32) indicated that a small percentage of males (less than 5%) are underweight. A much smaller percentage of the male population, compared to the female population, is obese (ranging between 15% of African Black males to 36% of White males). The largest amount of males (ranging from 62% of White males to 80% of African Black males) had a normal mass (as classified according to BMI). Normal design rules, applicable in investigations such as the correlation between BMI and functional body strength, would therefore apply for the majority of the male population.

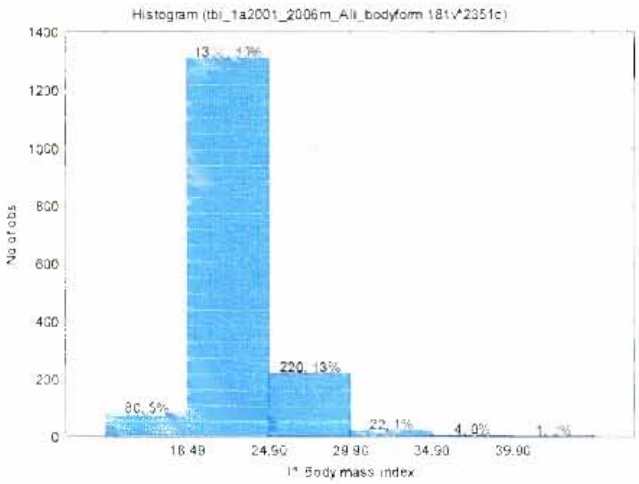

Figure 29 : BMI distribution for African Black males

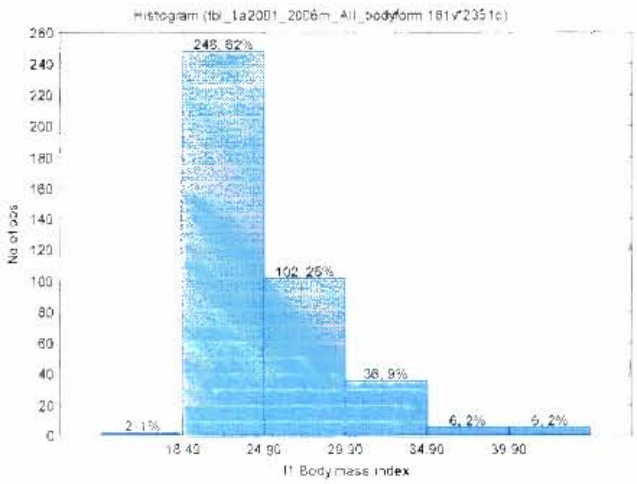

Figure 30 : BMI distribution for White males

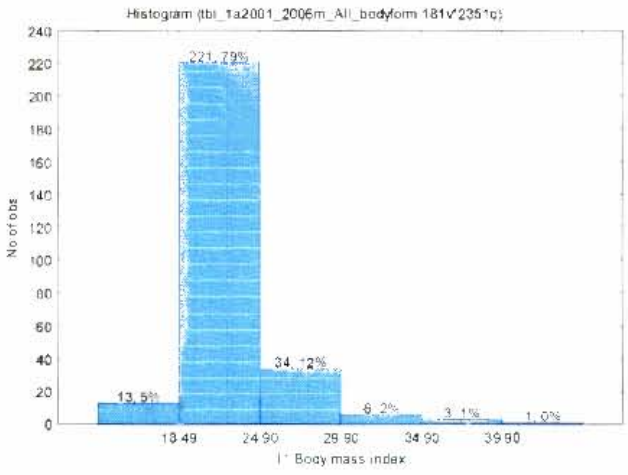

Figure 31 : BMI distribution for Coloured males

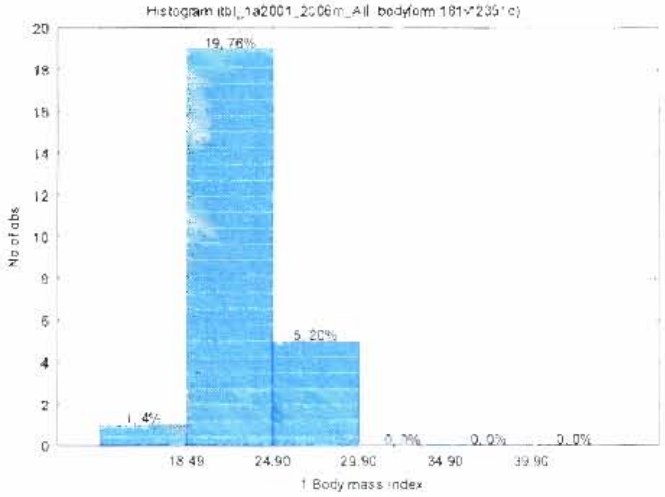

Figure 32 : BMI distribution for Asian males

4.1.2.2 Correlations

The Pearson's correlation coefficients are presented in Tables 9 to 11. Strong correlations were marked for $r^2 \geq 0.6$ (thus $r > 0.77$).

able 9 : Correlation coefficients for males (stratified according to SANDF distribution of four ethnic groupings, as indicated in the Department of Defence Annual Report FY 2006-2007 (2007)

	Mass	B1 Stature	B5 Acromial height	B6 Axilla height	B7 Chest height	B12 Elbow rest height	B13 Wrist height	B19 Armspan	B22 Inside arm length	B23 Outside arm length	B26 Cervical to waist back	B27 Cervical to waist front	B29 Under bust to waist	B30 Shoulder length	B35 Body rise	B40 Total crotch length	B41 Crotch height	B43 Thigh link	B44 Calf link	B48 Lateral malleolus height	Bs1 Sitting height	Trunk length
B1 Stature	0.32		0.90	0.89	0.84	0.88	0.77	0.78	0.50	0.55	0.38	0.33	0.09	0.25	0.24	0.12	0.65	0.29	0.37	0.21	0.70	0.59
B22 Inside arm length	-0.01	0.50	0.55	0.68	0.65	0.35	0.03	0.60		0.73	0.02	0.00	-0.10	-0.02	-0.07	-0.09	0.49	0.13	0.12	0.17	0.11	0.21
B41 Crotch height	0.08	0.65	0.67	0.63	0.64	0.59	0.42	0.63	0.49	0.56	0.14	0.09	-0.01	0.08	-0.08	-0.09		0.29	0.10	0.24	0.27	-0.07
Trunk length	0.40	0.59	0.58	0.53	0.46	0.56	0.53	0.38	0.21	0.33	0.34	0.36	0.06	0.18	0.34	0.31	-0.07	0.21	0.25	0.00	0.58	

Table 10 : Correlation coefficients for males (continued...)

	Bs20 Thigh clearance height	Bs21 Knee height	Bs22 Popliteal height	Bs23 Buttock to popliteal length	Bs24 Buttock to knee length	Bs25 Functional leg length	f1 Foot length	h1 Hand length	H1 Head length	H2 Head width	C1 Head circ	C2 Neck circ	C3 Shoulder circ	C4 Chest circ	C5 Standing vertical trunk circ	C6 Armscye circ	C7 Upper arm circ	C9 Waist circ	C12 Wrist circ	C13 Hip circ	C14 Thigh circ	C18 Ankle circ	Trunk length
B1 Stature	0.63	0.79	0.70	0.49	0.63	0.63	0.68	0.57	0.18	0.18	0.22	0.32	0.38	0.33	0.55	0.35	0.18	0.23	0.43	0.31	0.25	0.45	0.55
B22 Inside arm length	0.46	0.55	0.55	0.39	0.39	0.42	0.43	0.40	0.14	0.12	0.09	0.04	0.12	0.05	0.13	0.04	0.05	0.00	0.11	-0.04	0.09	0.12	0.15
B41 Crotch height	0.56	0.70	0.69	0.45	0.51	0.56	0.55	0.46	0.14	0.09	0.08	0.07	0.11	0.05	0.18	0.10	-0.02	-0.01	0.13	-0.01	0.06	0.18	-0.10
Trunk length	0.29	0.34	0.24	0.25	0.37	0.24	0.31	0.26	0.07	0.19	0.20	0.34	0.40	0.38	0.54	0.38	0.30	0.34	0.41	0.50	0.28	0.41	

Table 11 : Correlation coefficients for males (continued...)

	C2 Neck circ	C3 Shoulder circ	C4 Chest circ	C5 Standing vertical trunk circ	C6 Armscye circ	C7 Upper arm circ	C8 Forearm circ	C9 Waist circ natural ind	C11 Elbow circ	C12 Wrist circ	C13 Hip circ	C14 Thigh circ	C16 Knee circ	C17 Calf circ	C18 Ankle circ	C21 Hip circ - 10cm below waist	C22 Hip circ - 20cm below waist	C23 Hip circ - 25cm below waist
C1 Head circumference	0.21	0.24	0.18	0.15	0.16	0.18	0.27	0.20	0.21	0.22	0.21	0.25	0.29	0.24	0.24	0.12	0.24	0.22
C2 Neck circumference		0.73	0.73	0.61	0.61	0.52	0.65	0.73	0.64	0.63	0.54	0.52	0.51	0.54	0.46	0.58	0.57	0.44
C3 Shoulder circumference			0.85	0.70	0.71	0.71	0.72	0.84	0.68	0.61	0.61	0.69	0.59	0.61	0.49	0.72	0.74	0.58
C4 Chest circumference				0.70	0.72	0.64	0.68	0.89	0.64	0.61	0.70	0.69	0.58	0.59	0.48	0.72	0.74	0.58
C5 Standing vertical trunk circumference					0.62	0.58	0.59	0.70	0.59	0.58	0.61	0.62	0.59	0.60	0.52	0.67	0.69	0.59
C6 Armscye circumference						0.70	0.60	0.71	0.59	0.53	0.56	0.58	0.53	0.51	0.45	0.59	0.61	0.49
C7 Upper arm circumference biceps (max)							0.65	0.68	0.63	0.50	0.45	0.61	0.55	0.55	0.40	0.58	0.63	0.53
C8 Forearm circumference max								0.70	0.71	0.70	0.57	0.64	0.66	0.66	0.57	0.60	0.66	0.53
C9 Waist circumference natural ind									0.67	0.61	0.71	0.71	0.62	0.62	0.48	0.79	0.78	0.59
C11 Elbow circumference										0.66	0.50	0.58	0.59	0.59	0.53	0.56	0.60	0.51
C12 Wrist circumference											0.50	0.50	0.59	0.58	0.60	0.51	0.51	0.46
C13 Hip circumference												0.71	0.61	0.57	0.47	0.63	0.75	0.66
C14 Thigh circumference													0.73	0.71	0.52	0.71	0.87	0.79
C16 Knee circumference mid-patella														0.74	0.62	0.59	0.71	0.65
C17 Calf circumference max															0.68	0.61	0.69	0.62
C18 Ankle circumference																0.37	0.49	0.48
C21 Hip circ - 10cm below waist																	0.80	0.53
C22 Hip circ - 20cm below waist																		0.80

For the males, stratified according to representation of ethnic groupings (African Black, White, Coloured and Asian) in the SANDF, strong correlations were observed between the following anthropometric variables:

- Stature and acromial, axilla, chest, elbow rest height, wrist heights as well as armspan
- Neck circumference and shoulder, chest, waist, and forearm circumference
- Shoulder circumference and chest, forearm circumference
- Chest circumference and waist, forearm circumference
- Waist circumference and hip, hip 10cm below waist, hip 20cm below waist circumference
- Hip circumference and under bust, hip 20cm below waist, hip 25cm below waist circumference
- Thigh circumference and hip 20cm below waist, hip 25cm below waist circumference
- Knee circumference and hip 20cm below waist circumference
- Hip 10cm below waist and hip 20cm below waist circumference
- Hip 20cm below waist and hip 25cm below waist circumference

The correlations above indicated that, similar to the findings for the females, very few length variables were correlated. The correlations also indicated that neck circumference was strongly correlated with the upper torso circumferences (shoulder and chest) and overall, all the adjoining torso circumferences (shoulders to chest, chest to waist and waist to hip) were strongly correlated. However, it is evident that all torso circumferences were not necessarily correlated (such shoulder to waist and hip and chest to hip).

It should be noted that although variables may be correlated, it does not imply that no variance in body shapes will be observed for these variables (such as males with large waist in relation to hip circumference and other males with small waist in relation to hip circumferences). It could however be expected that such variances in body shapes will be for smaller percentages of the population.

4.1.2.3 *Principal Component Analysis*

The results of the PCA for the different combination of body variables for males are presented in Figure 33 and Tables 12 and 13.

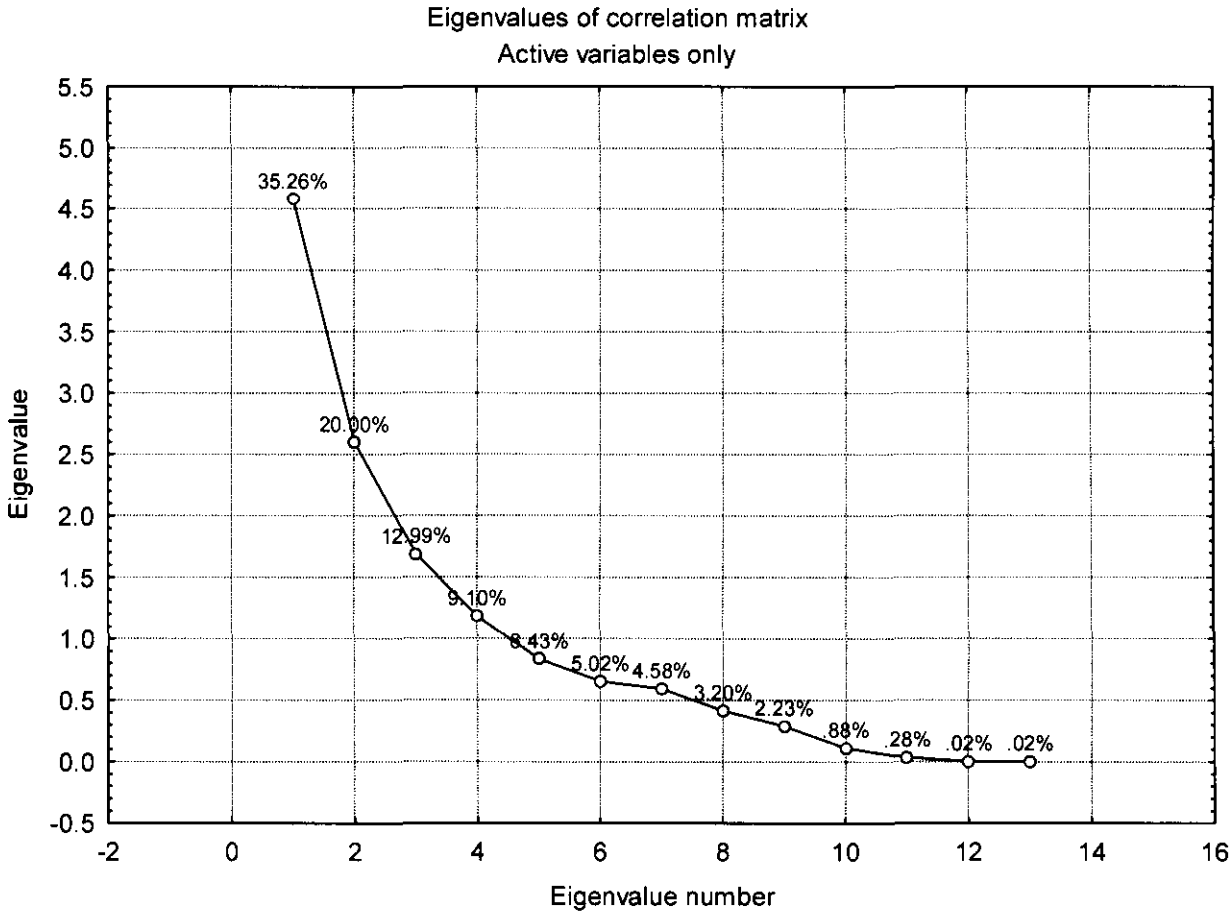

Figure 33 : Scree plot of Eigenvalues of PCA (indicated in Table 12)

Table 12 : Eigenvalues of PCA for males

	Eigenvalue	% Total	Cumulative Eigenvalues	Cumulative %
1	4.583	35.26	4.58	35.26
2	2.600	20.00	7.18	55.26
3	1.689	12.99	8.87	68.25
4	1.183	9.10	10.05	77.35
5	0.836	6.43	10.89	83.77
6	0.652	5.02	11.54	88.79
7	0.595	4.58	12.14	93.37
8	0.416	3.20	12.55	96.57
9	0.290	2.23	12.84	98.80
10	0.114	0.88	12.96	99.68
11	0.036	0.28	12.99	99.96
12	0.003	0.02	13.00	99.98
13	0.002	0.02	13.00	100.00

Visual inspection of the Scree plot indicated that the majority of the variance in body shape of the data (and so the SANDF male population) is described by the first four PCs. Due to the small amounts of variances described by each of the remaining components, it is impractical to consider, and design for, these variances. The first four PCs describe 77% of the variance in the male data.

The anthropometric variances described by each PC are indicated in Table 13. The PCs described are very similar overall body shape variances as those found for the female data.

Table 13 : Contribution of variables to Principal Components for men

	Factor 1	Factor 2	Factor 3	Factor 4
B1 Stature	-0.29	**0.86**	0.02	-0.12
I1 BMI	**-0.89**	-0.18	-0.14	-0.06
I2 Cormic index	-0.32	**-0.51**	0.19	-0.37
I5 Chest to waist drop	0.42	0.24	0.22	**-0.72**
I6 Waist to hip drop ratio	-0.06	-0.25	**-0.91**	-0.14
B22 Inside arm	0.01	**0.77**	-0.28	0.10
B37 Buttock depth	**-0.58**	-0.03	-0.25	-0.42
B41 Crotch height	0.07	**0.83**	-0.30	0.07
Bs18 Abdominal depth	**-0.81**	-0.11	-0.04	0.30
C4 Chest circumference	**-0.84**	0.12	-0.10	-0.34
C9 Waist circumference (natural indentation)	**-0.95**	-0.04	-0.20	0.14
C13 Hip Circumference	**-0.75**	0.17	0.54	0.22
B49 Trunk length	**-0.51**	0.33	0.43	-0.18

Similar to females, the first PC describes a "fatness" variance. The one end of the range is represented by males who have small chest, waist and hip circumferences, abdominal and buttock depths and a low BMI. However, different to the variances described by the first female PC, variances in trunk length are also described by the first PC for males. The "thinner" males have shorter trunk lengths than the "fatter" males. The other end of the variance is represented by males who have larger circumferences, greater abdominal and buttock depths, higher BMI and longer trunk lengths.

The second PC is also similar to that describing female body shape. This PC describes a length variance. The shape variance ranges from short males with short arm and leg length to taller males with longer arms and legs. Also similar to the variances described for the second PC for females, this PC for males also includes a trunk length variance (indicated by the Cormic index). The shorter males have longer trunk lengths in relation to their stature and taller males have shorter trunk lengths in relation to their stature.

The third and fourth PCs describe shape variance of the trunk, with the third describing variances in waist to hip ratios as well as hip circumferences, and the fourth variances in chest to waist ratios. Relatively large variances were also observed in buttock depth under the fourth PC males with a larger chest than waist circumferences having larger buttock depths.

4.1.3 Anthropometric inputs to biomechanical models

The anthropometric dimensions of the boundary cases for the 4 male and 4 female biomechanical models are presented in Table 14.

Table 14 : Anthropometric dimensions of the eight biomechanical models [mm]

Anthropometric variables	Anthropometric dimensions [mm]							
	MPC1-	MPC1+	MPC2-	MPC2+	FPC 1-	FPC 1+	FPC 2-	FPC 2+
Mass	51	92	62	69	49	90	57	71
Stature*#	1672	1793	1630	1799	1596	1630	1497	1717
BMI*	18.2	28.7	23.3	21.4	19.2	33.9	25.4	24.1
Cormic Index*#	50.1	52.8	53.4	49.0	51.9	53.1	54.9	50.6
Upper limb index*#	34.4	33.6	32.0	36.2	34.2	32.5	31.1	33.7
Lower limb index*#	53.2	52.0	51.0	55.7	51.5	54.3	51.1	52.6
Chest to waist drop index*	1.24	1.14	1.16	1.22	1.30	1.18	1.22	1.19
Waist to hip drop index*	0.86	0.91	0.87	0.87	0.71	0.87	0.72	0.87
Inside arm length*#	485	489	451	537	457	430	398	511
Inside leg length*	792	806	742	862	741	724	681	805
Trochanterion height#	890	932	831	1002	822	884	765	903
Sitting height#	838	925	871	881	828	865	822	868
Chest circumference*	820	1048	894	902	788	1160	849	890
Waist circumference*	663	916	769	741	609	983	697	750
Hip circumference*	775	1010	883	859	852	1132	966	860
Trunk length*	624	737	657	696	639	693	585	678

* Anthropometric variables used during PCA

Anthropometric variables used during the selection of participants for the recording of motion data.

4.2 INVESTIGATING CORRELATION BETWEEN ANTHROPOMETRY AND FUNCTIONAL BODY STRENGTH VARIABLES

The Pearson's correlation coefficient for anthropometry and functional body strength data compared is summarised in Tables 15 to 18. Table 15 illustrates correlation between data that had been collected during 2001, Tables 16 and 17 data collected during 2002 and Table 18 data collected during 2003.

Due to the indication that muscle cross section is more closely related to arm circumferences of persons with a smaller percentage body fat (see Section 2.2), correlations between anthropometric data were investigated for only males and females with a BMI that indicated a normal body mass.

For the females, the majority of correlations were observed between stature as an anthropometric variable and functional body strength variables knee, waist and shoulder force exertion, grip strength and right concentric extension, and left concentric extension. Several other length variables were to a lesser extent randomly correlated to functional body strength variables such as lateral femoral epicondyle to malleolus height with grip strength, left arm concentric extension, left arm eccentric extension, left and right arm concentric flexion, and left and right leg concentric extension. Very few circumference anthropometric variables were available for inclusion in the investigation. A medium correlation was indicated between waist circumference and shoulder force.

For males, very few anthropometric variables correlated with functional body strength variables. Mass and chest circumferences were slightly correlated to waist force and mass with grip strength. For males not screened for normal BMI, mass was also slightly correlated with trolley pull, clockwise wheel turning, wrench turning, left arm pull and left arm lever adduction.

Table 15 : Correlation coefficients of 2001 functional body strength and anthropometry data for SANDF Males and Females

	Grip strength left	Grip strength right	Trolley push	Trolley pull	Leg strength left	Leg strength right	Wheel turning clockwise	Wheel turning counter-clockwise	Wrench turning	Arm push left	Arm pull left	Arm push right	Arm pull right	Lever push (adduction) left	Lever pull (abduction) left	Lever push (adduction) right	Lever pull (abduction) right	Overhead lift left	Overhead lift right
Females																			
Age	0.06	0.11	0.14	0.14	0.07	0.11	0.20	0.23	0.01	0.33	0.21	0.31	0.19	0.16	0.10	0.22	0.16	0.04	-0.04
Mass	0.20	0.22	0.27	0.65	0.00	-0.04	0.30	0.25	0.15	0.38	0.44	0.47	0.43	0.10	0.23	0.28	0.20	0.24	0.21
Height	0.13	0.11	-0.04	0.24	0.05	0.05	0.02	-0.02	0.04	0.00	0.01	0.09	0.01	-0.27	-0.05	-0.20	-0.17	0.03	0.01
Females with BMI indicating normal mass																			
Mass	0.01	0.05	0.12	0.31	0.00	0.05	0.01	0.05	0.07	0.07	0.10	0.09	0.09	-0.10	0.08	-0.03	-0.11	-0.15	-0.12
Height	0.16	0.17	-0.01	0.15	0.13	0.21	-0.06	-0.03	0.14	-0.17	-0.01	-0.05	-0.04	-0.31	-0.08	-0.15	-0.14	-0.24	-0.05
BMI	-0.16	-0.12	0.15	0.21	-0.14	-0.16	0.07	0.08	-0.06	0.25	0.12	0.15	0.15	0.18	0.17	0.11	0.01	0.06	-0.09
Males																			
Age	-0.11	-0.17	-0.10	0.02	0.01	-0.03	-0.04	-0.01	0.09	0.02	0.01	-0.11	0.14	-0.04	0.09	-0.13	-0.03	-0.11	-0.10
Mass	0.40	0.37	0.49	0.66	0.52	0.49	0.61	0.42	0.56	0.49	0.56	0.46	0.47	0.55	0.52	0.44	0.46	0.30	0.29
Height	0.29	0.38	0.23	0.39	0.27	0.31	0.45	0.29	0.34	0.20	0.32	0.19	0.05	0.21	0.12	0.25	0.16	0.23	0.18
Males with BMI indicating normal mass																			
Mass	0.35	0.39	0.37	0.58	0.46	0.43	0.55	0.37	0.48	0.48	0.46	0.42	0.32	0.43	0.36	0.48	0.39	0.33	0.31
Height	0.28	0.34	0.28	0.44	0.33	0.37	0.54	0.32	0.45	0.26	0.40	0.25	0.15	0.28	0.18	0.31	0.20	0.20	0.17
BMI	0.23	0.23	0.25	0.40	0.34	0.25	0.23	0.21	0.23	0.43	0.26	0.35	0.31	0.33	0.34	0.39	0.36	0.27	0.27

Table 16 : Correlation coefficients of 2002 functional body strength and anthropometry data for SANDF Females

arm_CF	Concentric arm flexion
arm_EF	Eccentric arm flexion
arm_CE	Concentric arm extension
arm_EE	Eccentric arm extension
leg_CF	Concentric leg flexion
leg_EF	Eccentric leg flexion
leg_CE	Concentric leg extension
leg_EE	Eccentric leg extension

Anthropometric variables	Grip strength right	Grip strength left	Back strength	arm_CF left	arm_CF right	arm_EF left	arm_EF right	arm_CE left	arm_CE right	arm_EE left	arm_EE right	leg_CF left	leg_CF right	leg_EF left	leg_EF right	leg_CE left	leg_CE right	leg_EE left
Age	0.20	0.45	0.19	0.05	0.36	-0.05	0.30	0.02	0.16	0.10	0.12	0.15	0.09	-0.27	0.18	-0.15	-0.08	-0.34
Stature	0.38	0.56	0.04	0.29	0.30	0.11	0.24	0.28	0.12	0.11	0.12	0.25	0.29	0.24	0.07	0.33	0.46	0.24
Mass	0.31	0.51	0.32	0.19	0.19	0.04	0.08	0.22	0.16	0.01	-0.04	0.29	0.11	0.16	-0.03	0.46	0.57	0.28
Trochanter-lateral femoral epicondyle length	0.02	0.08	-0.15	0.30	0.17	0.29	-0.12	0.14	0.01	-0.23	-0.09	0.12	0.21	0.45	0.09	0.33	0.39	0.46
Trochanter-lateral femoral epicondyle length	0.48	0.47	-0.15	0.01	0.13	-0.08	0.30	0.17	0.04	0.23	0.13	0.26	0.21	0.07	0.26	0.26	0.18	0.00
Trochanter-floor length	0.26	0.39	-0.16	0.26	0.27	0.16	0.06	0.20	0.02	-0.03	-0.08	0.17	0.08	0.24	-0.02	0.37	0.33	0.21
Acromion-lateral humeral epicondyle length	0.53	0.68	0.15	0.45	0.54	0.16	0.32	0.54	0.38	0.44	0.21	0.22	-0.05	-0.01	-0.01	0.39	0.37	-0.03
Lateral humeral condyle-styloid process length	0.45	0.53	-0.01	0.34	0.43	-0.11	-0.01	0.20	0.02	0.24	0.01	0.09	-0.12	-0.30	-0.14	0.05	0.04	-0.38
Acromion-styloid process length	0.53	0.65	0.06	0.43	0.53	0.01	0.15	0.38	0.20	0.36	0.11	0.16	-0.10	-0.19	-0.09	0.22	0.21	-0.25
Arm length left	0.28	0.49	-0.11	0.17	0.09	0.07	0.07	0.25	0.02	-0.04	0.01	0.11	0.25	0.27	0.09	0.13	0.35	0.32
Arm length right	0.22	0.42	-0.11	0.19	0.10	0.13	0.07	0.22	-0.02	-0.08	-0.04	0.09	0.27	0.25	0.06	0.13	0.26	0.29
Leg length left	0.30	0.41	0.34	0.38	0.52	0.03	0.15	0.39	0.21	0.30	0.19	0.09	-0.03	-0.09	-0.10	0.23	0.19	-0.13
Leg length right	0.33	0.36	0.31	0.25	0.45	0.00	0.26	0.25	0.19	0.29	0.20	0.11	0.09	-0.21	-0.05	0.09	0.02	-0.28

Females with BMI indicated normal mass																		
Anthropometric variables	Grip strength right	Grip strength left	Back strength	arm_CF left	arm_CF right	arm_EF left	arm_EF right	arm_CE left	arm_CE right	arm_EE left	arm_EE right	leg_CF left	leg_CF right	leg_EF left	leg_EF right	leg_CE left	leg_CE right	leg_EE left
Stature	0.51	0.60	-0.02	0.51	0.42	0.26	0.39	0.71	0.28	0.42	0.40	0.29	0.42	0.35	0.09	0.33	0.60	0.40
Mass	0.35	0.32	0.04	0.44	0.34	0.36	0.29	0.59	0.35	0.28	0.10	0.38	0.30	0.24	-0.05	0.53	0.59	0.42
BMI	-0.09	-0.21	0.07	0.03	0.01	0.20	-0.04	0.02	0.15	-0.08	-0.28	0.15	-0.09	-0.10	-0.17	0.30	0.10	0.08
Trochanter-lateral femoral epicondyle length	0.20	0.39	-0.06	0.21	0.23	0.14	0.03	0.63	0.08	0.08	0.02	0.01	0.03	0.37	0.02	0.22	0.41	0.43
Trochanter-lateral femoral epicondyle length	0.79	0.71	-0.06	0.32	0.36	0.10	0.40	0.55	0.14	0.56	0.36	0.59	0.58	0.09	0.28	0.62	0.68	0.09
Trochanter-floor length	0.38	0.53	-0.20	0.34	0.37	0.15	0.11	0.61	0.14	0.22	0.05	0.22	0.09	0.24	-0.12	0.37	0.43	0.26
Acromion-lateral humeral epicondyle length	0.49	0.52	-0.04	0.64	0.53	0.36	0.28	0.61	0.31	0.42	0.18	0.34	0.10	0.04	-0.10	0.39	0.33	0.07
Lateral humeral condyle-styloid process length	0.45	0.59	-0.23	0.29	0.42	-0.12	0.04	0.23	0.01	0.10	-0.09	0.09	0.04	-0.30	-0.13	-0.04	-0.04	-0.36
Acromion-styloid process length	0.52	0.63	-0.16	0.49	0.52	0.09	0.16	0.43	0.15	0.26	0.03	0.22	0.07	-0.17	-0.13	0.16	0.14	-0.19
Arm length left	0.38	0.63	-0.32	0.42	0.29	0.20	0.15	0.71	0.11	0.32	0.29	0.03	0.21	0.27	0.11	0.04	0.41	0.31
Arm length right	0.40	0.64	-0.33	0.42	0.28	0.21	0.15	0.71	0.09	0.31	0.27	0.04	0.22	0.26	0.11	0.06	0.41	0.30
Leg length left	0.27	0.38	0.26	0.28	0.40	-0.02	0.10	0.34	0.12	0.17	0.10	0.14	0.12	-0.01	-0.11	0.16	0.19	0.00
Leg length right	0.38	0.43	0.27	0.21	0.40	-0.06	0.24	0.16	0.16	0.14	0.13	0.19	0.22	-0.11	-0.03	0.11	0.13	-0.15

Table 17 : Correlation coefficients of 2002 functional body strength and anthropometry data for SANDF Males

Anthropometric variables	Grip strength right	Grip strength left	Back strength	arm_CF left	arm_CF right	arm_EF left	arm_EF right	arm_CE left	arm_CE right	arm_EE left	arm_EE right	leg_CF left	leg_CF right	leg_EF left	leg_EF right	leg_CE left	leg_CE right	leg_EE left
Age	-0.11	-0.18	0.12	0.16	0.09	0.21	0.17	0.17	0.13	0.01	-0.24	-0.02	-0.13	0.01	-0.17	-0.12	-0.20	-0.09
Stature	0.37	0.46	0.18	0.04	0.04	0.06	-0.04	0.05	0.07	0.18	0.25	0.14	0.12	0.01	0.13	0.26	0.32	0.03
Mass	0.33	0.40	0.41	0.28	0.31	0.17	0.09	0.32	0.35	0.35	0.44	0.40	0.31	-0.06	0.40	0.48	0.43	0.00
Trochanter-lateral femoral epicondyle length	0.26	0.27	-0.06	0.09	0.06	0.00	-0.08	0.05	0.08	0.06	0.09	0.10	0.16	-0.18	0.11	0.16	0.27	-0.16
Trochanter-lateral femoral epicondyle length	0.10	0.10	-0.06	-0.12	-0.21	-0.03	-0.19	-0.21	-0.08	0.01	0.01	-0.19	-0.19	0.20	-0.19	-0.13	-0.08	0.18
Trochanter-floor length	0.24	0.28	0.01	0.04	-0.03	0.05	-0.09	-0.05	0.05	0.05	0.05	-0.02	0.00	0.09	-0.01	0.07	0.12	0.11
Acromion-lateral humeral epicondyle length	0.19	0.25	0.12	0.03	0.06	0.13	0.10	0.07	0.09	0.21	0.17	0.11	0.08	0.04	0.06	0.15	0.24	0.07
Lateral humeral condyle-styloid process length	0.26	0.20	0.14	0.01	-0.08	0.02	-0.07	-0.07	-0.01	0.11	0.11	-0.08	-0.09	-0.09	-0.05	0.06	0.12	-0.02
Acromion-styloid process length	0.25	0.26	0.14	0.02	-0.01	0.08	0.01	0.00	0.05	0.19	0.17	0.02	0.00	-0.03	0.01	0.12	0.21	0.02
Arm length left	0.15	0.19	0.05	0.09	0.13	0.07	0.08	-0.03	0.02	-0.18	-0.03	-0.03	-0.06	-0.05	-0.07	0.15	0.12	0.06
Arm length right	0.28	0.29	0.17	0.14	0.16	0.14	0.10	0.06	0.12	-0.02	0.01	0.05	-0.03	-0.02	-0.02	0.23	0.20	0.06
Leg length left	0.24	0.29	0.20	-0.02	-0.08	-0.05	-0.08	-0.05	-0.06	0.11	0.08	0.02	-0.01	0.20	-0.03	0.09	0.13	0.13
Leg length right	0.21	0.28	0.15	-0.06	-0.08	-0.01	-0.03	-0.10	-0.09	0.06	0.10	0.02	-0.07	0.14	-0.07	0.10	0.07	0.09
Males with BMI indicated normal mass																		
Stature	0.32	0.43	0.09	0.00	0.04	-0.05	-0.13	0.03	-0.08	0.17	0.27	0.12	0.16	-0.02	0.10	0.18	0.26	0.03
Mass	0.46	0.56	0.21	0.10	0.15	0.12	0.07	0.19	0.18	0.37	0.46	0.31	0.33	0.13	0.28	0.41	0.46	0.20
BMI	0.29	0.32	0.20	0.13	0.16	0.21	0.22	0.22	0.31	0.31	0.33	0.28	0.27	0.18	0.26	0.36	0.34	0.23
Trochanter-lateral femoral epicondyle length	0.18	0.22	-0.10	0.09	0.12	-0.13	-0.13	0.06	-0.01	0.03	0.08	0.14	0.20	-0.31	0.16	0.16	0.25	-0.28
Trochanter-lateral femoral epicondyle length	0.07	0.07	-0.05	-0.09	-0.19	-0.01	-0.16	-0.14	-0.10	0.02	0.03	-0.18	-0.16	0.26	-0.17	-0.15	-0.12	0.26
Trochanter-floor length	0.24	0.29	-0.02	0.09	0.03	0.00	-0.13	0.00	-0.03	0.06	0.14	0.03	0.09	0.07	0.08	0.06	0.12	0.11
Acromion-lateral humeral epicondyle length	0.20	0.28	0.11	0.02	0.02	0.09	0.03	0.06	0.02	0.21	0.19	0.05	0.03	0.01	0.03	0.13	0.21	0.08
Lateral humeral condyle-styloid process length	0.16	0.18	0.11	0.07	0.04	0.06	0.05	-0.06	-0.06	0.03	0.13	-0.05	-0.07	-0.07	-0.02	0.06	0.13	0.03
Acromion-styloid process length	0.19	0.26	0.12	0.05	0.04	0.07	0.03	0.00	-0.02	0.14	0.19	0.00	-0.02	-0.03	0.01	0.11	0.19	0.06
Arm length left	0.16	0.16	-0.02	0.01	0.10	-0.02	0.05	-0.08	-0.06	-0.22	-0.05	-0.07	-0.04	0.00	-0.05	0.11	0.13	0.09
Arm length right	0.27	0.23	0.10	0.03	0.14	0.04	0.08	0.00	0.01	-0.06	-0.03	0.02	-0.02	0.06	-0.01	0.17	0.18	0.10
Leg length left	0.20	0.23	0.18	-0.01	-0.02	-0.13	-0.13	-0.01	-0.09	0.15	0.11	0.04	0.10	0.22	0.03	0.02	0.14	0.14
Leg length right	0.18	0.23	0.15	-0.08	-0.06	-0.09	-0.11	-0.08	-0.12	0.12	0.18	0.03	0.02	0.15	0.01	0.01	0.06	0.09

Table 18 : Correlation coefficients of 2003 functional body strength and anthropometric data for SANDF Males and Females

Females			
Anthropometric variables	**Knee push strength**	**Waist push strength**	**Shoulder push strength**
Stature	0.61	0.80	0.55
Mass	0.68	0.65	0.45
BMI	0.55	0.36	0.26
Leg length	0.59	0.70	0.42
Acromion height	0.64	0.78	0.55
Stylion height	0.57	0.74	0.49
Arm Length	0.58	0.65	0.51
Chest Circumference	0.63	0.51	0.37
Waist circumference	0.57	0.37	0.24
Females with BMI indicated normal mass			
	KneeP	WaistP	ShP
Stature	0.83	0.58	0.55
Mass	0.50	0.34	0.42
BMI	-0.07	-0.05	0.04
Leg length	0.77	0.62	0.41
Acromion height	0.81	0.55	0.47
Stylion height	0.76	0.55	0.28
Arm Length	0.62	0.36	0.58
Chest Circumference	0.47	0.21	0.53
Waist circumference	0.46	0.03	0.56
Males			
	KneeP	WaistP	ShP
Stature	0.34	0.47	0.27
Mass	0.50	0.58	0.43
BMI	0.35	0.35	0.33
Leg length	0.26	0.26	0.19
Acromion height	0.31	0.44	0.24
Stylion height	0.26	0.44	0.21
Arm Length	0.27	0.27	0.19
Chest Circumference	0.53	0.55	0.49
Waist circumference	0.36	0.39	0.29
Males with BMI indicated normal mass			
	KneeP	WaistP	ShP
Stature	0.38	0.52	0.34
Mass	0.44	0.53	0.40
BMI	0.21	0.19	0.21
Leg length	0.32	0.34	0.29
Acromion height	0.35	0.48	0.30
Stylion height	0.30	0.51	0.25
Arm Length	0.27	0.26	0.26
Chest Circumference	0.49	0.54	0.46
Waist circumference	0.26	0.32	0.21

4.3 REPRESENTATIVE BIOMECHANICS FULL BODY MODELS

4.3.1 Participants

Eight participants with statures, seated heights, arm lengths (inside arm length), leg lengths (Trochanterion height), Cormic index, Upper limb index and lower limb index values similar to the anthropometric dimensions indicated to represent the biomechanical models (see Section 3.1.3), volunteered to simulate the functional body strength postures and movement actions required for the collection of motion data. The anthropometric dimensions of these participants are indicated in Table 19.

Table 19 : Anthropometric dimensions of participants used in the collection of motion data for the eight biomechanical models

Anthropometric variable	Anthropometric dimensions [mm]							
	MPC1-	MPC1+	MPC2-	MPC2+	FPC1-	FPC1+	FPC2-	FPC2+
Stature#*	1712	1820	1602	1791	1602	1615	1501	1715
Seated Height#*	865	955	860	886	860	868	787	865
Inside arm length#	475	490	460	540	460	450	415	475
Trochanterion height#	900	950	811	980	811	882	785	900
Cormic index#	50.5	52.8	52.3	49.5	52.3	53.5	52.4	50.5
Upper limb index#	27.7	26.9	28.7	30.2	28.7	27.8	27.6	27.7
Lower limb index#	52.6	52.2	50.5	54.7	50.5	54.4	52.3	52.6
Shoulder Height*	1425	1500	1322	1475	1322	1400	1206	1425
Armpit Height*	1275	1335	1214	1350	1214	1250	1130	1275
Waist Height*	1105	1094	1010	1105	1010	1030	940	1105
Head Length*	188	202	195	196	195	193	191	188
Head Breadth*	148	159	154	154	154	141	149	148
Head to chin height*	227	230	220	128	220	226	205	227
Shoulder Breadth*	500	505	460	400	460	465	354	500
Chest Depth*	260	273	223	236	223	351	234	260
Chest Breadth*	302	355	305	299	305	364	283	302
Waist Depth*	188	251	205	215	205	266	172	188
Waist Breadth*	265	343	280	281	280	315	240	265
Buttock Depth*	234	270	219	220	219	295	254	234
Hip Breadth*	320	378	316	320	316	383	315	320
Shoulder-elbow Length*	330	370	325	343	325	315	275	330

Anthropometric variable	Anthropometric dimensions [mm]							
	MPC1-	MPC1+	MPC2-	MPC2+	FPC1-	FPC1+	FPC2-	FPC2+
Forearm-hand Length*	470	505	431	525	431	416	392	470
Knee Height*	542	570	482	565	482	515	435	542
Ankle Height*	142	140	122	120	122	120	110	142
Foot Breadth*	94	110	92	96	92	92	83	94
Foot Length*	256	276	247	280	247	240	227	256

Anthropometric variables used to select participants

* Anthropometric variables used as input to building the biomechanical models in LifeMod™

4.3.2 Ethics Clearance

Ethics clearance was obtained from the 1 Military Hospital Ethics Committee to conduct this study using military participants. Clearance was also obtained from the UCT Ethics Committee.

4.3.3 Functional body strength data

The average functional body strength data for males and females with BMI's ranging between the values indicated in Table 20 were used to provide force values required to simulate the respective peak muscles contractions. The force values used are presented in Table 20.

Table 20 : Averaged functional body strength values used to simulate muscle contractions for functional tasks

Anthropometric boundary condition and Biomechanical model			Biomechanical models	Range of BMI	Leg strength [N]	Overhead arm strength [N]	Back strength [N]
Male	PC1	Small	MPC1-	18.08 – 18.4	1115	157	273
		Large	MPC1+	27.82 – 29.37	1337	217	432
	PC2	Small	MPC2-	22..2 – 24.8	1227	195	368
		Large	MPC2+	21.2 – 21.5	1115	172	331
Female	PC1	Small	FPC1-	18.7 – 19.96	700	80	206
		Large	FPC1+	34.9 – 36.8	894	142	383
	PC2	Small	FPC2-	24.61 – 26.09	784	121	318
		Large	FPC2+	23.28 – 25.5	748	117	306

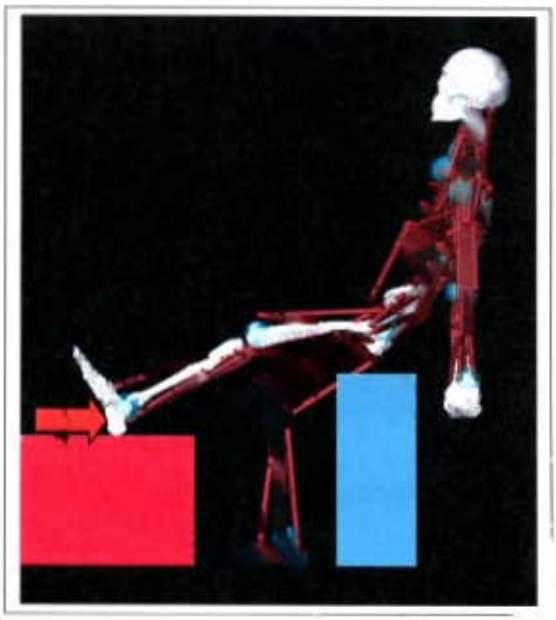

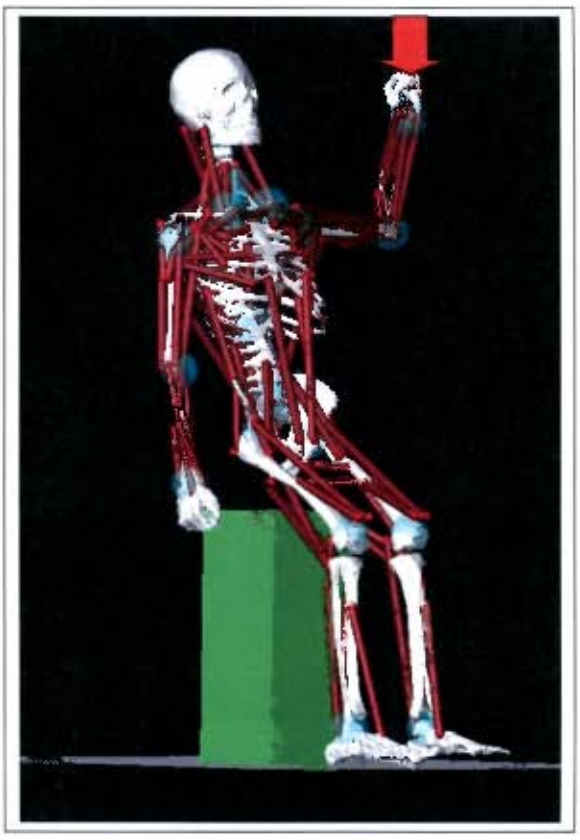

Figure 35 : The biomechanics model simulating overhead arm strength

The simulation of the overhead arm strength failed for several LifeMod™ models. The main cause for this failure was determined to be due to poor model representation of the human shoulder biomechanics. Due to inadequate muscle representation as well as joint stability, task execution when the shoulder joint exceeded 90 degrees was not possible. In attempts to create longer force lever arms to ensure more shoulder joint stability as well as larger shoulder forces, several of the models still failed to execute the task. No generic solution that ensured that all 8 biomechanics models could execute the overhead lift task could be generated. As a result, it was decided to remove this task from the tasks utilised for building the representative biomechanics models.

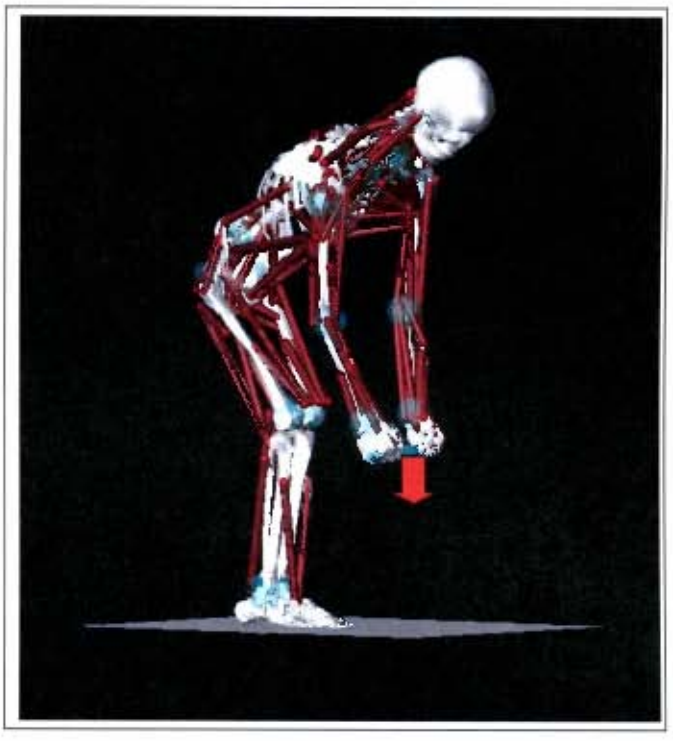

Figure 36 : The biomechanics model simulating back strength

Simulation errors were experienced on two out of the eight models during the simulation of the back functional strength tasks on the small case of the principal component group 2 for the males and the females. As a result these conditions could not be simulated (see Section 5.3 for further discussions).

4.3.5 Muscle properties

The maximum muscle stress (σ_{max}) of 35 N/cm^2 was utilised for all the muscle sets for all 8 biomechanical models.

The primary muscles that contributed to the leg push and back strength functional strength tasks were identified to be the following ;

1. Leg strength task
    a. Rectus femoris
    b. Vastus medialis
    c. Vastus lateralis
2. Back strength task
    a. External oblique
    b. Erector spinae 1, 2 and 3

The maximum muscle forces for the primary leg muscles that contributed to the execution of the leg push functional strength task as well as the primary back muscles that contributed to the execution of the back strength functional strength task are presented in Table 21.

The maximum muscle force values indicated in Table 21 are counter intuitive in that larger muscle force values were obtained for the smaller (and supposedly weaker) biomechanical models (MPC1- and FPC1-). In addition, very small muscle force values were observed for the larger female model of the principal component 2 group (FPC2+), where it would be expected that this model would exert larger muscle forces.

Table 21 : The maximum primary leg muscle forces that contributed to the leg strength task as well as primary back muscle forces that contributed to the back strength task

Muscles	Maximum muscle forces [N]							
	Males				Females			
	Principal component 1		Principal component 2		Principal component 1		Principal component 2	
	small	large	small	large	small	large	small	large
	MPC1-	MPC1+	MPC2-	MPC2+	FPC1-	FPC1+	FPC2-	FPC2+
Leg strength task								
Rectus femoris	4965	1979	-	4406	3514	3258	-	892
Vastus medialis	1810	1555	-	1346	1814	521	-	1006
Vastus lateralis	1638	1494	-	1239	1530	521	-	946
Sum	**8413**	**5028**	**-**	**6991**	**6858**	**4300**	**-**	**2844**
Back strength task								
External oblique	905	454	-	0	4218	1196	-	2377
Erector spinae 1	2004	2030	-	5638	0	1380	-	1155
Erector spinae 2	697	3530	-	0	2828	1973	-	477
Erector spinae 3	1054	0	-	2493	0	0	-	0
Sum	**4660**	**6014**	**-**	**8131**	**7046**	**4549**	**-**	**4009**

- Due to simulation errors, no values could be obtained

The pCSA values for the muscles were generated by the LifeMod^{TM} software program and automatically scaled according to the gender, mass and anthropometric segment lengths of the model parameters entered into the software when creating

the biomechanical models. Based on the σ_{max} as well as the maximum muscle forces generated by the primary muscles in each task (leg and back strength tasks) (see Table 21), the functional strength scaling factors were calculated (see Section 3.4.3.1). The default pCSAs were then adjusted with the functional strength scaling factors. The final pCSAs for the biomechanical models are listed in Table 22.

Since the pCSAs are directly related to the magnitude of the maximum force that can be generated by each muscle (see Section 3.4.3.1), the pCSA values indicated in Table 22 are, similar to the maximum force values, also counter intuitive. Larger pCSA values were obtained for the smaller (and supposedly weaker) biomechanical models (MPC1- and FPC1-).

Table 22 : pCSA values for each biomechanical model

Muscles	pCSA [mm^2]							
	Males				Females			
	Principal component 1		Principal component 2		Principal component 1		Principal component 2	
	small	large	small	large	small	large	small	large
	MPC1-	MPC1+	MPC2-	MPC2+	FPC1-	FPC1+	FPC2-	FPC2+
LEG								
Rectus femoris	6728	3643	-	5692	5298	3701	-	1977
Semitendinosus	1880	1018	-	1591	1481	1034	-	553
Vastus medialis	9366	5072	-	7927	7378	5153	-	2753
Biceps femoris1	2052	1111	-	1737	1618	1129	-	603
Iliac	3641	1972	-	3081	2869	2003	-	1070
Gluteus maximus 1	4378	2371	-	3705	3448	2409	-	1287
Gastrocnemius 1	8369	4533	-	7083	6594	4606	-	2460
Tibialis anterior	4088	2214	-	3460	3222	2249	-	1201
Soleus	23782	12879	-	20127	18734	13086	-	6991
Gluteus medius 1	4327	2343	-	3661	3407	2380	-	1272
Gluteus medius 2	3364	1822	-	2847	2651	1851	-	989
Gluteus maximus 2	4378	2371	-	3705	3448	2410	-	1287
Adductor magnus	3403	1844	-	2880	2683	1874	-	1001
Psoas major	2771	1500	-	2345	2183	1525	-	815
Vastus lateralis	13788	7466	-	11667	10859	7586	-	4052
Biceps femoris 2	5773	3126	-	4886	4547	3176	-	1697
Gastrocnemius 2	3988	2160	-	3374	3142	2194	-	1172

Muscles	pCSA [mm^2]							
	Males				Females			
	Principal component 1		Principal component 2		Principal component 1		Principal component 2	
	small	large	small	large	small	large	small	large
	MPC1-	MPC1+	MPC2-	MPC2+	FPC1-	FPC1+	FPC2-	FPC2+
TRUNK								
Scalene anterior	1683	2397	-	3525	1478	1520	-	867
Scalene medial	1547	2214	-	3269	1353	1402	-	803
Scalene posterior	1532	2196	-	3237	1353	1389	-	794
Splenius cervicis	1502	2141	-	3173	1317	1363	-	775
Splenius capitis	1577	2251	-	3301	1371	1415	-	812
Sternocleidomastoid	1532	2196	-	3237	1353	1389	-	794
Rectus abdominis	6640	9516	-	13972	5839	6000	-	3442
External oblique	17577	25162	-	36981	15434	15892	-	9116
Erector spinae 1	2719	3898	-	5704	2385	2463	-	1412
Erector spinae 2	2854	4099	-	6025	2510	2581	-	1486
Erector spinae 3	2869	4117	-	6057	2528	2594	-	1486

- Due to simulation errors, no values could be obtained

4.3.6 Muscle force output

4.3.6.1 Leg strength task

The primary leg muscle forces that contributed to execute the leg push task for the large cases of both principal components for the males and females are presented in Figures 37 to 42.

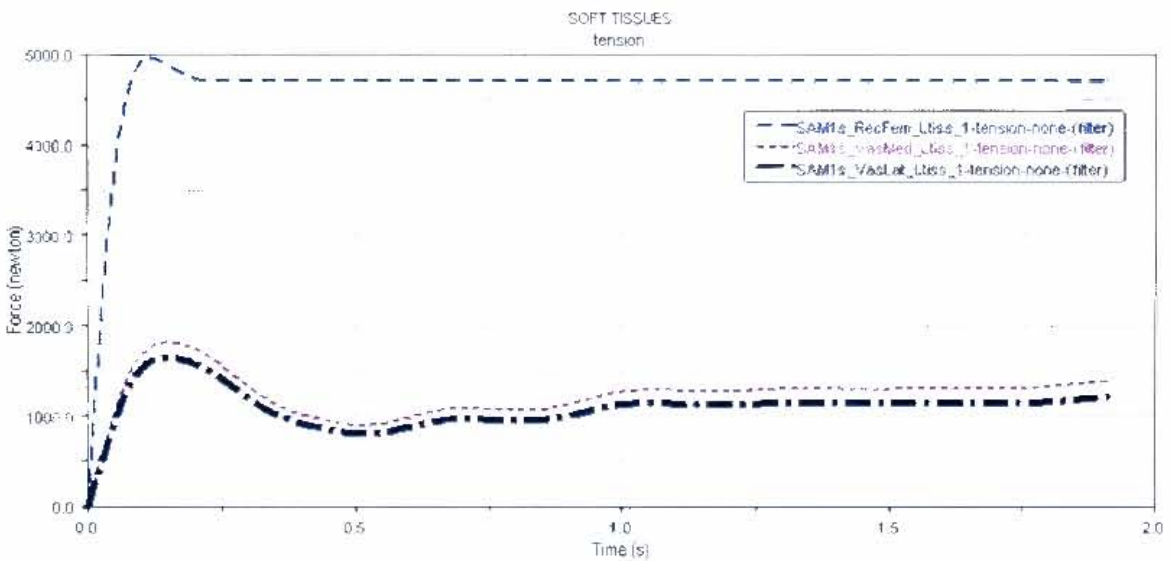

Figure 37 : Leg muscle forces of the small male case in principal component group 1

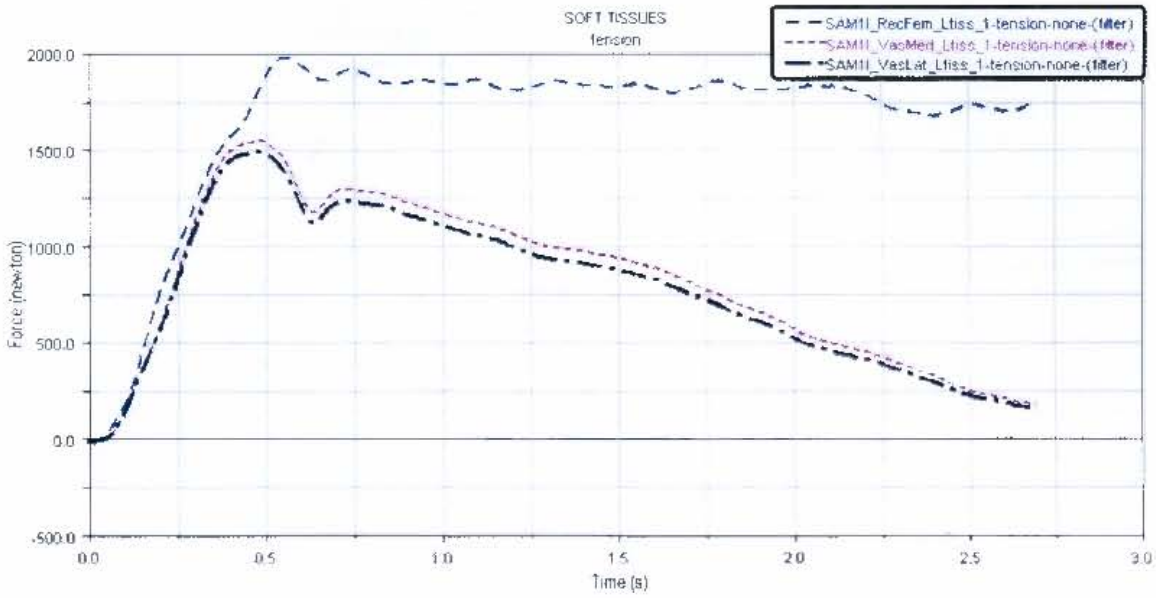

Figure 38 : Leg muscle forces of the large male case in principal component group 1

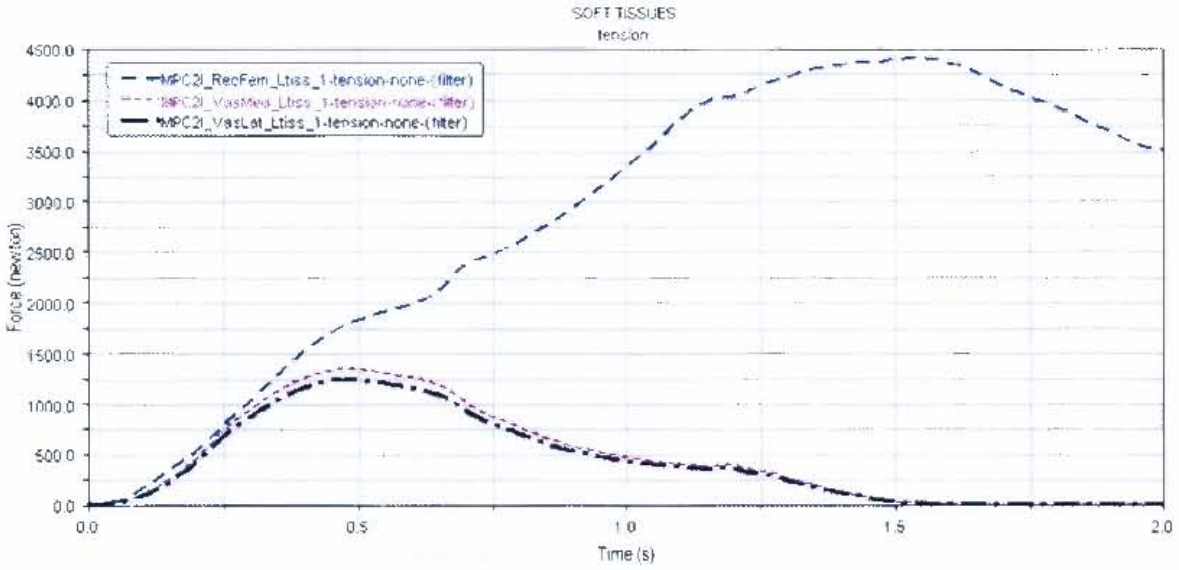

Figure 39 : Leg muscle forces of the large male case in principal component group 2

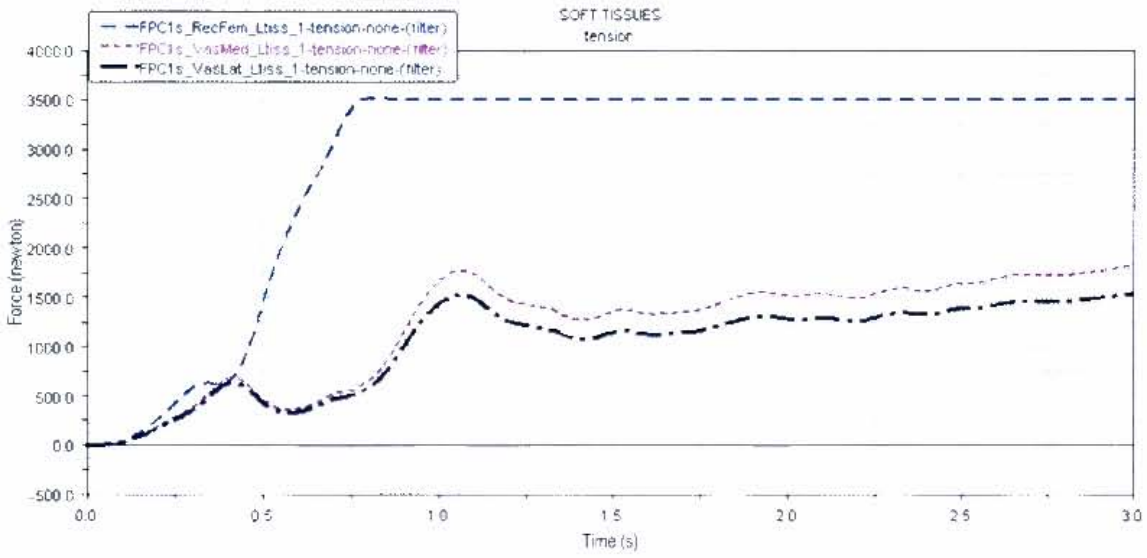

Figure 40 : Leg muscle forces of the small female case in principal component group 1

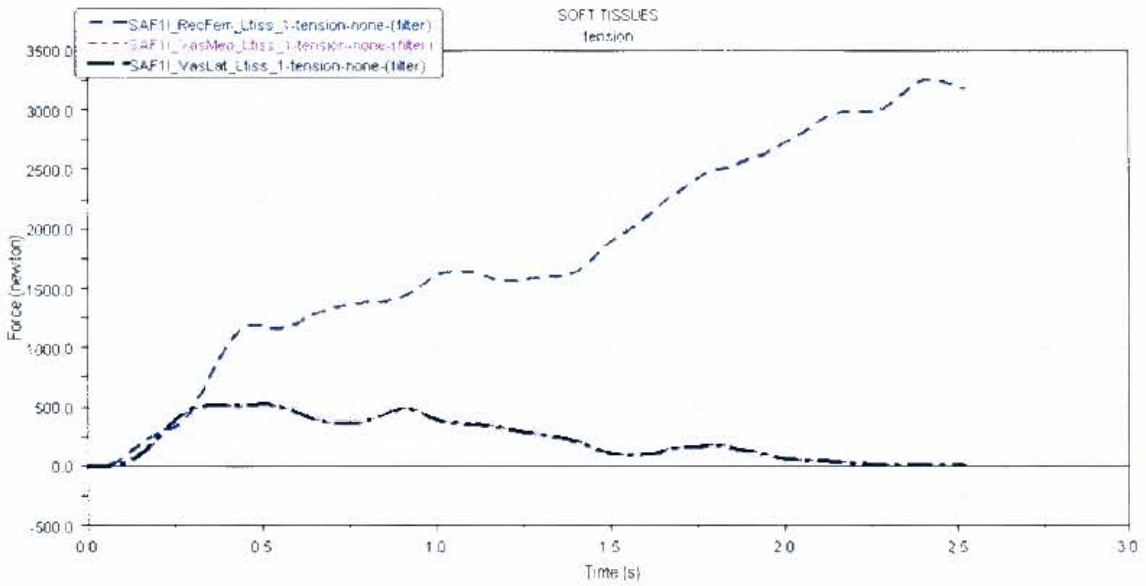

Figure 41 : Leg muscle forces of the large female case in principal component group 1

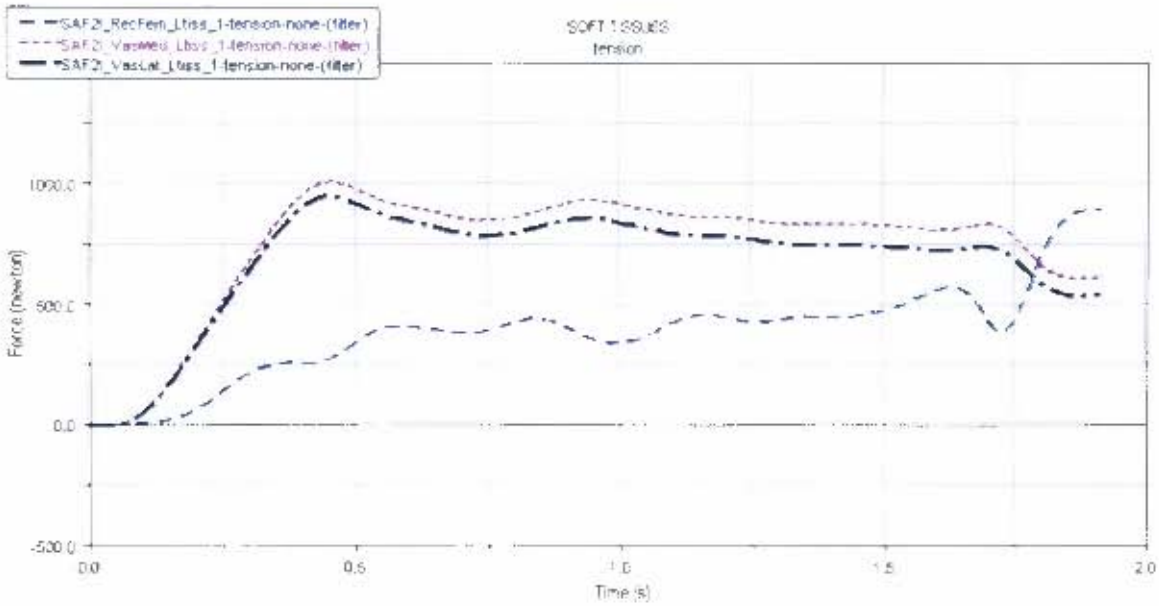

Figure 42 : Leg muscle forces of the large female case in principal component group 2

The maximum muscle forces for the primary leg muscles that contributed to the execution of the leg push functional strength task are presented in Table 21. Front and side views of the models in the starting leg push position are presented in Figures 43 to 54.

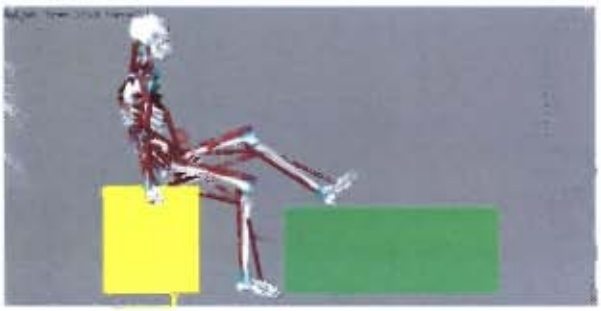

Figure 43 : Small male principal component 1 leg push side view

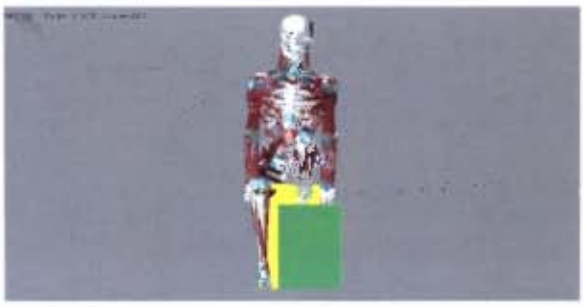

Figure 44 : Small male principal component 1 leg push front view

Figure 45 : Large male principal component 1 leg push side view

Figure 46 : Large male principal component 1 leg push front view

Figure 47 : Large male principal component 2 leg push side view

Figure 48 : Large male principal component 2 leg push front view

Figure 49 : Small female principal component 1 leg push side view

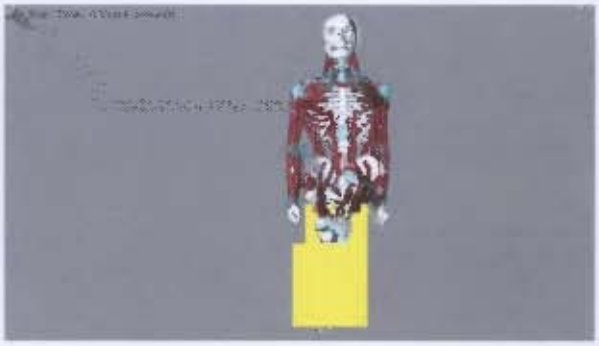

Figure 50 : Small female principal component 1 leg push front view

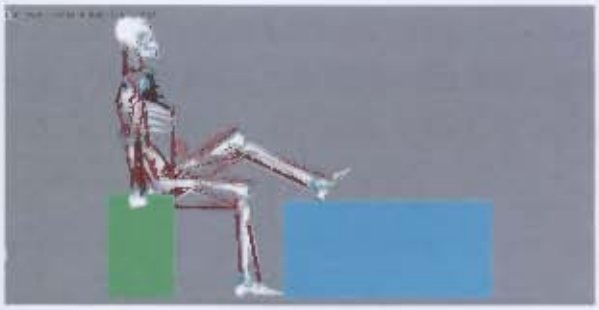

Figure 51 : Large female male principal component 1 leg push side view

Figure 52 : Large female principal component 1 leg push front view

Figure 53 : Large female principal component 2 leg push side view

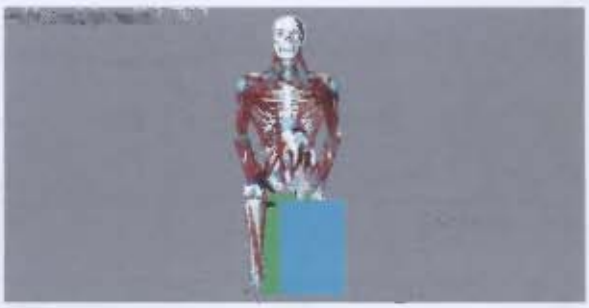

Figure 54 : Large female principal component 2 leg push front view

4.3.6.2 *Back strength*

The primary back muscle forces that contributed to execute the back strength task for the large cases of both principal components for the males and females are presented in Figures 55 to 60.

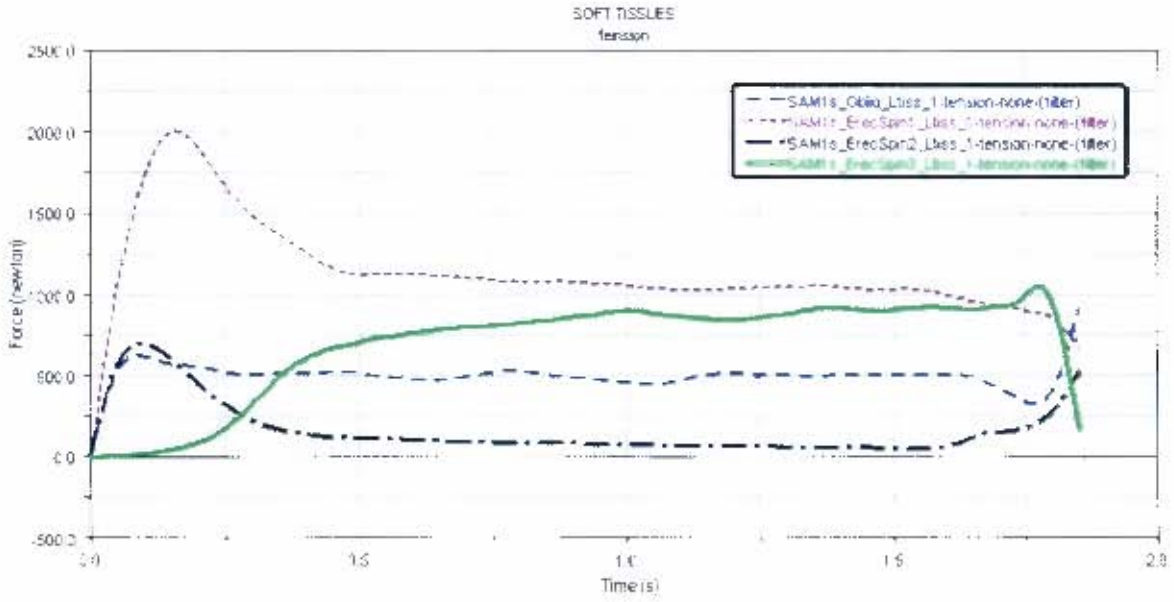

Figure 55 : Back muscle forces of the small male case in principal component group 1

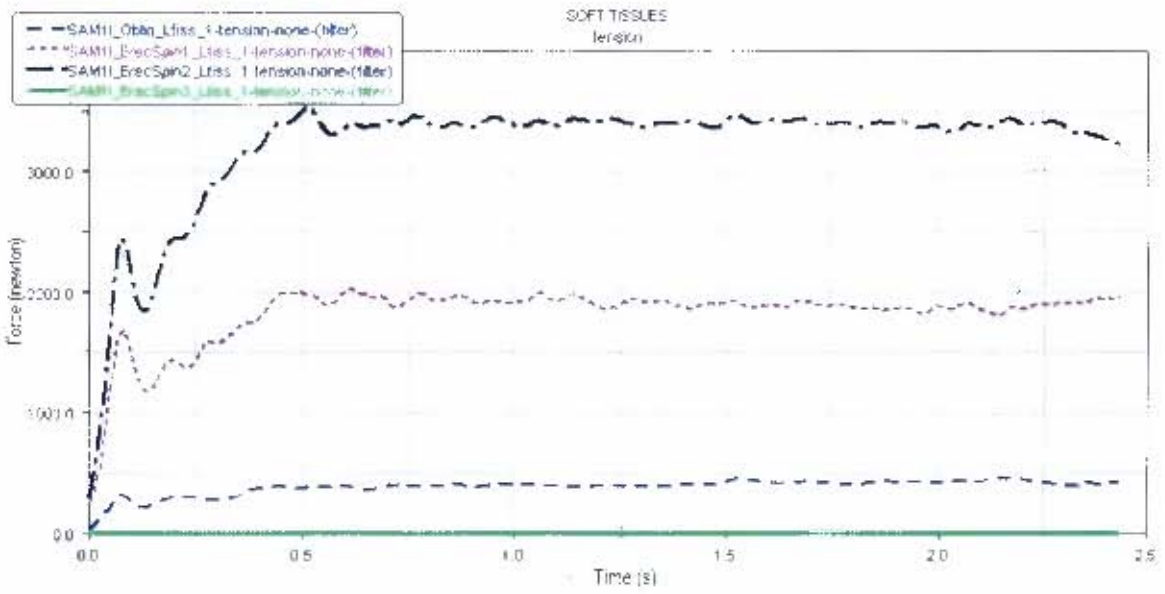

Figure 56 : Back muscle forces of the large male case in principal component group 1

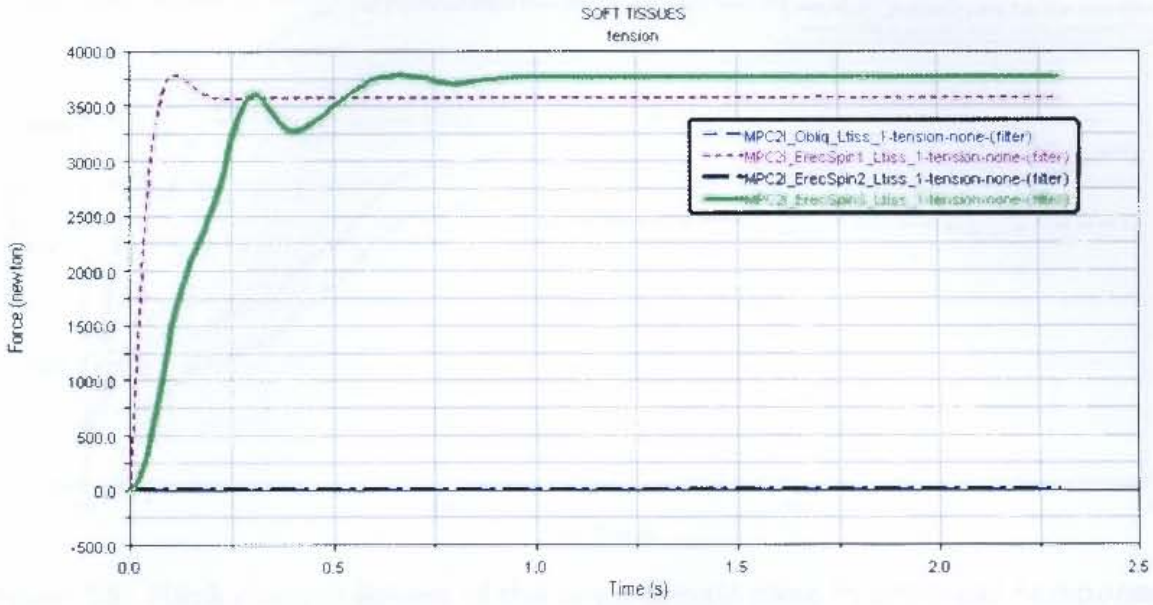

Figure 57 : Back muscle forces of the large male case in principal component group 2

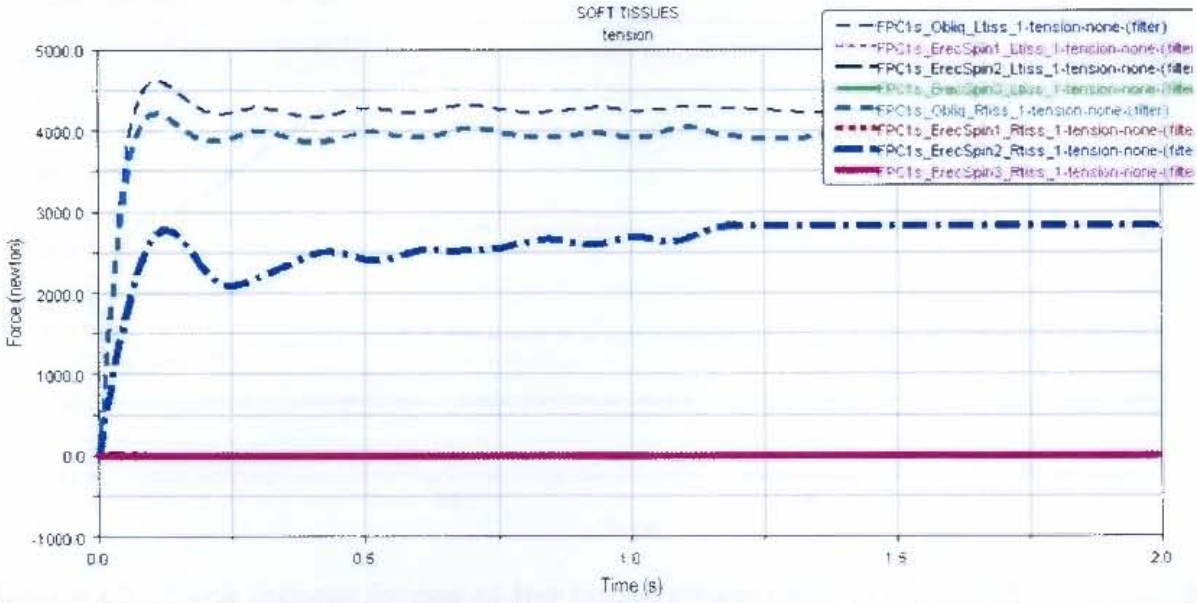

Figure 58 : Back muscle forces of the small female case in principal component group 1

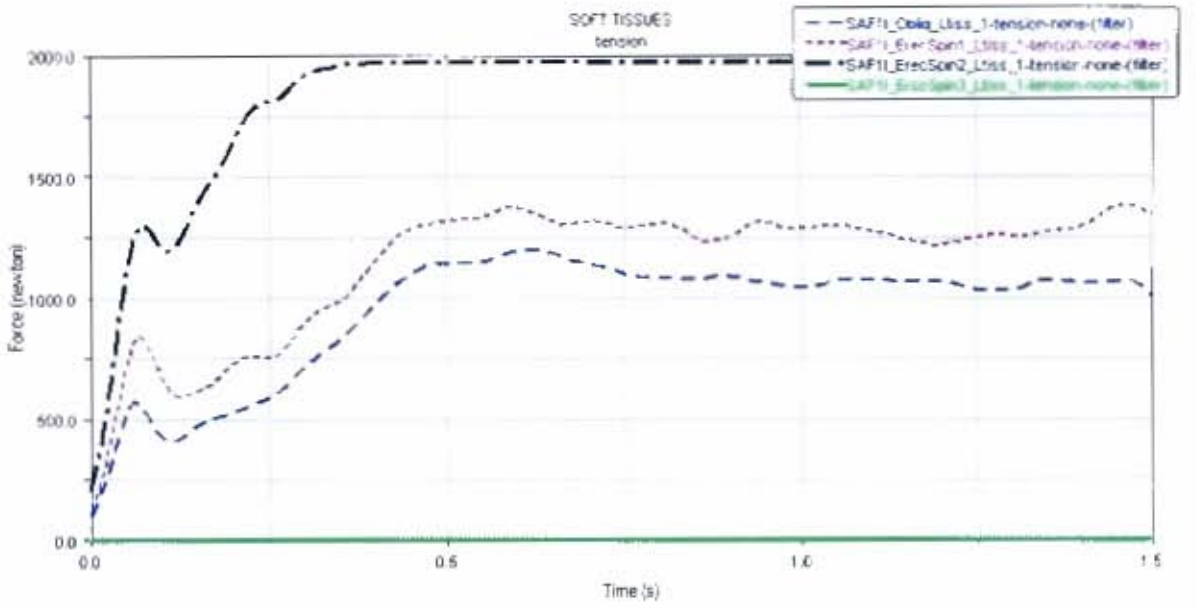

Figure 59 : Back muscle forces of the large female case in principal component group 1

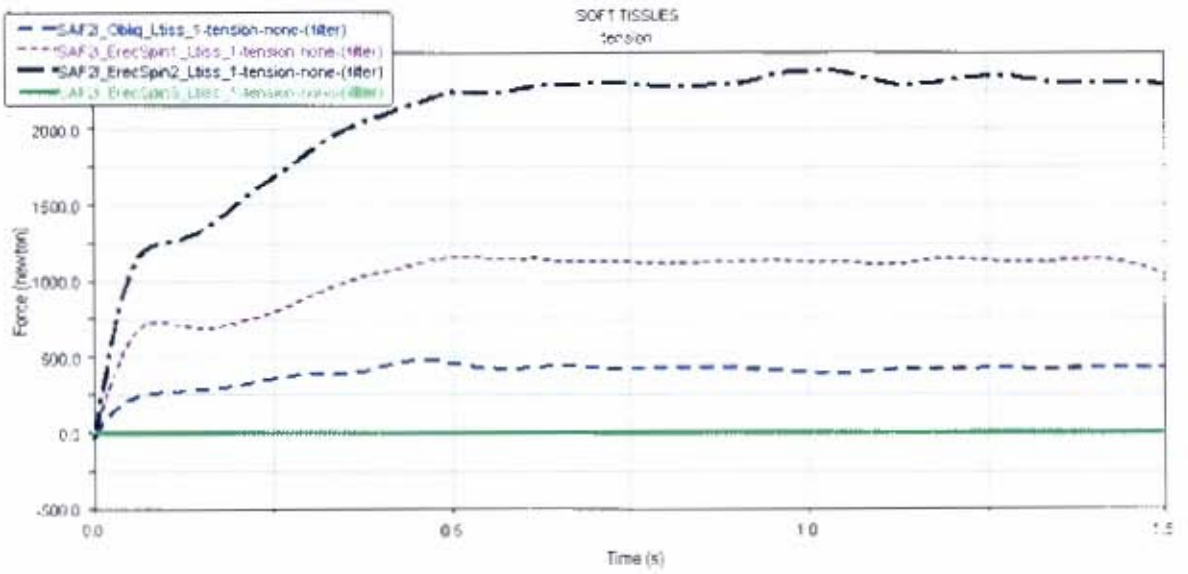

Figure 60 : Back muscle forces of the large female case in principal component group 2

The maximum muscle forces for the primary back muscles that contributed to the execution of the back strength functional strength task are presented in Table 21. The side view of the models in the back strength postures are illustrated in Figures 61 to 66.

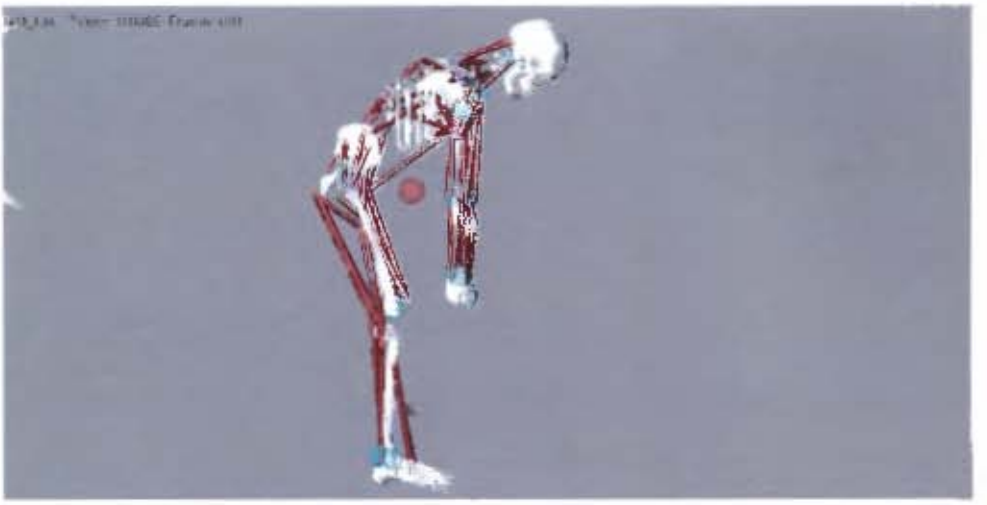

Figure 61 : Small male principal component 1 back strength side view

Figure 62 : Large male principal component 1 back strength side view

Figure 63 : Large male principal component 2 back strength side view

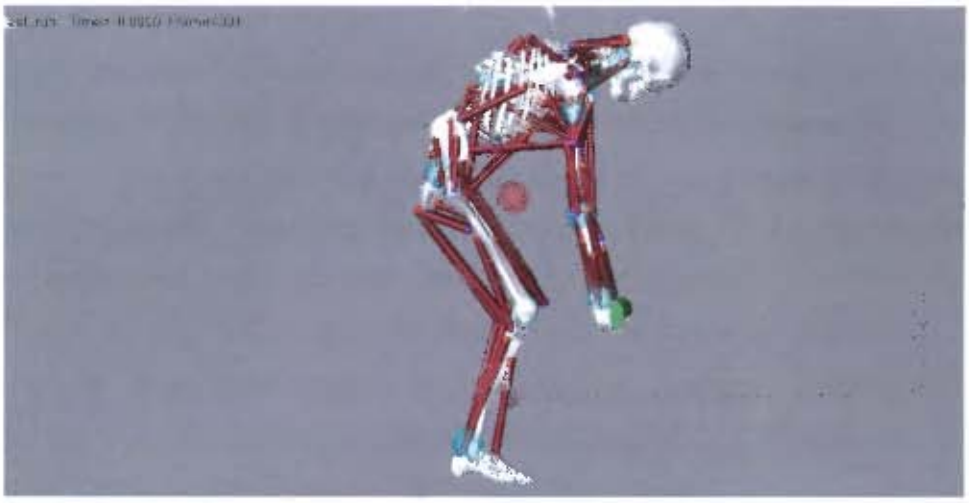

Figure 64 : Small female principal component 1 back strength side view

Figure 65 : Large female principal component 1 back strength side view

Figure 66 : Large female principal component 2 back strength side view

4.3.7 Validation of model

Box lift from the knee to waist height was simulated by using the biomechanical model (see Figure 67). The maximum box mass that the biomechanical model could lift compared to the mass that the corresponding boundary case SANDF males and females would typically be able to lift is indicated in Table 23. Also indicated in Table 23 is the percentage error between the model and actual functional body strength values. Three of the verification models failed. A possible reason for this was reported to be large joint angles and insufficient muscle representation at the respective joints in the model to execute the expected box lift task. No verification values could therefore be obtained for these three models.

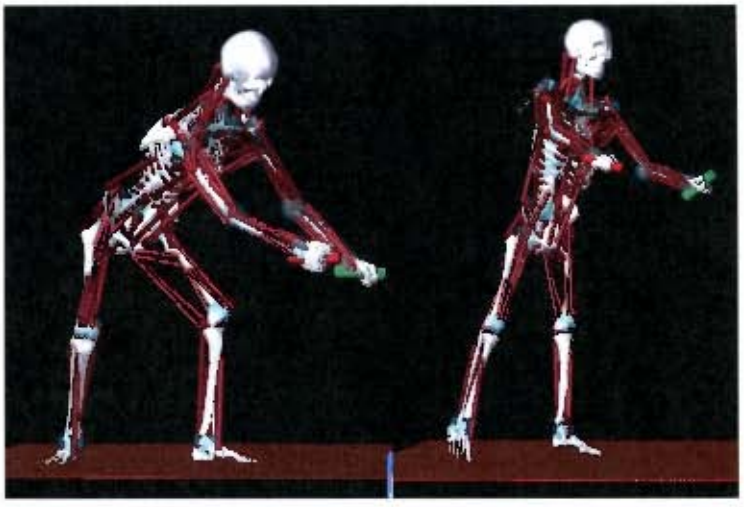

Figure 67 : The biomechanics model simulating box lift

Table 23 : Model versus actual SANDF functional body strength values compared

Biomechanical models			Box lift mass that could be lifted [kg]		% error
			Biomechanical model	SANDF functional body strength	
Male	PC1	Small	26	39.5	34
		Large	*	64.5	*
	PC2	Small	*	44	*
		Large	50	41.6	22
Female	PC1	Small	24	27	11
		Large	44	34.5	27.5
	PC2	Small	*	26.5	*
		Large	18	27	33

* No verification data available

CHAPTER 5 : DISCUSSION

5.1 ANTHROPOMETRY ANALYSIS

In order to characterise body forms, analysis of 3D anthropometric data is the ideal analysis approach. Analysis of 3D anthropometric data includes shape information otherwise lost when relying on the analysis of 1D anthropometric data (linear and contour measurements) only (Robinette and Whitestone, 1992; Ben Azouz *et al.,* 2005; Veitch *et al.,* 2007; Bredenkamp and Skelton, 2009). In the absence of 3D anthropometric data, several scientists have used photographs in combination with 1D measurement data to derive the required body form information (Douty, 1954). During the analysis approach used during this study, neither 3D anthropometric data nor photographs were available. Somatotyping (Heath-Carter technique (Carter, 2002; Fox *et al.,* 1993)) was yet another analysis technique that could have added value to this analysis approach, but due to the lack of skinfold and bi-epicondylar widths in the current SANDF anthropometric database, this technique could not be used.

As a result, a combination of analysis techniques was used to attain the most complete understanding of the body form variation for the males and females in the SANDF. This analysis approach relied solely on objective analysis of measurements and no visual parameters (photographs or 2D plots) were included. The data analysis included investigation of BMI distribution, correlations between anthropometric variables and PCA. The use of BMI and correlation between anthropometric variables were used as investigative techniques and provided additional insight to body form variation for the SANDF populations. The BMI classification provided information with regard to the distribution of mass (underweight, normal mass or obese) within the male and female populations. The investigation of correlations between anthropometric measurement variables highlighted areas where very limited form variation can be expected (thus where variables are correlated), such as chest to waist body form variation for SANDF females. The investigations of correlations furthermore indicated where shape variations can be expected within a population group (thus where poor to no correlations were observed), such as stature vs. body circumferences for SANDF males and females. Finally, PCA provided an analysis technique which could quantify the largest contributors to body form variation, highlight the percentage of form variation described by specific factors and indicate

the total percentage of body form variation which could be included in the design/modelling process. Regardless of the omission of certain recognized analysis techniques, the analysis approach used during this study was successful in highlighting variation in body forms of males and females in the SANDF.

The BMI for the South African males and females indicated high percentages of overweight (BMI > 25) and obesity (BMI > 30) (see Figures18 to 21 for females and Figures 29 to 32 for males). This is true especially for females, with the highest levels prominent in African (black) females (see Figures 18 to 21). This trend agrees with the findings for American and Canadian females (Stevens *et al.*, 2008; Chiu *et al.*, 2010). Obesity is however a worldwide trend with reported percentages for obese Native Latino females (Puerto Rican, Cuban, Mexican and Other Latinos) of 28% (Bates *et al.*, 2008). A study conducted by Niskar *et al.* (2009) reported percentages of overweight (BMI > 25) Israeli females of 44.3% for Jewish women and 55.9% for Arabian women. Obesity figures for different American ethic groups indicated 31% white females to be overweight and 23% obese, 35% black females as overweight and 48% obese (Stevens *et al.*, 2008). Lower obesity levels were reported for Canadians, where 13% white females are obese, 17% black females and 3 to 9% Asian females (Chinese and south Asian respectively) (Chiu *et al.*, 2010). When compared to the obesity figures for white and black females in the USA, the South African population have smaller percentages of obese females (17% vs. 23% for white females (see Figure 19) and 25% vs. 48% for black females (see Figure 18)) (Stevens *et al.*, 2008). The South African females have however higher obesity figures than Canadian females (17% vs. 13% for white females and 25% vs. 17% for black females) (Chiu *et al.*, 2010). For South African men, the largest occurrence of overweight and obesity was observed for white males (see Figures 29 to 32). Bates *et al.* (2008) reported that 30% of Native Latino males are overweight (BMI > 30). Similar to that observed for the females, South African males have lower obesity levels than American men (13% vs. 22% for white males (see Figure 30) and 1% vs. 28% for black males (see Figure 29)) (Stevens *et al.*, 2008). South African men were also observed to have lower obesity levels than Canadian men (13% vs. 15% for white males and 1% vs. 11% for black males) (Chiu *et al.*, 2010).

It should however be noted that the BMI data used during this study applies to the South African military (SANDF) population and not the general South African

population. If compared to reported values for percentages of overweight and obese South African black males and females in the general populations, the percentages reported during this study fall within the percentage ranges reported by Walker *et al.* (2001) for females, but slightly below reported ranges for males. For black females this study reports 32% overweight and 25% obese (see Figure 18) compared to Walker *et al.* (2001) 29 – 42% for overweight and 22 – 34% obese, and for black males this study reports 13% overweight and 1% obese (see Figure 29) compared to 17 – 36% overweight and 4 – 8% obese.

Several studies have indicated a correlation between BMI and functional body strength, illustrating those persons with higher BMI displayed higher functional body strengths (Xiao et al, 2005; Meyer et al, 1996; Geladas et al, 2005; Van den Tillaar and Ettema, 2004). As a result, it is expected that the functional body strength figures observed for the South African population should be slightly lower than that for American males and females but higher than Canadian females and lower than Canadian males (see discussion on BMI > 25 above) (Stevens *et al.*, 2008; Chiu *et al.*, 2010).

The variations in body forms that were identified for males and females in the SANDF agree with body forms identified for other populations (see Table 8 and Figures 23 to 28 for females and Table 13 for males). National sizing systems used by the United Kingdom, Germany, Netherlands, Canada and America incorporates the body form variation in terms of height, ratio value (difference between hip and bust circumference) and hip type (hip circumference) for females, and body length and ratio values (chest to waist circumference) for males (Fan *et al.*, 2004). The American sizing systems commonly use the figure types called junior petite, junior, miss petite, miss, half-size, and woman. These figure types vary from each other with regard to body length (back length for upper body garments and inside leg length for lower body garments) and body circumference (bust, waist and hip for upper body garments, and waist and hip for lower body garments).

The body forms that were identified for SANDF males and females would furthermore impact on the functional body strength variations in this population. Several studies have indicated a correlation between BMI and functional body strength, illustrating those persons with higher BMI displayed higher functional body strengths (Xiao et al,

2005; Meyer et al, 1996; Geladas et al, 2005; Van den Tillaar and Ettema, 2004). This can clearly be observed in the South African data. The body form variances described by the first principal component is body circumferences (and depths for males) and BMI (see Table 8 and Figures 23 and 24 for females and Table 13 for males). The functional body strengths modelled for the boundary cases of this principal component illustrate that lower functional body strength is modelled for the boundary case with a lower BMI values (see MPC1- and FPC1- in Table 20) and higher functional body strength for the higher BMI values (see MPC1+ and FPC1+ in Table 20). Very similar functional body strengths were observed for models with similar BMI values (see MPC2- vs. MPC2+ and FPC2- vs. FPC2+ in Table 20). This trend is observed for both the SANDF male and female groups. In addition to this, several studies have indicated correlations between segment lengths and functional body strengths related to the segment lengths (Meyer *et al.*, 1996; Maeda *et al.*2001; Geladas *et al.*, 2005), and between stature and functional body strength (Sinaki et al, 2001; Geladas *et al.*, 2005; Van den Tillaar and Ettema, 2004). These correlations suggest that longer segment lengths and statures would result in higher functional body strengths. However, this trend was not observed in the South African data. The second principal component described variances in stature for the SANDF males and females. The functional body strengths modelled for the boundary cases of this principal component shows only slight variations, with the variations keeping in line with the slight variations observed in BMI and opposite to the variations in stature (see MPC2- vs. MPC2+ and FPC2- vs. FPC2+ in Table 20).

5.2 INVESTIGATING CORRELATION BETWEEN ANTHROPOMETRY AND FUNCTIONAL BODY STRENGTH VARIABLES

Very few *consistent* indications of strong correlations between anthropometric body dimensions and functional body strength variables were observed in the literature or when investigating correlations for the SANDF data. However some form of relationship between anthropometry and biomechanical strength must be assumed in order to accommodate both of these aspects in the biomechanical models. The most frequent medium correlations observed were between stature and mass (characterised as BMI) and functional body strength data (Xiao et al, 2005; Meyer et al, 1996; Geladas et al, 2005; Van den Tillaar and Ettema, 2004). Therefore, a correlation between BMI and functional body strength was assumed for the SANDF

population for the purpose of building these biomechanical models. Similar assumptions have previously been made in biomechanics full body model simulations (Rasmussen *et al.,* 2007; Andersen *et al.*, 2007; Annegarn *et al.*, 2007).

5.3 REPRESENTATIVE BIOMECHANICS FULL BODY MODELS

5.3.1 Muscle properties

The muscles used during this study were simple elements which consisted only of active elements and not of passive elements. In addition to the omission of passive elements, the active muscle elements did not incorporate any of the complexity typically associated with human muscle tissue. The active muscle elements included in this study incorporated only maximum muscle force (F_{max}). The complexity of the muscle is discussed in Section 2.4 of this document. The most widely published models include 1) the Force-Velocity Relationship where the muscle force generated varies with velocity, 2) the Force-Length Relationship where muscle tension varies at different muscle lengths and 3) Force-Time Relationship which refers to a delay in the development of muscle tension of the whole muscle tendon unit. The muscle force generated in the simple LifeMod muscle did not incorporate velocity, length or time variables. Several studies have used a similar simple muscle formulation during Biomechanical modelling (Pierce and Li, 2005; Amarantini *et al.*, 2010; Pel *et al.*, 2008). Arjmand and Shirazi-Adl (2006) incorporated active as well as passive muscle elements, but incorporating only the force-length relationship in the active elements.

In order to incorporate the complexity of the human muscle tissue, several studies have implemented Hill-type muscle models as well as electromyographic (EMG) information (de Oliveira and Menegaldo, 2010; Raasch *et al.*, 1997; Neptune and Hull, 1998). Although simple LifeMod muscle formulations were used in the development of these biomechanics models, later versions of LifeMod have implemented the Hill-type muscle formulation. Hill-type muscle models are developed from the material behaviour of the muscle model adopted from the original work by Hill (1970). Hill-type muscle models operate on the traditional combination of an active contractile element and a passive parallel elastic element. The contractile element are elastic and contains a muscle activation state which controls the active muscle force capability, while the parallel elastic element exerts opposing forces that more accurately simulate the movement and force exertion of real muscles. The

combination introduces the Force-Velocity relationship and the Force-Length relationship of the muscle force generation into the formula. The passive element incorporates visco-elastic material properties. A schematic representation of the Hill-type muscle formula is illustrated in Figure 68. The muscle force is calculated by the following series of equations :

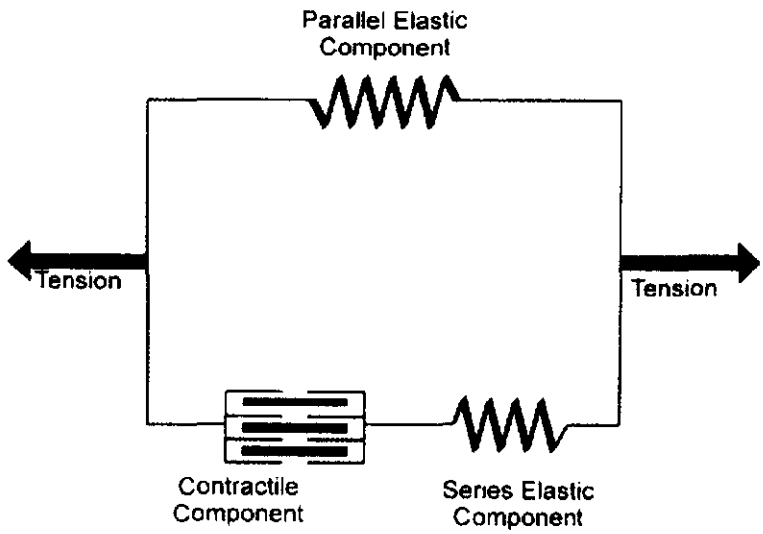

Figure 68 : Schematic representation of the Hill-type muscle formula (Knudson, 2007)

$$F_{muscle} = F_{CE} + F_{PE}$$

Where : F_{CE} = Active muscle element
F_{PE} = Passive muscle element

$$F_{PE} = \sigma \times pCSA$$

Where : σ = passive muscle stress; σ = (k x ε) / (1-ε/asym)
$pCSA$ = physiological cross sectional area
ε = strain defined as the elongation relative to the resting length of the muscle; ε = (l_{curr} – l_{free}) / l_{free}

k = passive muscle stiffness
asym = strain asymptote
l_{curr} = current (instantaneous) length of the muscle
l_{free} = free length of the muscle at rest when it is removed from the body

$$F_{CE} = A(t) \times \sigma_{max} \times pCSA \times f_H(v_r) \times f_L(l_r)$$

Where : $A(t)$ = activation state (normalized between 0-resting and 1-maximum activation)
σ_{max} = maximum isometric muscle stress
$pCSA$ = physiological cross sectional area
$f_H(v_r)$ = normalized active force-velocity relation (Hill-curve)
$f_L(l_r)$ = Normalized active force-length relation
v_r = dimensionless lengthening velocity
l_r = dimensionless muscle length

Several other researchers attempted to incorporate even more aspects of muscle complexity in addition to that incorporated in the Hill-type muscle models. Lu *et al.* (2010) developed a skeletal muscle that incorporates visco-hyperelastic properties. This method used the definition of a Helmhotlz free energy function (Ogden, 1984). The Helmholtz energy function can be decoupled into an elastic energy function and a viscous energy function. The strain energy function was furthermore divided into volumetric and isochoric parts to describe a quasi-incompressible solid. The skeletal muscle is modelled as an active, quasi-incompressible, transversely isotropic and visco-hyperelastic composite, comprising of an isotropic solid ground substance and the muscle fibres.

A maximum muscle stress (σ) of 35 N/cm^2 was used in the LifeMod whole body models. This value is similar to that used by McGill and Norman (1986) and Cholewicki *et al.* (1995). This value furthermore falls within the range of values reported for maximum muscle stress by several researchers (17.2 - 23.5 N/cm^2 reported by Bodine *et al.* (1987), 22.5 N/cm^2 reported by Powel *et al.* (1984), 30

N/cm^2 reported by Brand *et al.* (1986) and Friederich and Brand (1990), 40 N/cm^2 reported by Amarantini *et al.* (2010), 50 N/cm^2 reported by Sverdlova and Witzel (2010), and 73 N/cm^2 reported by Wickiewicz *et al.* (1983)).

The ranges of muscle cross sectional areas (pCSAs) observed in this range of models compares to findings in the literature. De Oliveira and Menegaldo (2010) found pCSAs of the Soleus muscles to be between 98.4 and 140.4cm^2, the gastrocnemius medialis to be between 36.8 and 57.9cm^2, and the gastrocnemius lateralis to be between 19.6 and 32 cm^2. During this study, pCSAs for the Soleus ranged from 69.9 to 237.8 cm^2, for the gastrocnemius medialis from 24.6 to 83.7cm^2, and for the gastrocnemius lateralis from 11.7 to 39.9cm^2 (see Table 22).

The physiological cross sectional areas (pCSA) of the muscles in the separate models describe the differences in muscle force output ability between the models. Taking into consideration the stature, mass, BMI and functional body strengths, certain trends were expected in the variances in pCSA values between models. Because all factors influencing the pCSA, that is stature, BMI, mass and input functional body strengths, of the smaller models are less than that of the larger models in the principal component 1 group for both males and females, the pCSAs for the smaller models should be smaller than that of the larger models (see Table 14 for anthropometric dimensions of the models, Table 20 for the functional body strengths of the models, and Table 22 for pCSA values of the models). Similarly, because at least BMI, mass and functional body strengths, of the large models of the second principal component is smaller than that of the first principal component for males and females, it is expected that the pCSAs for the larger male and female models of the second principal component should be smaller than those of the first principal component (see Tables 14, 20 and 22). These trends were however not observed, especially for the pCSAs of the leg muscle groups. For both the males and females the pCSAs of the smaller model were larger than those of the larger model of principal component 1 (see MPC1- vs. MPC1+ and FPC1- vs. FPC1+ in Table 22). Also, the pCSAs for the larger male model of the second principal components were not smaller than those of the first principal components, as would be expected (see MPC2+ vs. MPC1+ in Table 22). The pCSA for the larger female model of the second principal component, although smaller than the large model of the first principal

component, was also smaller than the small model, which again does not agree with the expected trend (see FPC2+ vs. FPC1+ and FPC1- in Table 22).

The pCSAs for the back muscles groups were more in line with the expected trends. The pCSAs of the small male and female models of the first principal components were smaller than the large models (see MPC1- vs. MPC1+ and FPC1- vs. FPC1+ in Table 22). Differences in the expected trends were again observed with the male and female models of the second principal components. The large male and female models of the second principal components were smaller than the large models of the first principal components, as expected. However, the pCSAs of these models were also smaller than the small models in the first principal component groups, which were not expected (see MPC2+ vs. MPC1+ and MPC1-, and FPC2+ vs. FPC1+ and FPC1- in Table 22).

The pCSA values are directly linked to the maximum force that can be generated by each individual muscle in the models (see Section 3.4.3.1). A model with the capability of producing larger muscle forces, will be expected to produce larger functional strength outputs. As a result, the trends observed in pCSA values for the eight biomechanical models (Table 22) would result in overall functional strengths of biomechanical models that are not in-line with the functional strength values that have been used as inputs to build these models. This will also result in biomechanical models that are for example required to represent weaker persons in the SANDF population, but which have functional strengths that far exceed the functional strengths of the actual population.

5.3.2 Muscle force output and functional body strength

Several studies rely on one biomechanical model to provide an indication of muscle force output under a range of tasks and conditions (Sverdlovo and Witzel, 2010). It was evident from the muscle force outputs that a large range in maximum muscle forces resulted from this range of models representing a population of military personnel. Similar findings were reported by de Oliveira and Menegaldo (2010).

5.3.2.1 Leg strength functional task

The results indicated that the knee extensor muscle groups, Rectus femoris, Vastus medialis and Vastus lateralis consistently produced the largest muscle force outputs during the leg push functional task. The Vastus intermedius muscle group is not modelled in the LifeMod Biomechanical modelling muscle set. The forces produced by these three muscle groups ranged between 892 – 4965 N for the Rectus femoris, 521 – 1814 N for the Vastus medialis, and between 521 – 1638 N for the Vastus lateralis (see Table 21). These values are lower than the values reported by Svedlova and Witzel (2010), who estimated maximum muscle force for the Vastus medialis and lateralis to be 3220N and 3340N respectively. The values observed during this study were also lower than the findings of Amarantini *et al.* (2010). Amarantini *et al.* (2010) modelled a half squat movement with a load of 14 kg on the shoulders and by means of an EMG assisted biomechanical model generated Vastus medialis and Vastus lateralis muscle forces ranging up to a maximum of approximately 3500 N.

The trends between models in the total muscle forces generated by the primary knee extensor muscles, Rectus femoris, Vastus medialis and Vastus lateralis, agrees with the findings of the pCSAs of the leg muscle groups (as discussed in Section 5.3.1). Again the expected trends were not observed. Rather, the total muscle forces produced by the small male and female models of the first principal component were larger than those of the large models (see Table 21). Also, the total muscle forces of the large male model of the second principal component was not smaller than that of the first principal component, and the large female model of the second principal component was smaller than both the small and large models for the first principal component.

Closer investigation of the muscle force graphs highlighted some similarities between the models. The muscle force generated by the Rectus femoris to execute the leg push functional task, was consistently higher than that produced by the Vastus medialis and lateralis muscles (see Figures 37 to 41), with the exception of the large female model of the second principal component (see Figure 42). In addition, the forces generated by the Vastus medialis and lateralis are very similar, and that produced by the Vastus medialis is slightly larger than that of Vastus lateralis (see Figures 37 to 42). Since all the models produced the same functional leg push task, it

was expected that similar muscle force graphs would be observed for all the models. The only consistency in the muscle force graphs was observed for the Vastus medialis and Lateralis muscles, where the muscle forces increased to a peak with the start of the leg push, and decreased as the leg moved into full extension. The only exception in this trend was observed for the small male and female models of the first principal components (see Figures 37 and 40). Several differences in the muscle force graphs were observed, the largest of which is the force graph of the Rectus femoris muscle. No consistent trend was observed for where the maximum force of the Rectus femoris muscle was reached or what the magnitude of the Rectus femoris muscle maximum force was, in comparison with the Vastus medialis and lateralis muscles.

Although a lot of care was taken to ensure that model postures were similar during capture of the motion data, and that the leg push task was executed at the same isokinetic speed, closer inspection of the initial leg push posture highlighted some differences in the models (see Figures 43 to 54). From the front, the leg positions in relation to the models' hips, are similar and in line for the small male principal component 1 model and the female largest principal components 1 and 2 models (Figures 44, 52 and 54). The leg position of the male largest principal components 1 and 2 models was more lateral to the hip (Figures 46 and 48) and for the small female principal component 1 model was more medial (Figure 50). In addition to these variations in leg position in relation to the hip, the feet for the small male principal component 1 and large male principal component 2 were everted in varying degrees (Figures 44 and 48). From the side, a similar posture was observed for the large male and female principals 1 and 2 models (Figures 45, 47, 51 and 53). The small male and female models of principal component 1 had a pelvis that was more tilted towards the back and the male model had a much more stooped trunk (Figures 43 and 49). These variances in side postures could be caused by the variances in body and segment lengths, since the same seat and foot support heights were utilised during the capturing of motion data.

Due to the magnitude of a muscle force required to execute a task being directly related to the lever arm and angle at which the force is being exerted, it can be expected that any variances in model postures would result in differences in muscle force totals and muscle force graphs. It is therefore speculated that the differences

observed in pCSA, force magnitudes and force graphs are a direct result of the differences in model postures. Similar findings were noted by Hoffmann *et al.* (2007), which was the driving force for significant research work being conducted at the University of Michigan to determine "standardized" postures for execution of certain tasks (Hoffmann *et al.*, 2007 and Wagner *et al.*, 2007).

The differences in force graphs highlighted the fact that the same functional task executed by different individuals with different body dimensions, would result in slight variations in postures, which in turn would result in variations in muscle requirement patterns. In spite of these differences, each individual would inevitably be able to execute the same task in a visibly similar manner.

5.3.2.2 Back strength functional task

The results indicated that the back extensor muscle groups, External oblique, and Erector spinae 1, 2 and 3, consistently produced the largest muscle force outputs during the back strength functional task (see Figures 55 to 60).

The trends observed between models in the maximum muscle forces generated by the External oblique, and Erector spinae 1, 2 and 3 muscles, agree with the findings of the pCSAs of the back muscle groups (as discussed in Section 5.3.1) (see Tables 21 and 22). The observed trends agreed partly with the expected results for pCSA values based on the model stature, mass, BMI and functional strength values (see Tables 14, 20 and 22). The observed trends agreed with the expected trends for the male principal component 1 models (MPC1- vs. MPC1+ in Table 21), where the total muscle forces produced by the small model is smaller than that of the large model, as well as between the two large female models (FPC1+ vs. FPC2+ in Table 21), where the model of principal component 1 is larger than that of principal component 2. On the other hand, the observed trends did not agree with the expected trends for the female principal component 1 (FPC1- vs. FPC1+ in Table 21) or for the large male models of principal components 1 and 2 (MPC1+ vs. MPC2+ in Table 21).

These discrepancies in the observed maximum muscle force output trends compared to the expected trends, would result in biomechanical models that fail to predict functional body strengths for the target SANDF population groups correctly. Per

example, the smaller, weaker biomechanical models will fail to predict the inability of the weaker SANDF population group to execute a specific task.

Closer investigation of the muscle force graphs highlighted a few similarities in some of the models (see Figures 55 to 60). Since a similar functional task was being executed by all the models, it was expected that similar primary back muscle force magnitudes over time would be observed. These similarities were observed in the back muscle force graphs for the large female principal components 1 and 2 models and the large male principal component 1 model. For these models, the largest muscle forces were produced by the Erector spinae 2, followed by the Erector spinae 1 and then the External oblique muscles (see Figure Figures 56, 59 and 60). Variations from this trend were observed for the small male and female principal component 1, and large male principal component 2 models (see Figures 55, 57 and 58). No similarities were observed between the muscle force patterns of these models.

Although a lot of care was taken to ensure that model postures were similar during capturing of the motion data, closer inspection of the initial body postures highlighted some differences in the models. Similar postures were observed between the male large principal component 1 model, and the female large principal components 1 and 2 models (see Figures 62, 65 and 66), where the models executed the back strength functional task with straight legs and the pelvis more tilted to allow for a more horizontally aligned back, than that of the other models (Figures 61, 63 and 64). The muscle force patterns of these three models displayed similar muscle force graphs (Figures 56, 59 and 60). The small male principal component 1, although also having straight legs, had a more upright pelvis and back (see Figure 61). The large male principal component 2 model and the small female principal component 1 model executed the back strength functional task with bent knees. Although differences were observed in the muscle force graphs for these two models, some similarities (when compared to the other back strength muscle force graphs (Figures 55, 56, 59 and 60)) could be observed (see Figures 57 and 58).

Similar to the findings for the leg push muscle force graphs, the differences in force graphs for the back strength functional task highlighted the fact that the same functional task executed by different individuals with different body dimensions, would

result in slight variations in postures, which in turn would result in variations in muscle requirement patterns.

5.3.3 Challenges in modelling Biomechanical muscles/ Biomechanical risk analysis

The biomechanics of the human body is a very complicated synergy of muscle, joint, ligament and bone segment interaction. To be able to create all these elements in a model that represents human movement and force output is a substantial challenge which has been accomplished to a large extent in the LifeMod^{TM} biomechanical software package. However, as is inherent in any simulation of the real event, some modelling challenges occurred due to shortcomings in the default LifeMod Human body model. In spite of these challenges, *the advantages* of being able to run predictive biomechanics models for research and evaluation purposes still outweigh the challenges inherent to the modelling process. The biomechanical simulation of the human body remains a work in progress.

The first challenge focused around joints and joint stability. During the inverse dynamics simulation, all the segments and muscle elements were passive and were moved by splines created from the Qualisys motion data imported into the model for this purpose. The function of the joint elements was to keep segments connected to each other with a degree of stiffness and dampening. Any noise in the motion data (however small) was transferred to the biomechanical model as irregular motion and caused instability in this dynamical model. Joints with higher stiffness assisted in providing stability to the moving model and overrode the irregular motion caused by small noise in the motion data. Higher joint stiffness also provided stability during forward dynamics, especially where adequate stability was not provided across a joint by muscle and ligament elements.

Even though the default LifeMod biomechanical model represents the human biomechanical system, no ligaments are provided across joints. As a result, certain modelling scenarios, such as joint angles larger than 90 degrees, rely on joint stiffness to provide stability across the joints. The joint stiffness however does not afford only positive contribution to the model. If joints are too stiff in any of the movement planes (sagittal, frontal or transverse), it causes artificial restraint against the muscles, which requires additional muscle strength to overcome in the forward

dynamics models. Thus, when the researcher is interested in the most accurate muscle force representation of the real life event, joint stiffness of near zero should be used. Therefore, each movement and functional strength task requires a careful balance between slightly higher joint stiffness in some axes to provide stability to the moving model, and lower joint stiffness in other axes to provide as little resistance to muscle force exertion as possible. Joints where poor support is provided due to too few muscles included the scapula, lumbar and thoracic joints.

Another aspect of the modelling process that produced significant challenges included the effect of the model posture on the force exertion and also the model's ability to execute a task. Discrepancies between recorded motion data marker locations (imported into LifeMod as motion splines) and the motion marker locations on the model, resulted in awkward postures either at the initial/start condition (if the simulation analysis function in LifeMod was used) or during the motion and task execution. Even though considerable care was taken to place the markers on the human subjects (used during the recording of the motion data) as close to the defined locations in the LifeMod manual as possible, small discrepancies between marker locations between the human subjects and the model were still observed. Awkward body postures resulting from marker location discrepancies frequently resulted in muscle force requirements that exceeded the ability of the model. Such scenarios were difficult to identify, and required careful inspection of the model and each joint posture. Once identified, these settings were furthermore very difficult to correct and sometimes required the model to be rebuilt with slight adjustments in segment lengths to ensure better correlation between the recorded motion data and marker locations on the model. The impact of skin movement during marker location capture remains undefined.

Another challenge surrounded the trouble shooting approach advised to provide solutions to failures in modelling simulations. A synergy of settings can be adjusted in the LifeMod modelling software package. Identifying which setting required adjustment to solve specific problems, remains a challenge. Poor guidance by the LifeMod Support team contributed to this challenge. Settings include those discussed earlier in this Section. Other settings that also had to be optimized included the motion tracker agent stiffness, contact element properties, muscle force servo proportional and derivative gain and contact bushing settings.

Finally, errors were identified in the LifeMod software package during the use of Hill's muscle elements. The software erroneously assigned a 0 value to random muscles. The LifeMod software developers are aware of this error in the software package and are busy correcting it in the new update. The temporary solution to this problem was to utilize only simple muscle elements.

CHAPTER 6 : CONCLUSIONS AND RECOMMENDATIONS

In order to determine anthropometric (body form) variations for SANDF males and females that should be included in the biomechanical models in order to represent these population groups, a combination of analysis techniques was used. This analysis approach included investigation of BMI distribution, correlations between anthropometric variables and PCA. Regardless of the omission of certain recognized analysis techniques, such as somatotyping or visual body form identification, the analysis approach used during this study was successful in highlighting variations in body forms typically observed for males and females in the SANDF.

Extensive modelling has been conducted in the LifeMod^{TM} biomechanics software with the aim of creating a range of biomechanical models, consisting of four female and four male models that represent the SANDF in anthropometry and functional body strength. The modelling process required multiple iterations to identify optimal model characteristics such as joint stiffness and damping, foot-floor contact characteristics, motion tracking settings and muscle properties. Validation of the functional body strength capabilities of the models indicated a maximum of 34 percentage estimation error when compared to the actual functional body strength data. Errors in functional strength values predicted by the model could be attributed to a range of modelling anomalies, such as inconsistencies between motion data and the model, poor muscle representation in specific areas such as the abdomen and shoulders, as well as joint instability and poor force exertion at large (> 90 degrees) joint angles.

All the challenges encountered during the modelling process require an in depth understanding and extensive experience in the LifeMod^{TM} software environment, to solve. It also requires enough modelling time to ensure that all aspects of the model are optimised for the specific biomechanical problem being investigated.

Taking all the above results and conclusions into consideration, it is finally concluded that the LifeMod^{TM} software does not lend itself to the current approach of using a range of models to investigate biomechanical risks by representing functional body strength of the SANDF population. The detail required when modelling a biomechanical task in the LifeMod^{TM} software, makes the software a very powerful

APPENDIX A :
EQUIPMENT LIST

Table A-1 : Equipment list

Equipment	Date of calibration
LifeMod™ Biomechanics Software	N/A
Qualisys Motion Capture System	Calibration in-house before use.

APPENDIX B :
ANTHROPOMETRY AND FUNCTIONAL BODY STRENGTH VARIABLES FOR WHICH CORRELATION WAS INVESTIGATED

Table B-1 : SANDF Anthropometry and functional body strength variables for which correlations were investigated

Year of survey (dataset)	Anthropometry variables	Biomechanics variables
2001	Stature	Left and Right Grip Strength
	Mass	Trolley Push & Pull
		Left and right Leg Strength
		Wheel Turning clockwise and counter-clockwise
		Wrench Turning
		Left and right Arm Push & Pull
		Left and right Horizontal Lever Push (Adduction) & Pull (Abduction)
		Left and right Vertical (overhead) Lift
2002	Stature	Left and right Grip strength
	Body mass	Back strength
	Trochanter to lateral femoral epicondyle length	Left and right concentric arm flexion
	lateral femoral epicondyle to lateral malleolus length	Left and right eccentric arm flexion
	Trochanter to floor length	Left and right concentric arm extension
	Acromion to lateral humeral epicondyle length	Left and right eccentric arm extension
	Acromion to styloid process length	Left and right concentric leg flexion
	Left and right arm length	Left and right eccentric leg flexion
	Left and right leg length	Left and right concentric leg extension
		Left and right eccentric leg extension
2003	Stature	Knee strength
	Mass	Waist strength
	Leg Length	Shoulder strength
	Acromion height	
	Stylion height	
	Arm Length	
	Chest circumference	
	Waist circumference	

APPENDIX C :
LIST OF MUSCLES MODELLED IN LIFEMOD WHOLE-BODY MODEL

Full Body Muscle Set

A detailed set of 118 muscles is automatically generated and attached to the bones at anatomical landmarks. The set is scalable with the skeletal geometry. Each muscle consists of a "learning" or contractile element in series with a spring damper.

Sections:
Upper Arm Muscle Set
Lower Arm Muscle Set
Leg Muscle Set
Neck/Trunk Muscle Set
Back View

Upper Arm Muscle Set

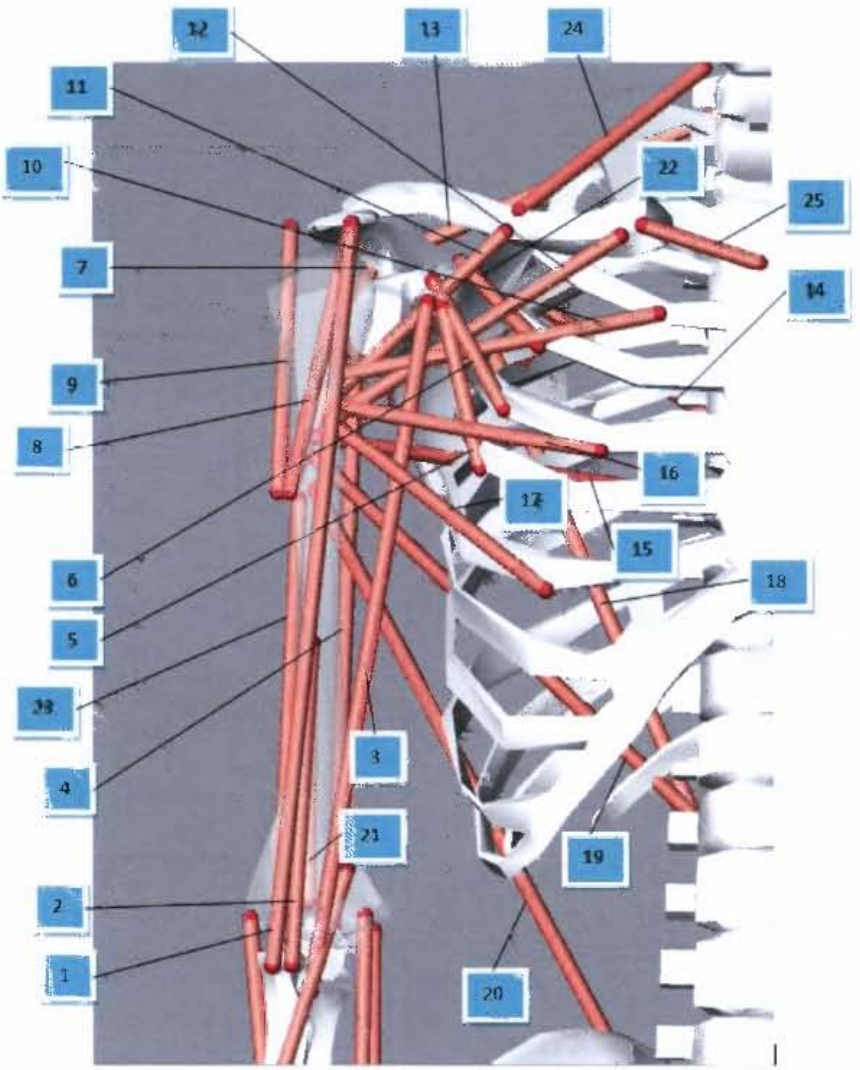

Figure 1: Muscle set for upper arms (front view)

ID	Muscle	Attach Proximal	Attach Distal
1	Biceps Brachii 2	scapula	lower_arm
2	Brachioradialis	upper_arm	lower_arm
3	Biceps Brachii 1	scapula	lower_arm
4	Triceps Brachii 1	scapula	lower_arm
5	Pectoralis Minor 3	scapula	upper_torso
6	Pectoralis Minor 2	scapula	upper_torso
7	Deltoideus 3	scapula	upper_arm
8	Deltoideus 1	scapula	upper_arm
9	Deltoideus 2	scapula	upper_arm
10	Pectoralis Major 1	upper_torso	upper_arm
11	Pectoralis Major 4	scapula	upper_arm
12	Pectoralis Major 5	scapula	upper_arm
13	Trapezius 1	neck	scapula
14	Trapezius 2	upper_torso	scapula
15	Latissimus Dorsi 1	upper_torso	upper_arm
16	Pectoralis Major 2	upper_torso	upper_arm
17	Pectoralis Major 3	upper_torso	upper_arm
18	Trapezius 3	scapula	central_torso
19	Latissimus Dorsi 2	upper_arm	central_torso
20	Latissimus Dorsi 3	upper_arm	lower_torso
21	Triceps Brachii 2	upper_arm	lower_arm
22	Pectoralis Minor 1	scapula	upper_torso
23	Triceps Brachii 3	upper_arm	lower_arm
24	Trapezius 4	neck	scapula
25	Subclavius	upper_torso	scapula

Lower Arm Muscle Set

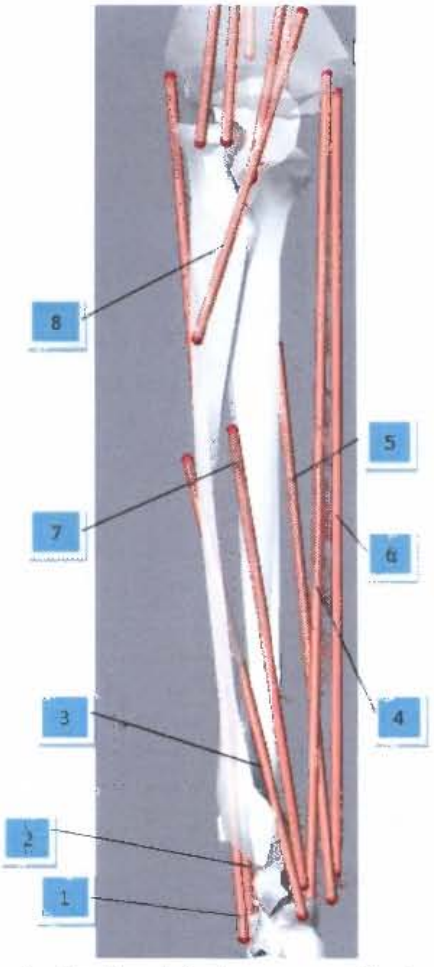

Figure 2: Muscle set for lower arms (front view)

ID	Muscle	Attach Proximal	Attach Distal
1	Extensor Carpi Rad. Longus	upper_arm	hand
2	Extensor Digiti Minimi	lower_arm	hand
3	Abductor Pollicis Longus	lower_arm	hand
4	Flexor Capi Radialis	upper_arm	hand
5	Flexor Dititorum Profundus	lower_arm	hand
6	Flexor Carpi Ulnaris	upper_arm	hand
7	Flexor Pollicus Longus	upper_arm	hand
8	Pronator Teres	upper_arm	lower_arm

Leg Muscle Set

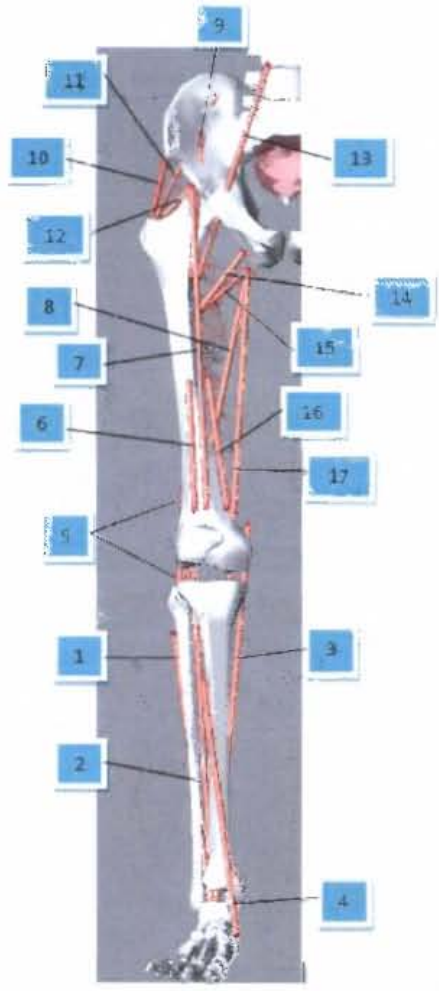

Figure 3: Muscle set for legs (front view)

ID	Muscle	Attach Proximal	Attach Distal
1	Soleus	lower_leg	foot
2	Gastrocnemius 2	upper_leg	foot
3	Gastrocnemius 1	upper_leg	foot
4	Tibialis Anterior	lower_leg	foot
5	Biceps Femoris 1	upper_leg	lower_leg
6	Vastus Lateralis	upper_leg	lower_leg
7	Rectus Femoris	lower_torso	lower_leg
8	Biceps Femoris 2	lower_torso	lower_leg
9	Iliacus	lower_torso	upper_leg
10	Gluteus Medius 1	lower_torso	upper_leg
11	Gluteus Medius 2	lower_torso	upper_leg
12	Gluteus Maximus 2	lower_torso	upper_leg
13	Psoas Major	central_torso	upper_leg
14	Gluteus Maximus 1	lower_torso	upper_leg
15	Adductor Magnus	lower_torso	upper_leg
16	Vastus Medialis	upper_leg	lower_leg
17	Semitendinosus	lower_torso	lower_leg

Neck/Trunk Muscle Set

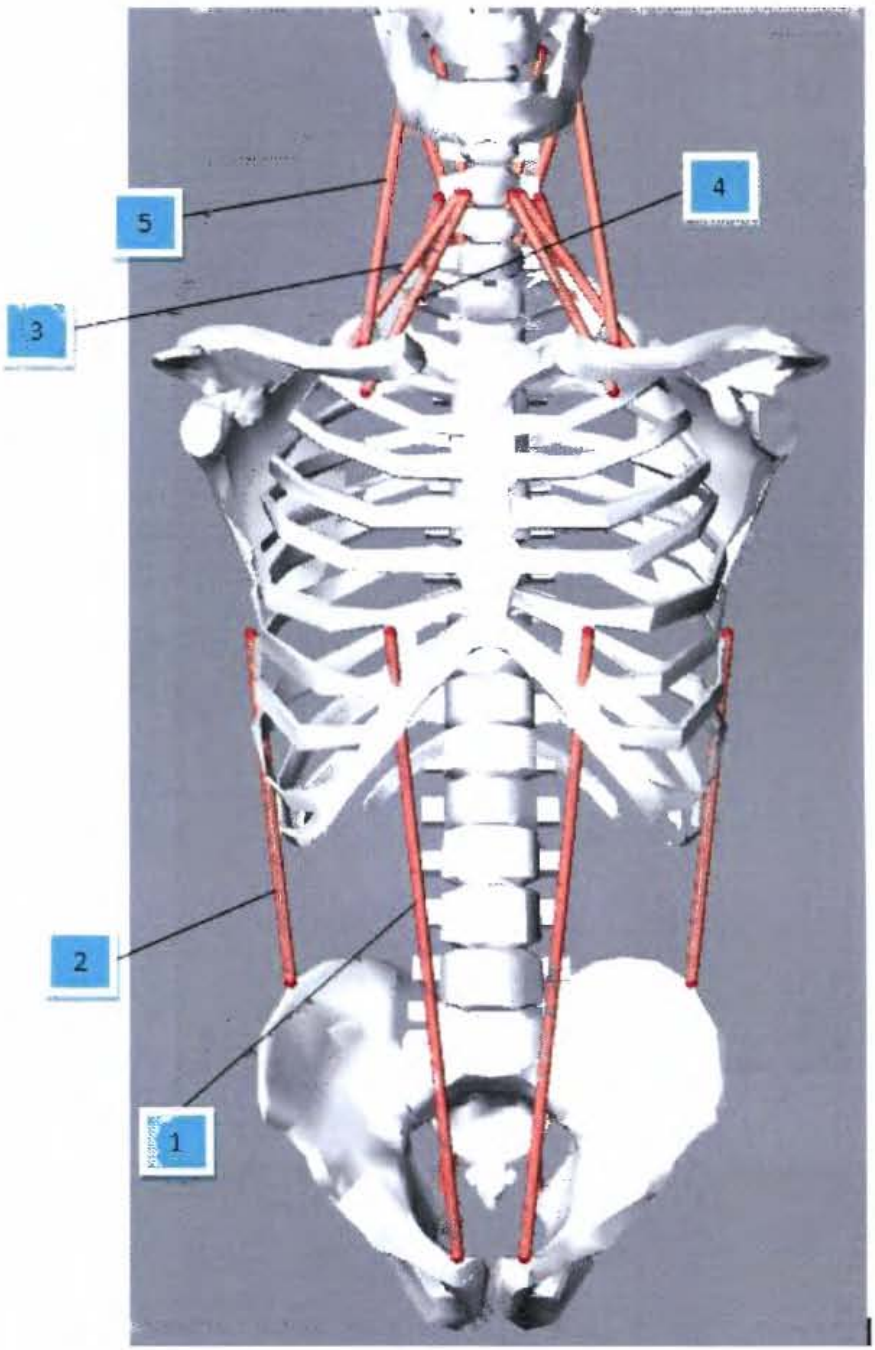

Figure 4: Muscle set for trunk (front view)

ID	Muscle	Attach Proximal	Attach Distal
1	Rectus abdominis	upper_torso	lower_torso
2	Oblique external	upper_torso	lower_torso
3	Scalene medius	neck	upper_torso
4	Scalene anterior	neck	upper_torso
5	Sternocleidomastoid	neck	scapula

REFERENCES

Alemany, S., Nacher, B., Gonzalez, J.C., Alcantara, E., Gomez, F., Montero, J., Vera, P. and Garcia, A.C. (2006). Prediction model of children footprints growing using geometric morphometric techniques. *Proceedings of the International Ergonomics Association (IEA) Conference.* Maastricht, 10-14 July.

Amarantini, D., Rao, G. And Berton, E. (2010). A two-step EMG-and-optimization process to estimate muscle force during dynamic movement. *Journal of Biomechanics,* 43, 1827-1830.

Andersen, M.S., Rasmussen, J. and Damsgaard, M. (2007). Scaling and local marker coordinates determination of musculoskeletal systems. *Proceedings of the 2007 Digital Human* Modelling *for Design and Engineering Conference.* Seattle, 12-14 June.

Annegarn, J., Rasmussen, J., Savelberg, H.H.C.M., Verdijk, L.B. and Meijer, K. (2007). *Scaling strength in human simulation models.* Retrieved July 15, 2007, from www.anybodytech.com.

Anybody Technology A/S. (2008). *The Anybody Modelling System™.* Retrieved August 15, 2008, from www.anybodytech.com.

Arjmand, N. and Shirazi-Adl, A. (2006). Model and in vivo studies on human trunk load partitioning and stability in isometric forward flexions. *Journal of Biomechanics*, 39, 510-521.

Bataller, A., Alcantara, E., Gonzalez, J.C., Garcia, A.C. and Alemany, S. (2001). Morphological Grouping of Spanish Feet Using Clustering Techniques. *Proceedings of the 5th Symposium on Footwear Biomechanics.* Zurich, 5-7 July.

Bates, L.M., Acevedo-Garcia, D., Alegría, M. and Krieger, N. (2008). Immigration and Generational Trends in Body Mass Index and Obesity in the United States: Results of the National Latino and Asian American Survey, 2002–2003. *American Journal of Public Health*, 98(1), 70–77.

Ben Azouz, Z., Roux, M., Shu, C. and Lepage, R. (2005). Characterizing Human Shape Variation Using 3-D Anthropometric Data. *The Visual Computer International Journal of Computer Graphics*, 22 (5), 302-314.

Biomechanics Research Group, Inc. (2008). *LifeMod™ Biomechanics Modeller.* Retrieved on August 15, 2008 from www.biomechanicsresearchgroup.com.

Bodine, S.C., Roy, R.R., Eldred, E., Edgerton, V.R. (1987). Maximal force as a function of anatomical features of motor units in the cat tibialis anterior. *Journal of Neurophysiology*, 57, 1730-1745.

Brand, R.A., Pedersen, D.R., Friederich, J.A. (1986). The sensitivity of muscle force predictions to changes in physiologic cross-sectional area. *Journal of Biomechanics*, 19, 589-596.

Bredenkamp, K. (2005). Investigation of the design of the SANDF service dress clothing. *ERGOTECH Document P0533/2005/02.* Centurion: ERGOnomics TECHnologies.

Bredenkamp, K. (2007). The characterisation of the male and female body forms of the SANDF. *ERGOTECH Document P0683/2007/01.* Centurion: ERGOnomics TECHnologies.

Bredenkamp, K. and Skelton, S. (2009). Footwear Programme: Foot form characterisation and detailed footwear development plan. *ERGOTECH Document P0837/2009/01.* Centurion: ERGOnomics TECHnologies.

Calisse, J., Rohlmann, A. and Bergmann, G. (1999). Estimation of trunk muscle forces using the finite element method and in vivo loads measured by telemeterized internal spinal fixation devices. *Journal of Biomechanics*, 32 (7), 727-731.

Carlsteds, C.A. and Nordin, M. (1989). Biomechanics of tendons and ligaments. In M. Nording & V.H. Frankel, (Eds.). *Basic biomechanics of the musculoskeletal system*. Philadelphia: Lea & Febiger.

Carter, J.E.L. (2002). *Anthropometry Illustrated*. Surrey: Ross, Carr & Carter in association with TeP and Rosscraft.

Chaffin, D.B. (1997). Development of Computerized Human Static Strength Simulation Model for Job Design. *Human Factors and Ergonomics in Manufacturing,* 7(4), 305-322.

Chaffin, D.B., Woolley, C., Dickerson, C. and Parkinson, M. (2004). Modelling of object movement capability in the spinal cord injured population. *International Journal of Industrial Ergonomics*, 33, 229-236.

Chiu, M., Austin, P.C., Manuel, D.G. and Tu, J.V. (2010). Comparison of cardiovascular risk profiles among ethnic groups using population health surveys between 1996 and 2007. *Canadian Medical Association Journal*, 182(8), E301–E310.

Cholewicki, j. and McGill, S.M. (1994). EMG assisted optimization: a hybrid approach for estimating muscle forces in an indeterminate biomechanical model. *Journal of Biomechanics,* 27(10), 1287-1289.

Cholewicki, J., McGill, S.M. and Norman, R.W. (1995). Comparison of muscle forces and joint load from an optimization and EMG assisted lumbar spine model: Towards development of a hybrid approach. *Journal of Biomechanics*, 28 (3), 321-331.

Coblentz, A., Mollard, R. and Ignazi, G. (1991). Three-dimensional face shape analysis of French adults, and its application to the design of protective equipment. *Ergonomics*, 34 (4), 497 – 517.

Cooper, G. and Ghassemieh, E. (2007). Risk assessment of patient handling with ambulance stretcher systems (ramp/(winch), easi-loader, tail-lift) using biomechanical failure criteria. *Medical Engineering & Physics*, 29, 775-787.

Cyron, B.M. and Hutton, W.C. (1978). The fatigue strength of the lumbar neural arch in spondylolysis. *Journal of Bone and Joint Surgery*, 60B, 234-238.

Davis, K.G., Jorgensen, M.J. and Marras, W.S. (2000). An investigation of perceived exertion via whole body exertion and direct muscle force indicators during the determination of the maximum acceptable mass of lift. *Ergonomics*, 43 (2), 143-159.

Daynard, D., Yassi, A., Cooper, J.E., Tate, R., Normal, R. and Wells, R. (2001). Biomechanical analysis of peak and cumulative spinal loads during simulated patient-handling activities: a substudy of a randomized controlled trial to prevent lift and transfer injury of health care workers. *Applied Ergonomics*, 32, 199-214.

De Oliveira, L.F. and Menegaldo, L.L. (2010). Individual-specific muscle maximum force estimation using ultrasound for ankle joint torque prediction using an EMG-driven Hill-type model. *Journal of Biomechanics*, Article in Press, doi: 10,1016/j.jviomwxh.2010.05.035.

Delp, S.L., Loan, J.P., Hoy, M.G., Zajac, F.E., Topp, E.L. and Rosen, J.M. (1990). An interactive graphics-based model of the lower extremity to study orthopaedic surgical procedures. *IEEE Transactions on Biomedical Engineering*, 37, 757-767.

Delp, S.L., Anderson, F.C., Arnold, A.S., Loan, P., Habib, A., John, C., Guendelman, E., Thelen, D.G. (2007). OpenSim: Open-source software to create and analyze dynamic simulations of movement. *IEE Transactions on Biomedical Engineering,* 54, 1940-1950.

Department of Defence Annual Report FY 2006-2007. (2007). Retrieved on December 15, 2007, from www.dod.mil.za.

Dietrich, M., Kedzior, K. and Zagrajek, T. (1991). A biomechanical model of the human spinal system. *Proceedings of the Institution of Mechanical Engineers-Part H – Journal of engineering in medicine*, 1, 19-26.

Dolan, P. and Adams, M.A. (1993). The relationship between EMG activity and extensor moment generation in the erector spinae muscles during bending and lifting activities. *Journal of Biomechanics*, 26(4-5), 513-522.

Douty, H. J. (1954). Objective Figure Analysis. *Journal of Home Economics,* 46 (1), 24-26.

Dysart, M.J. and Woldstad, J.C. (1996). Posture prediction for static sagittal-plane lifting. *Journal of Biomechanics*, 29 (10), 1393-1397.

Fan, J. Yu, W. and Hunter, L. (2004). *Clothing appearance and fit: Science and technology*. Cambridge: Woodhead Publishing.

Fox, E., Bowers, R. and Foss, M. (1993). *The physiological basis for exercise and sport.* Dubuque: Brown Communications Inc.

Friederich, J.A., Brand, R.A. (1990). Muscle fiber architecture in the human lower limb. *Journal of Biomechanics*, 23, 91-95.

Gardner-Morse, M.G., Stokes, I.A.F. and Laible, J.P. (1995). Role of muscles in lumbar spine stability in maximum extension efforts. *Journal of Orthopaedic Research*, 13(5), 802-808.

Gardner-Morse, M.G. and Stokes, I.A.F. (1998). The effects of abdominal muscle coactivation on lumbar spine stability. *Spine*, 23(1), 86-92.

Gaetan, M. (1989). Bringing anthropometric data into the 20th century. *Apparel Manufacturer*, 1(3), 24 – 31.

Geladas, N.D., Nassis, G.P. and Pavlicevic, S. (2005). Somatic and physical traits affecting sprint swimming performance in young swimmers. *International Journal of Sports Medicine,* 26, 139-144.

Godil, A. (2007). 3D Shape representation and analysis of the human head and body. *World Engineering Anthropometry Resource (WEAR) Conference proceedings.* Banff, 31 July – 1 August.

Gagnon, D., Lariviere, C. and Loisel, P. (2001). Comparative ability of EMG, optimization, and hybrid modelling approaches to predict trunk muscle forces and lumbar spine loading during dynamic sagittal plane lifting. *Clinical Biomechanics*, 16(5), 359-372.

Goldberg, S.R. and Kepple, T.M. (2009). Muscle-induced accelerations at maximum activation to assess individual muscle capacity during movement. *Journal of Biomechanics,* 42, 952-955.

Gordon, C.C. and Brantley, J.D. (1997). Statistical Modelling of Population Variation in the Head and Face. *Proceedings of The Design and Integration of Helmet Systems International Symposium.* Boston, 3-5 December.

Granata, K.P. and Marras, W.S. (1993). An EMG-assisted model of loads on the lumbar spine during asymmetric trunk extensions. *Journal of Biomechanics*, 26(12), 1429-1438.

Granata, K.P. and Marras, W.S. (1995). An EMG-assisted model of biomechanical trunk loading during free-dynamic lifting. *Journal of Biomechanics*, 28(11), 1309-1317.

Gupta, D., Garg, AN. Arora, K. and Priyadarshini, N. (2006). Developing body measurement charts for garment manufacture based on a linear programming approach. *Journal of textile and apparel, technology and management*, 5 (1), 1-5.

Heath-Carter body types. (2008). Retrieved July 30, 2008, from www.brianmac.co.uk/bodytype.htm.

Hennessy, R.J., McLearie, S., Kinsella, A. and Waddington, J.L. (2005). Facial surface analysis by 3D laser scanning and geometric morphometrics in relation to sexual dimorphism in cerebral-craniofacial morphogenesis and cognitive function. *Journal of Anatomy*, 207, 283-295.

Hill, A.V. (1970). *The first and last experiments in muscle mechanics*. Cambridge: Cambridge University Press.

Hoffman, S.G., Reed, M.P. and Chaffin, D.B. (2007). Predicting force-exertion postures from task variables. *Proceedings of the 2007 Digital Human* Modelling *for Design and Engineering Conference.* Seattle, 12-14 June.

Hornby, S.T., Nunes, Q.M., Hillman, T.E., Stanga, Z., Neal, K.R., Rowlands, B.J., Allison, S.P. and Lobo, D.N. (2005). Relationships between structural and functional measures of nutritional status in a normally nourished population. *Clinical Nutrition,* 24, 421-426.

3D Imaging, modelling and visualisation. (2007). Retrieved August 15, 2007, from http://iit-iti.nrc-cnrc.gc.ac.

Hudson, J.A., Zehner, G.F. and Meindl, R.S. (1998). The USAD multivariate accommodation method. *Proceedings of the Human Factors and Ergonomics society (HFES) 42nd annual meeting.* Chicago, 5-9 October.

Hughes, R.E., Chaffin, D.B., Lavender, S.A. and Andersson, G.B.J. (1994). Evaluation of muscle force prediction models of the lumbar trunk using surface electromyography. *Journal of Orthopometric Research*, 12, 689-698.

Jorgensen, M.J., Davis, K.G., Kirking, B.C., Lewis, K.E.K. and Marras, W.S. (1999). The significance of biomechanical and physiological variables during the determination of the maximum acceptable mass of lift. *Ergonomics*, 42(9), 1216-1217.

Kim, H. and Martin, B.J. (2007). Estimation of Body Links Transfer Functions in Vehicle Vibration Environment. *Proceedings of the 2007 Digital Human* Modelling *for Design and Engineering Conference.* Seattle, 12-14 June.

Kim, J.H. and Whang, M.C. (1997). Development of a set of Korean manikins. *Applied Ergonomics,* 28 (5), 407-410.

Knudson, D. (2007). *Fundamentals of Biomechanics.* New York: Springer Science + Business Media, LLC.

Korkmaz, S.V., Hoyle, J.A., Knapkik, G.G., Splittstoesser, R.E., Yang, G., Trippany, D.R., Lahoti, P., Sommerich, C.M., Lavender, S.A. and Marras, W.S. (2006). Baggage handling in an airplane cargo hold: An ergonomic intervention study. *International Journal of Industrial Ergonomics,* 36, 301-312.

Kumar, S. (1996). Spinal compression at peak isometric and isokinetic exertions in simulated lifting in symmetric and asymmetric planes. *Clinical Biomechanics,* 11 (5), 281-289.

Laursen, B., Jensen, B.R., Nemeth, G. and Sjogaard, G. (1998). A model predicting individual shoulder muscle forces based on relationship between electromyographic and 3D external forces in static position. *Journal of Biomechanics,* 31, 731-739.

Lavender, S.A., Conrad, K.M., Reichelt, P.A., Johnson, P.W. and Meyer, F.T. (2000). Biomechanical analyses of paramedics simulating frequently performed strenuous work tasks. *Applied Ergonomics,* 31, 167-177.

Louhevaara, V. and Suurnakki, T. (1992). OWAS^{TM}: A method for the evaluation of postural load during work. *Finnish Institute for Occupational Health Training publication*. Helsinki: Finnish Institute for Occupational Health.

Lu, Y.T., Zhu, H.X., Richmond, S. and Middleton, J. (2010). A visco-hyperelastic model for skeletal muscle tissue under high strain rates. *Journal of Biomechanics*, (in publication) doi: 10.1016/ j.jbiomech.2010.05.030.

Mac Duff, L. (2001). Specific Functional Body Strength Data of the South African Military Population. *ERGOTECH Document P139/2001/01*. Centurion: ERGOnomics TECHnologies.

Mac Duff, L. (2004[1]). Male anthropometric data survey: 2004. *ERGOTECH Document P0433/2004/01*. Centurion: Ergonomics Technologies.

Mac Duff, L. (2004[2]). Functional body strength for lifting and carrying capabilities of the SANDF. *ERGOTECH Document P0337/2004/01*. Centurion: Ergonomics Technologies.

Mac Duff, L. and Bredenkamp, K. (2007). Final Report for the Fit and Ease Study of Male Combat Trousers. *ERGOTECH Document P0653/2007/07*. Centurion: ERGOnomics TECHnologies.

Mac Duff, L. and Slabbert, E. (2003). Identification of additional functional body strength parameters and classification of physical job demands. *ERGOTECH Document P0266/2002/01*. Centurion: Ergonomics Technologies.

Mac Duff, L. and Smit, K. (2002). Biomechanical postural analysis during backpack load carriage: refining the load carriage specification. *ERGOTECH Document P0296/2002/01*. Centurion: ERGOnomics TECHnologies.

Mac Duff, L. and Smit, K. (2004[1]). Methodology for biomechanical postural analysis during backpack load carriage with heavy masses. *ERGOTECH Document P0413/2004/01*. Centurion: ERGOnomics TECHnologies.

Mac Duff, L. and Smit, K. (2004[2]). Lower limb characterisation study of SANDF recruits wearing the current military boot. *ERGOTECH document P0438/2004/02.* Centurion: ERGOnomics TECHnologies.

Mac Duff, L., Smit, K., Malan, D. and Shaba, M. (2003). Artillery Manual Handling Project - Phase Two : Strength Measurements 2002. *ERGOTECH Document P0275/2002/02.* Centurion: Ergonomics Technologies.

Maeda, T., Oowatashi, A., Kiyama, R., Yoshida, Y. and Sakae, K. (2001). Prediction of muscle strength using length and width of the bone. *Journal of Physical Therapy,* 13, 27-30.

Marras, W.S. and Granata, K.P. (1995). A biomechanical assessment and model of axial twisting in the thoraco-lumbar spine. *Spine,* 20(13), 1440-1451.

Marras, W.S., Lavender, S.A. and Leurgans, S.E. (1993). The role of dynamic three-dimensional trunk motion in occupationally-related low back disorders. The effects of workplace factors, trunk position and trunk motion characteristics on risk of injury. *Spine,* 18(5), 617-628.

Marras, W.S., Lavender, S.A. and Leurgans, S.E. (1995). Biomechanical risk factors for occupationally related low back disorder risk. *Ergonomics,* 38(2): 377-410.

Marras, W.S., Knapkik, G.G. and Ferguson, S. (2009). Loading along the lumbar spine as influence by speed, control, load magnitude, and handle height during pushing. *Clinical Biomechanics,* 24, 155-163.

McAtamney, L. and Corlett, E.G. (1993). RULA: A survey method for the investigation of work-related upper limb disorders. *Applied Ergonomics,* 24, 91-99.

McGill, S.M. (1996). Searching for the safe biomechanical envelope for maintaining healthy tissue. *Pre-meeting workshop, International Society for the Study of the Lumbar Spine: The contribution of biomechanics to the prevention and treatment of low back pain,* Vermont, 25 June.

McGill, S.M and Norman, R.W. (1985). Dynamically and statically determined low back moments during lifting. *Journal of Biomechanics,* 18(12), 877-879.

McGill, S.M. and Norman, R.W. (1986). Partitioning of L4/L5 dynamic moment into disc, ligamentous and muscular components during lifting. *Spine,* 11, 666-678.

McGill, S.M., Norman, R.W., Yingling, V.R., Wells, R.P. and Neumann, P. (1998). Sheer happens! Suggested guidelines for ergonomists to reduce the risk of low back injury from shear loading. *Proceedings of the 30th Annual Conference of the Human Factors Association of Canada (HFAC).* Mississauga, Ontario.

Meyer, L.G., Polorski, T.L., Ortel, B.E., Saxton, J.L. and Collyer, P.D. (1996). Muscular strength and anthropometric characteristics of male and female naval aviation candidates. *Naval Aerospace Medical Research Laboratory Report NAMRL-1396.* Pensacola: Naval Aerospace Medical Research Laboratory.

Mochimaru, M. and Kouchi, M. (2007). Body shape browser based on homologous body modelling. *World Engineering Anthropometry Resource (WEAR) Conference proceedings.* Banff, 31 July – 1 August.

Mollard, R. (2007). The use of an on-line anthropometric database system for morphotype analysis and sizing system adaptation for different world market apparel sportswear. *World Engineering Anthropometry Resource (WEAR) Conference proceedings.* Banff, 31 July – 1 August.

MSC.Software Corporation. (2005). ADAMS™. USA.

Neptune, R.R. and Hull, M.L. (1998). Evaluation of performance criteria for simulation of submaximal steady-state cycling using a forward dynamic model. *Journal of Biomechanical Engineering,* 120, 334-341.

Niskar, A., Baron-Epel, O., Garty-Sandalon, N. and Keinan-Boker, L. (2009). Peer Reviewed: Body Mass Dissatisfaction Among Israeli Jewish and Arab Women With Normal or Overweight-Obese Body Mass Index. *Preventing Chronic Disease*, 6(2): A51.

Nolte, H. (2006). Development of a detailed foot model to conduct biomechanical analysis predictions on users of military footwear. *ERGOTECH Document P0609/2006/01.* Centurion : ERGOnomics TECHnologies.

Nolte, H. (2007). Biomechanical Modelling of the Neck. *ERGOTECH Document P0687/2007/01.* Centurion : ERGOnomics TECHnologies.

Norman, R., Wells, R., Neumann, P., Frank, J., Shannon, H. and Kerr, M. (1998). A comparison of peak vs. cumulative physical loading factors for reported low back pain in the automobile industry. *Clinical biomechanics*, 13, 561-573.

Ogden, R.W. (1984). *Non-Linear Elastic Deformations.* West Sussex: Ellis Horwood Ltd.

Paquet, E. (2004). Exploring Anthropometric Data Through Cluster Analysis. *Proceedings of the Digital Human Modelling for Design and Engineering.* Michigan, 15-17 June,

Pel, J.J.M., Spoor, C.W., Pool-Goudzwaard, A.L., Hoek van Dijke, G.A. and Snijders, C.J. (2008). Biomechanical analysis of reducing sacroiliac joint shear load by optimization of pelvic muscle and ligament forces. *Annals of Biomedical Engineering*, 36 (3), 415-424.

Pierce, J.E. and Li, G. (2005). Muscle forces predicted using optimization methods are coordinate system dependent. *Journal of Biomechanics,* 38, 695-702.

Pompeu, F.A.M.S., Gabriel, D., Pena, B.G. and Ribeiro, P. (2004). Arm cross-section areas: technical implications and applications for body composition and maximal dynamic strength evaluation. *Rev. Bras. Med. Esporte.*, 10 (3), 207-211.

Powell, P.L., Roy, R.R., Kanim, P., Bello, M.A., Edgerton, V.R. (1984). Predictability of skeletal muscle tension from architectural determinations in guinea pig hindlimbs. *Journal of Applied Physiology*, 57, 1715-1721.

Qualisys AB. (2006). *ProReflex MCU: Qualisys Motion Capture Unit.* Retrieved October 31, 2006, from http://qualisys.iweb.se/archive/Product_information_pdf/AN_ProReflex.pdf.

Raasch, C.C., Zajac, F.E., Ma, B. and Levine, W.S. (1997). Muscle coordination of maximum-speed pedalling. *Journal of Biomechanics*, 30, 595-602.

Rasband, J. (1994). *Fabulous Fit.* New York: Fairchild Publications.

Rasmussen, J., de Zee, M., Damsgaard, M., Christensen, S.T., Marek, C. and Siebertz, K. (2007). *A general method for scaling musculo-skeletal models.* Retrieved July 25, 2007, from www.anybodytech.com.

Ren, L., Jones, R.K. and Howard, D. (2005). Dynamic analysis of load carriage biomechanics during level walking. *Journal of Biomechanics*, 38, 853-863.

Robertson, R.J. (1982). Central signals of perceived exertion during dynamic exercise. *Medicine and science in Sport and Exercise*, 14, 390-396.

Robinette, K.M. and Whitestone, J.J. (1992). Methods for characterizing the human head for the design of helmets. *Armstrong Aerospace Medical Research Laboratory Report AL-TR-1992-0061.* Virginia: National Technical Information Service (NTIS).

Rohlmann, A., Bauer, L., Zander, T., Bergmann, G. and Wilke, H. (2006). Determination of trunk muscle forces for flexion and extension by using a validated finite element model of the lumbar spine and measured in vivo data. *Journal of Biomechanics*, 39, 981-989.

RSA-MIL-STD-127 Volume 1. (2004). Ergonomics design: Anthropometry and environment. Pretoria: RMSS.

RSA-MIL-STD-127 Volume 5. (2001). Ergonomic design: Biomechanics – Specific functional body strength. Pretoria: RMSS.

Schultz, A.B., Haderspeck, K., Warwick, D. and Portillo, D. (1983). Use of lumbar trunk muscles in isometric performance of mechanically complex standing tasks. *Journal of Orthopaedic Res*, 1, 77-91.

Sekulic, D., Zenic, N. and Markovic, G. (2005). Non linear relationships between anthropometric and motor-endurance variables. *Col. Antropol.*, 29 (2), 723-730.

Shaba, M.N. and Slabbert, E. (2002). Task and postural analysis in South African mining industry. *ERGOTECH Document P169/2002/01.* Centurion: ERGOnomics TECHnologies.

Shoaf, C., Genaidy, A., Karwowski, W., Waters, T. and Christensen, D. (1997). Comprehensive manual handling limits for lowering, pushing, pulling and carrying activities. *Ergonomics*, 40 (11), 1183-1200.

Simmons, K., Istook, C.L. and Devarajan, P. (2004). Female Figure Identification Technique (FFIT) for apparel Part I : Describing female shapes. *Journal of Textile and Apparel, Technology and Management*, 4 (1), 1-16.

Sinaki, M., Nwaogwugwu, S.M., Phillips, B.E. and Mokri, M. (2001). Effect of gender, age, and anthropometry on axial and appendicular muscle strength. *American Journal of Physical Medicine & Rehabilitation,* 80 (5), 330-338.

Shaba, M.N. (2005[1]). Female anthropometric data survey: 2005. *ERGOTECH Document P0530/2005/01.* Centurion: Ergonomics Technologies.

Shaba, M.N. (2005[2]). Male anthropometric data survey: 2005. *ERGOTECH Document P0531/2005/01.* Centurion: Ergonomics Technologies.

Shaba, M.N. (2006[1]). Female anthropometric data survey: 2006. *ERGOTECH Document P0601/2005/01.* Centurion: Ergonomics Technologies.

Shaba, M.N. (2006[2]). Male anthropometric data survey: 2005. *ERGOTECH Document P0602/2005/01.* Centurion: Ergonomics Technologies.

Shaba, M.N. (2007). Anthropometric data survey for specific age groups in the SANDF: 2007. *ERGOTECH Document P0681/2007/01.* Centurion: Ergonomics Technologies.

Slabbert, E. (2001[1]). Male anthropometric data: Update. *Ergotech Document P208/2002/01.* Centurion: Ergonomics Technologies.

Slabbert, E. (2001[2]). Female anthropometric data survey. *Ergotech Document P0260/2002/02.* Centurion: Ergonomics Technologies.

Slabbert, E. (2002[1]). Male anthropometric data survey: November 2002. *Ergotech Document P0261/2002/01.* Centurion: Ergonomics Technologies.

Slabbert, E. (2002[2]). Female anthropometric data survey 2003. *Ergotech Document P0333/2003/01.* Centurion: Ergonomics Technologies.

Slabbert, E. (2003). Male anthropometric data survey: June 2003. *Ergotech Document P0332/2004/01.* Centurion: Ergonomics Technologies.

Smit, K. (2001). First representative South African head model in a range of head models to be used for sizing and fit evaluations of face fitting headgear. *ERGOTECH Document P154/2001/01.* Centurion: ERGOnomics TECHnolgies.

Smit, K. (2003). Methodology for identification and description of representative SANDF head forms for head fitting headgear. *ERGOTECH Document P0259/2002/01.* Centurion: ERGOnomics TECHnologies.

Snook, S.H. (1978). The design of manual handling tasks. *Ergonomics*, 21, 963-985.

Snook, S.H. and Ciriello, V.M. (1991). The design of manual handling tasks: revised tables of maximum acceptable mass and forces. *Ergonomics*, 34, 1197-1213.

Statsoft. (2008). *Data Analysis Software System*. Retrieved on August 15, 2008 from www.statsoft.com.

Stevens, J., Truesdale, K.P., Katz, E.G. and Cai, J. (2008). Impact of Body Mass Index on Incident Hypertension and Diabetes in Chinese Asians, American Whites, and American Blacks: The People's Republic of China Study and the Atherosclerosis Risk in Communities Study. *American Journal of Epidemiology*, 167(11), 1365–1374.

Stokes, I.A.F. and Gardner-Morse, M. (1995). Lumbar spine maximum effort and muscle recruitment patterns predicted by a model with multijoint muscles and joints with stiffness. *Journal of Biomechanics*, 28(2), 173-175.

Stokes, I.A.F. and Gardner-Morse, M. (2001). Lumbar spinal muscle activation synergies predicted by multi-criteria cost function. *Journal of Biomechanics*, 34(6), 733-740.

Sverdlova, N.A. and Witzel, U. (2010). Principles of determination and verification of muscle forces in the human musculoskeletal system: Muscle forces to minimise bending stress. *Journal of Biomechanics*, 43, 387-396.

Thompson, D.D. and Chaffin, D.B. (1993). Can biomechanically determined stress be perceived? *Proceedings of the Human Factors and Ergonomics Society 37th Annual meeting*, Seattle, 11-15 October.

Van den Tillaar, R. and Ettema, G. (2004). Effect of body size and gender in overarm throwing performance. *European Journal of applied Physiology,* 91, 413-418.

Van Schalkwyk, C. (2004). Female anthropometric data survey: 2004. *ERGOTECH Document P0432/2004/01*. Centurion: Ergonomics Technologies.

Veitch, D., Veitch, L. and Henneberg, M. (2007). Sizing for the Clothing Industry Using Principal Component Analysis – An Australian Example. *Journal of ASTM International*, 4(3). 133-145. Retrieved October 10, 2008, from www.astm.org.

Wagner, D., Rasmussen, J. and Reed, M. (2007). Assessing the Importance of Motion Dynamics for Ergonomic Analysis of Manual Materials Handling Tasks using the Anybody Modelling System. *Proceedings of the 2007 Digital Human* Modelling *for Design and Engineering Conference*. Seattle, 12-14 June.

Walker, A.R.P., Adam, F. and Walker, B.F. (2001). World pandemic of obesity: the situation in Southern African populations. *Public Health (2001)*, 115, 368–372.

Waters, T.R., Putz-Anderson, V., Garg, A. and Fine, L. (1994). Revised NIOSH equation from the design and evaluation of manual lifting tasks. *Ergonomics*, 36 (7), 749-776.

Wickiewicz, T.L., Roy, R.R., Powell, P.L., Edgerton, V.R. (1983). Muscle architecture of the human lower limb. *Clinical Orthopaedics and Related Research*, 179, 275-283.

Wilke, H.J., Rohlmann, A., Neller, S., Graichen, F., Claes, L. and Bergmann, G. (2003). ISSLS Prize Winner: a novel approach to determine trunk muscle forces during flexion and extension: a comparison of data from an in vitro experiment and in vivo measurements. *Spine*, 28, 2585-2593.

Whitestone, J.J. and Robinette, K.M. (1994). Fitting to Maximize Performance of HMD Systems. In E.M. James & K.W. Moffitt, (Eds.). *Head-Mounted Displays: Designing for the User.* New York: McGraw-Hill Publishers.

Xiao, G., Lei, L., Dempsey, P.G., Lu, B. and Liang, Y. (2005). Isometric muscle strength and anthropometric characteristics of a Chinese sample. *International Journal of Industrial Ergonomics*, 35, 674-679.

Zangrillo, F.L. (1990). *Fashion Design for the Plus-Size*. New York: Fairchild Publications.

Zenk, R., Franz, M. and Bubb, H. (2007). Spine Load in the Context of Automotive Seating. *Proceedings of the 2007 Digital Human* Modelling *for Design and Engineering Conference*. Seattle, 12-14 June.